Chapter 11: Maps of Faults in Planar Beds

FAULTS ARE disruptions of the rock, accommodating relative displacement of the walls separated by them. On geological maps, faults usually show as abrupt terminations of otherwise smooth lithological boundaries. Accurate assessment of the displacement across faults may further be of economic importance. Fault surfaces commonly act as seals for hydrocarbon traps and, also, are preferential sites of mineralization, as faults often control hydrothermal circulation in the subsurface. Faults may involve displacements of up to several hundreds of kilometers, in which case the fault motion is frequently accompanied by earthquakes. Faults may have formed at any moment in geological history and can still be traced at present by the mapping of dislocated outcrop patterns in the field.

Contents: The tectonic setting of faults is discussed in section 11-1. The important distinction of fault slip and fault separation is explained in section 11-2. The effects on map patterns caused by dip-slip faulting are systematically discussed for horizontal beds in section 11-3 and for uniformly inclined beds in section 11-4. Map symbols, used to facilitate the reading of geological maps, are outlined in section 11-5. The map analysis of faulted strata in areas of rugged topography is outlined in section 11-6.

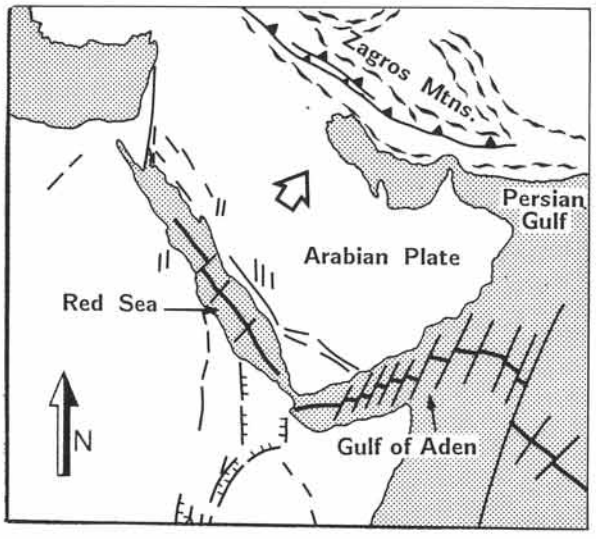

Figure 11-1a: *General tectonic map of the Arabian plate.*

11-1 Tectonic setting of faults

Penetrative disruption of crustal rocks by faulting is common along the boundaries of the major *lithospheric plates*. The boundaries of the plates themselves are faults, because they are

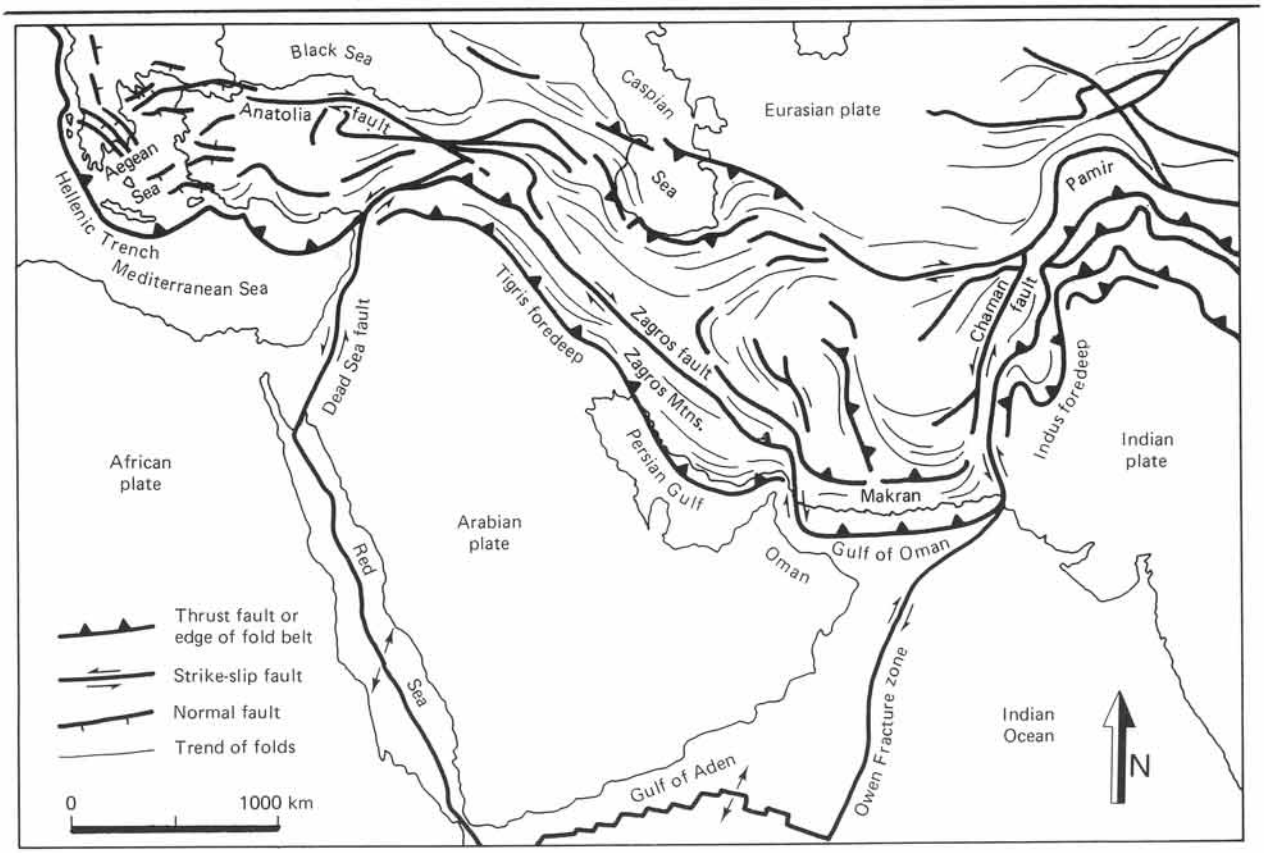

Figure 11-1b: *Detailed tectonic map of the Arabian plate.*

zones which accommodate the movement between juxtaposed plates. The Arabian plate provides a good example of a *tectonic plate*, surrounded by all of the three major types of plate boundaries (Fig. 11-1a & b). The plate is bordered in the south and west by the interconnected *spreading ridges* of the Gulf of Aden and the Red Sea. The northeast boundary of the Arabian plate is located in the diffuse *collision zone* with the adjacent Eurasian continent, that formed the Zagros Mountains. The differential horizontal movement of the Arabian plate is further accommodated by *transfer faults* along its northwest (Dead Sea fault) and southeast (Owen fracture zone) boundaries. Each of these boundaries includes one or more fundamental type(s) of fault(s), that will be outlined in turn below. The most commonly used classification distinguishes faults on the basis of their orientation and sense of displacement. Normal and reverse (dip-slip) faults and strike-slip faults are all introduced below.

Crustal extension and normal faults

The Red Sea has opened after thinning and rifting of the initially continuous continental crust, which led to the separation of the Arabian Peninsula from Africa about forty million years ago. The rifting itself was the result of northwestward propagation of the Indian spreading ridge, and subsequent opening of the Red Sea has occurred at an average annual rate of one to two centimeter(s). Figure 11-2a illustrates the incipient rift valley that was created by the extension and thinning of the crust above the propagating *spreading zone*. Progressive widening eventually allowed chemically fractionated mantle rocks to surface in the floor of the *rift valley*, which became flooded when the Indian Ocean transgressed into the growing Red Sea (Fig. 11-2b). The initial rifting and crustal *extension* were accommodated by *normal faults*, which, by definition, have a *hanging wall* that has moved

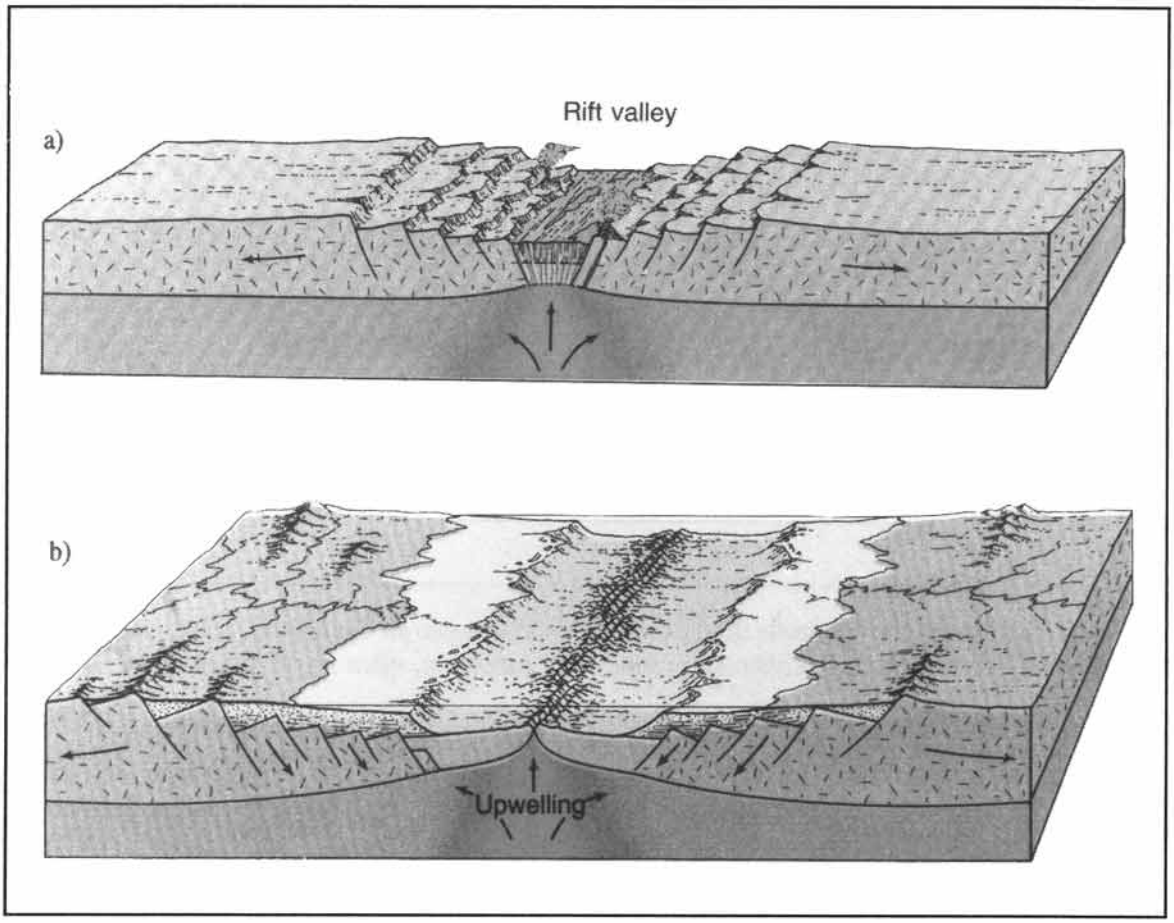

Figure 11-2: *a) & b) Stages in the break-up of a continent. a) Crustal thinning and rift valley formation by normal faulting. b) Accretion of oceanic crust by magmatic spreading of mid-oceanic rift zone.*

down relative to the *foot wall* (Fig. 11-3). The hanging wall always is understood as the crustal rock portion leaning against or onto the foot wall. The movement of normal faults can be described by *slip vectors* on the hanging wall, pointing down the dip of the fault plane. Normal faults form one particular class of so-called *dip-slip faults*. *Reverse faults*, like normal faults, also, move along slip vectors on the hanging wall, pointing in the direction of dip of the fault plane and constitute another class of *dip-slip faults* (see, also, section 11-2). Slip vectors are synonymous with the displacement vectors of formerly adjacent points on the fault plane, attached to either side of the faulted block.

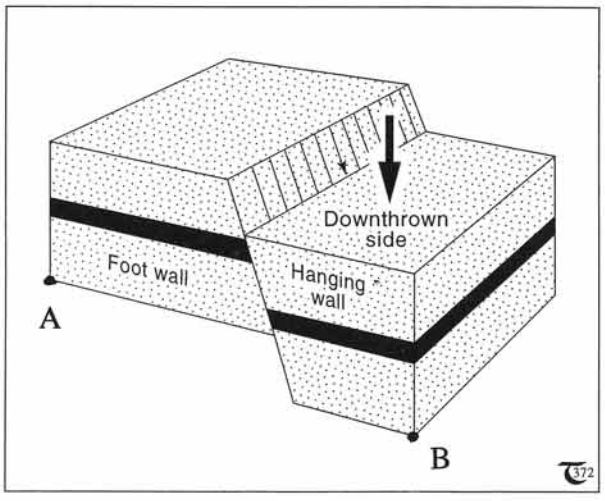

Figure 11-3: *Normal fault - the hanging wall moved down relative to the foot wall.*

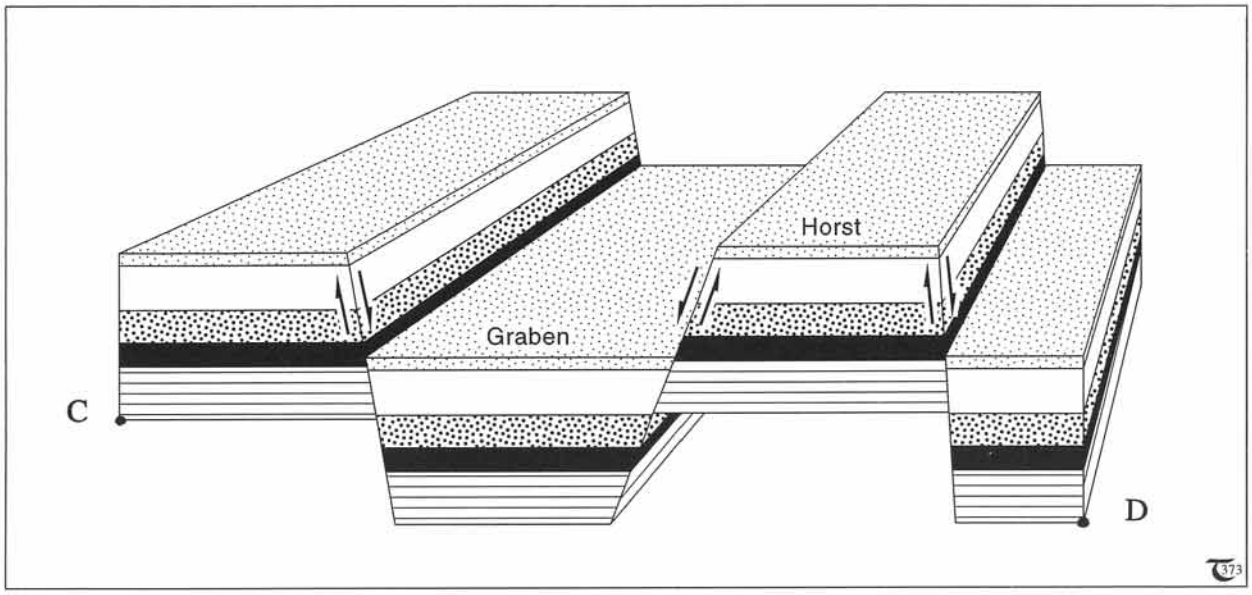

Figure 11-4: *Conjugate normal faults of opposite inclination separate upthrown (horst) and downthrown (graben) blocks. Normal faults accommodate horizontal extension, often in rift zones. See exercise 11-1.*

☐Exercise 11-1: a) Measure the crustal stretch associated with the single normal fault of Figure 11-3. The stretch can be calculated as the ratio of the final and the initial lengths between points A and B. b) Measure the crustal stretch between points C and D, caused by the system of normal faults separating downthrown (graben) and upthrown (horst) blocks in Figure 11-4. The terms graben and horst originate from the original German terminology.

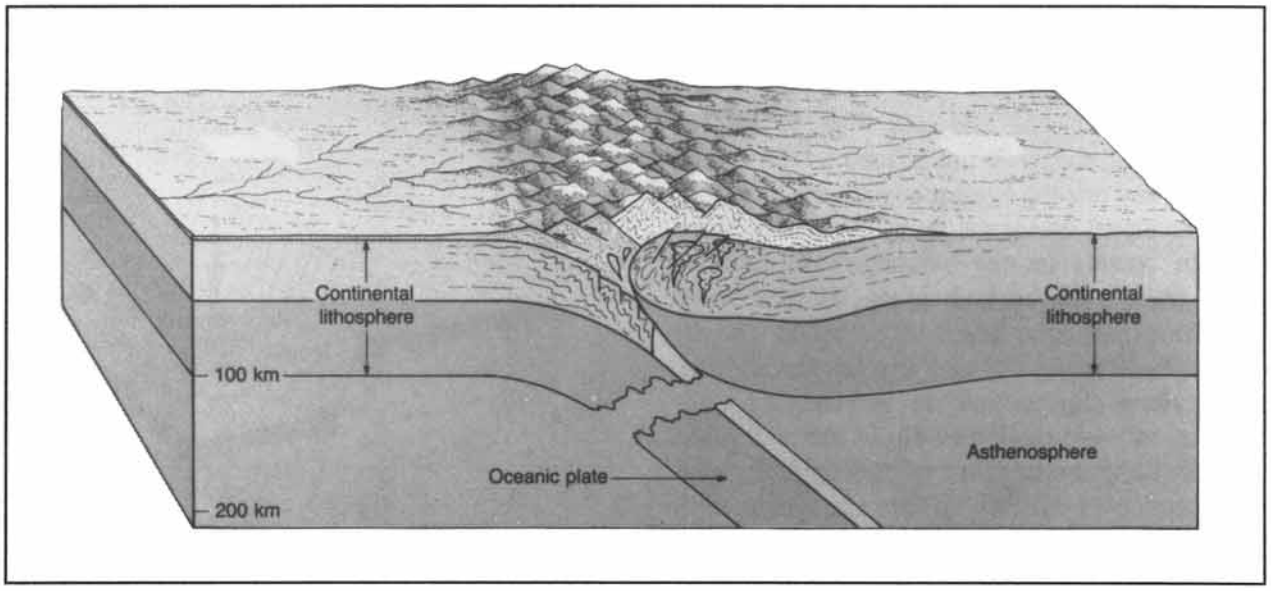

Figure 11-5: *Reverse faults accommodate crustal shortening, and the majority of them are formed in orogenic zones of active continental margins.*

Crustal shortening and reverse faults

The Zagros Mountains were uplifted by the impingement of the Arabian and Eurasian plates, which started after closure of the Tethys Ocean, which had separated the two continental areas until about twenty million years ago. The Zagros Mountains contain well-exposed, doubly plunging folds, and some of the crustal *shortening* associated with the plate collision has been accommodated by *reverse faults* (Fig. 11-5). These faults have a hanging wall that has moved up relative to the foot wall (Fig. 11-6). A special class of reverse faults is constituted by *thrust faults*. These are very low angle faults with hanging walls that may have translated for tens of kilometers over the foot wall (Fig. 11-7). Such translated masses of rock are termed *thrust nappes*. Estimates of

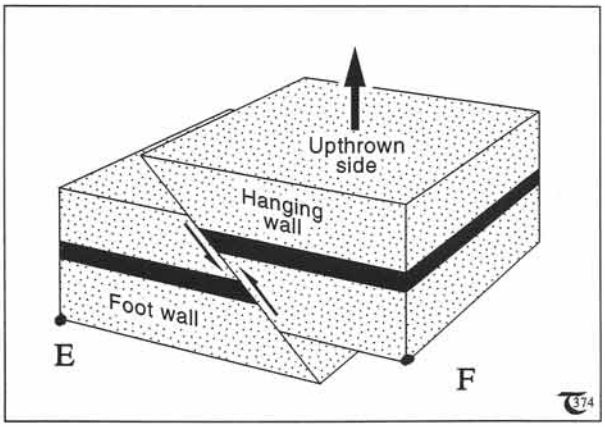

Figure 11-6: *Reverse fault - the hanging wall moved up relative to the foot wall.*

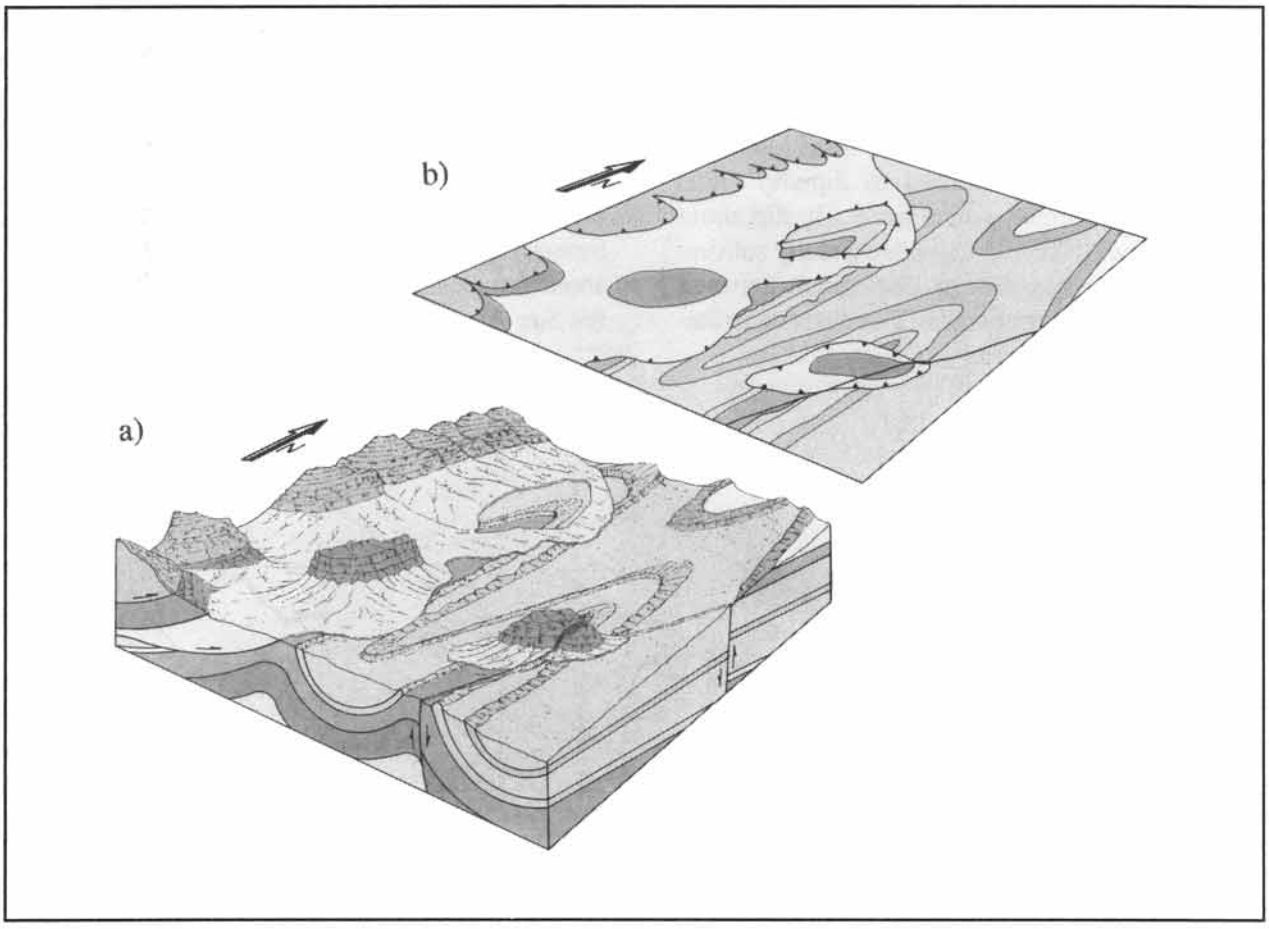

Figure 11-7: *a) Perspective diagram of thrust faults, transferring subhorizontal strata over a folded substratum. b) Geological map of the same area, showing the outlines of the eroded thrust fault contacts.*

☐Exercise 11-2: Measure the fractional change of crustal length EF (stretch, here leading to shortening) associated with the single reverse fault portrayed in Figure 11-6.

☐Exercise 11-3: Estimate the minimum horizontal displacement involved in the emplacement of the rock units above the major thrust plane in Figure 11-7b.

the minimum displacement over basal thrust faults can be inferred from the maximum distance between basement *inliers* (windows or fenster) and cover *outliers* (klippes).

Horizontal crustal transfer by strike-slip faults

The Owen fracture zone and the Dead Sea fault are examples of *strike-slip faults*. Such faults are typically vertical as opposed to dip-slip faults (normal and reverse), which generally dip about 60°. Because strike-slip faults are usually subvertical, it is not possible to distinguish between hanging walls and foot walls. The walls of strike-slip faults are displaced in opposite directions but mainly by horizontal slip, parallel to the trace or strike of the fault (Fig. 11-8). Unlike what is suggested in Figure 11-8, strike-slip faults are likely to terminate in the *asthenosphere*, where the motion of the juxtaposed plates is maintained by mantle rock convecting at differential rates. The sense of movement on strike-slip faults can be further described as clockwise, counterclockwise, right-lateral (dextral), or left-lateral (sinistral) (see examples below). The term strike-slip fault is entirely synonymous with *transfer fault*, *transcurrent fault*, *wrench fault*, *horizontal shear fault*, and, also, includes *transform faults* - the latter, by definition, occurring in oceanic crust only.

Figure 11-9 is a tectonic map of the Dead Sea fault, which accommodates the northward movement of the Arabian plate relative to the Sinai block by sinistral strike-slip movement. The complementary movement on the Owen fracture zone (Fig. 11-1b) can be described as clockwise or right-lateral (dextral). Some extension along the Dead Sea fault causes rifting and subsidence of its *central graben system*, which now hosts the Gulf of Aqaba and the Dead Sea. The estimated strike-slip displacement on the Dead Sea fault totals some 110 kilometers and started about 15 million years ago. The time-averaged rate of movement has varied between 0.5 and 1 millimeter per year.

Figure 11-10 is a tectonic map of the Alpine fault, New Zealand, with an estimated dextral strike-slip displacement of 480 kilometers. This fault is responsible for many earthquakes. The time-averaged rate of strike-slip is relatively fast - about 2.2 centimeters per year. For comparison, the San Andreas fault in California moves at a

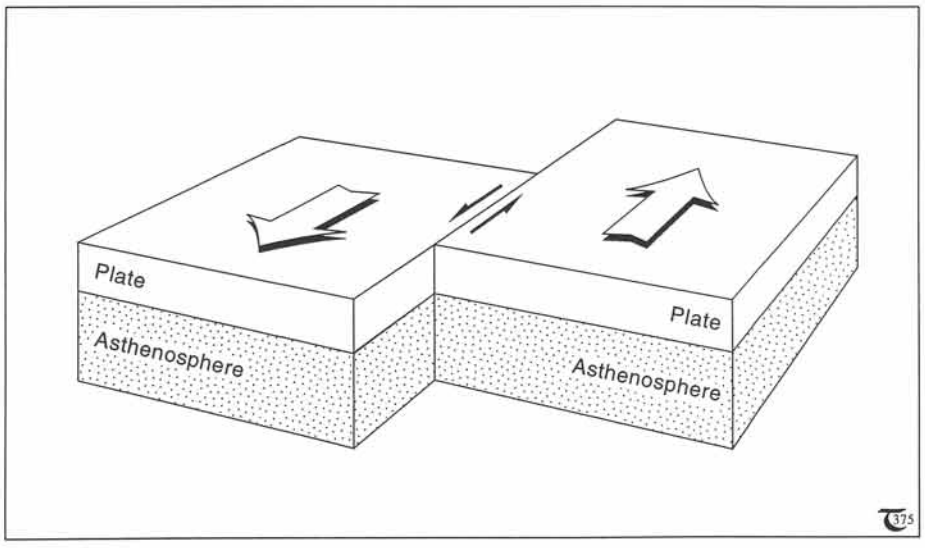

Figure 11-8: *Strike-slip faults, usually subvertical, separate two lithospheric plates moving in opposite directions, parallel to the fault trace.*

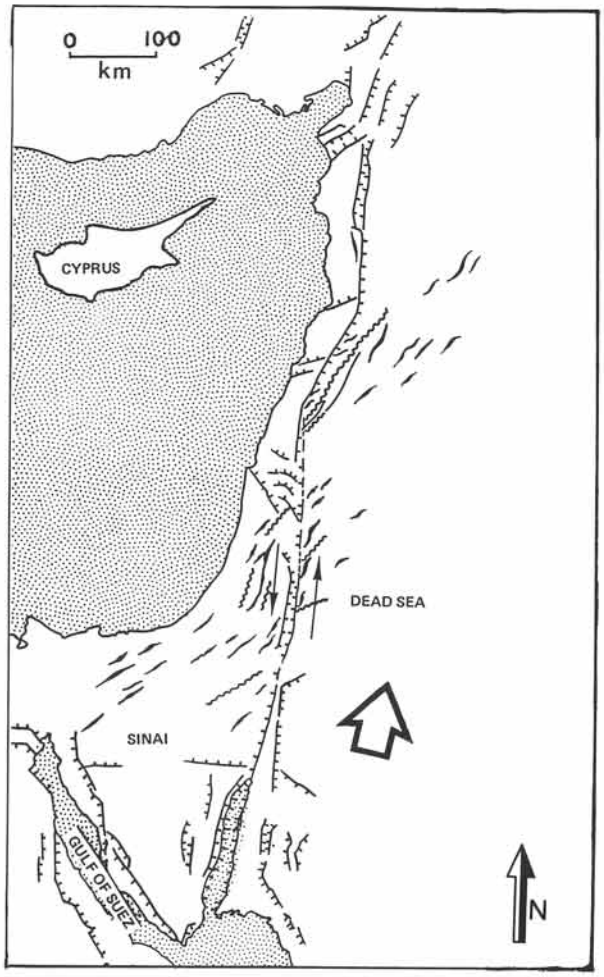

Figure 11-9: *Left-lateral (sinistral) strike-slip movement on the Dead Sea fault accommodates differential movement of the Arabian plate. The relative subsidence of the central graben results from transtension.*

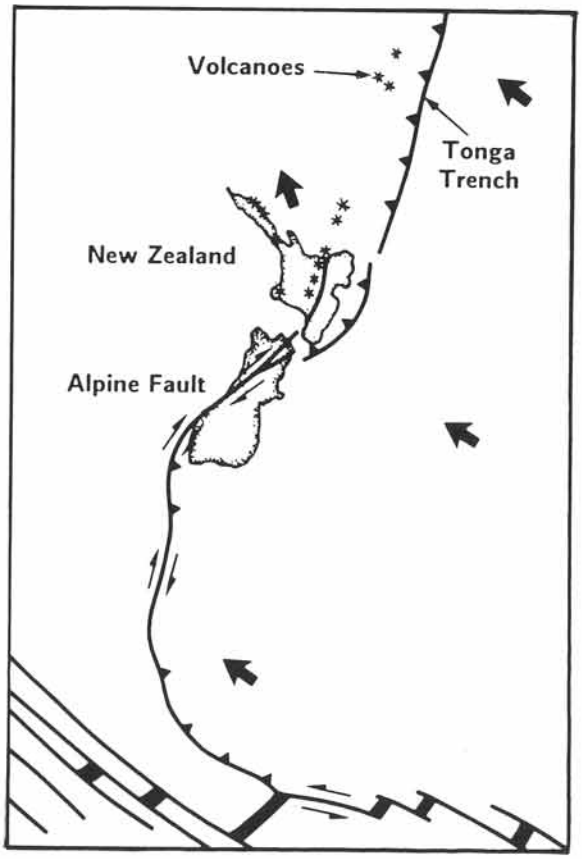

Figure 11-10: *Right-lateral (dextral) strike-slip movement on the Alpine fault accommodates part of the westward movement of the Pacific plate relative to the Australian plate. The uplift of the Alpine Mountains of New Zealand is due to a significant component of transpression near the Alpine fault.*

time-averaged rate of about 5 centimeters per year. It is worth noting that the strike-slip on the Alpine fault is accompanied by crustal thickening of its walls. Such thickening deformation, if accompanied by strike-slip movement, is termed *transpression*. Conversely, if a strike-slip motion is accompanied by extension, such as documented for the Dead Sea fault, *transtension* is said to occur.

☐Exercise 11-4: Consider the map of the Alpine fault, transecting New Zealand (Fig. 11-10). a) Is this a left- or right-lateral wrench? b) Give alternative terms for the same sense of shear. c) Describe, also, the sense of shear of the transform fault to the right of the spreading ridge in the south of the map area. d) Also, list all the alternative terms for this sense of shear.

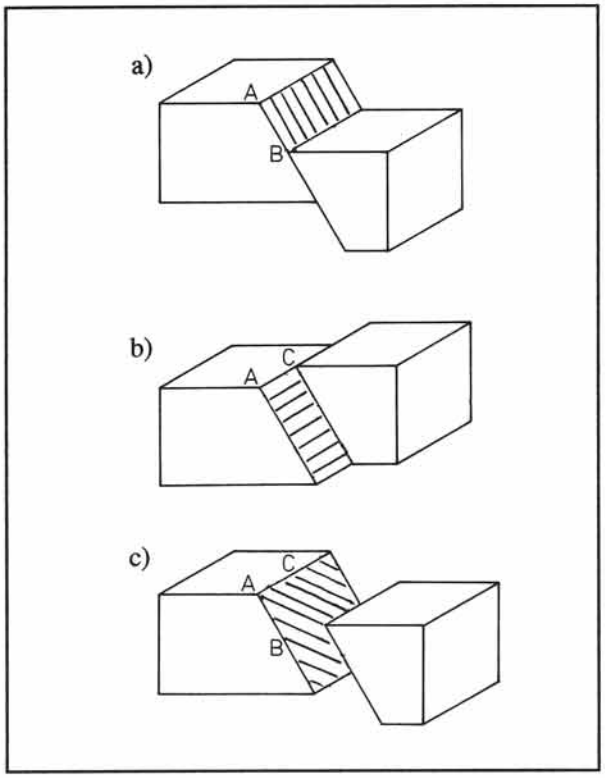

Figure 11-11: *a) to c) Examples of fault slip: (a) Dip-slip fault, (b) strike-slip fault, (c) oblique-slip fault.*

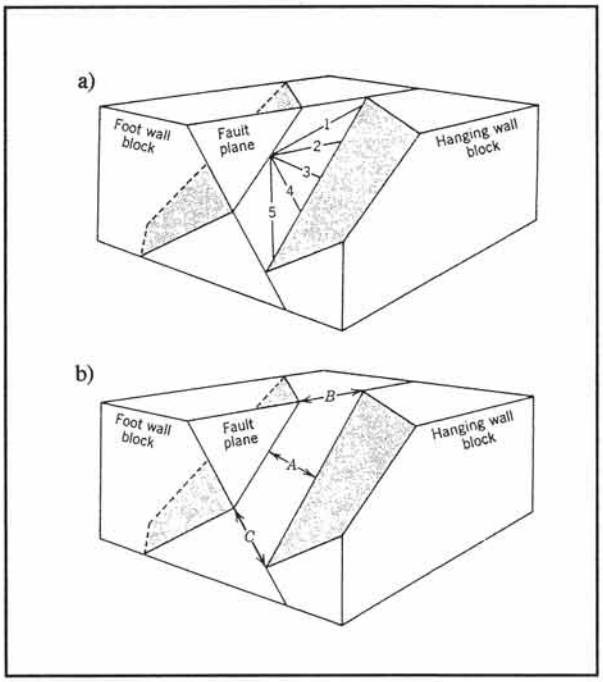

Figure 11-12: *a) Displaced marker plane, and five arbitrary slip directions. b) Various slip separations: net separation (A), strike separation (B), and dip separation (C).*

11-2 Fault slip and fault separation

Faults can be classified, on the basis of the actual movement on the fault surface, as dip-slip, strike-slip, or oblique-slip faults (Figs. 11-11a to c). The *fault slip* measures the relative movement of rock units, separated by the fault, by slip vectors that have displaced formerly adjacent points. Fault slip is different from *fault separation*, which does not refer to the actual fault movement. In determinations of the fault separation, distances between displaced marker planes are measured in a particular direction. Figure 11-12a illustrates an example of a fault displacing a hypothetical marker plane. The actual displacement may have been caused by an infinite number of possible slip movements (e.g., labeled 1 to 5 in Figure 11-12a). It is sometimes not possible to determine the unique direction of fault slip that led to this situation. However, the fault separation can be used to characterize displacements of a marker plane, as measured in a number of specified directions (Fig. 11-12b). The separation is measured in the plane of the fault. Indicated are: net separation (A), strike separation (B), and dip separation (C). Unlike fault slip, the term fault separation refers to the geometrical displacement only and does not imply any direction of actual movement.

11-3 Dip-slip faulted, horizontal beds

Normal and reverse faults, the two types of dip-slip faults distinguished, generally affect the map pattern of rock units. One or both of the walls on either side of a faulted block may have made the movement. It is usually impossible to tell which wall has moved, and only a *relative displacement* direction can be established. The sense of relative displacement is indicated by half-arrows (Figs. 11-13a & b). Dip-slip faulting in a region underlaid by subhorizontal strata will

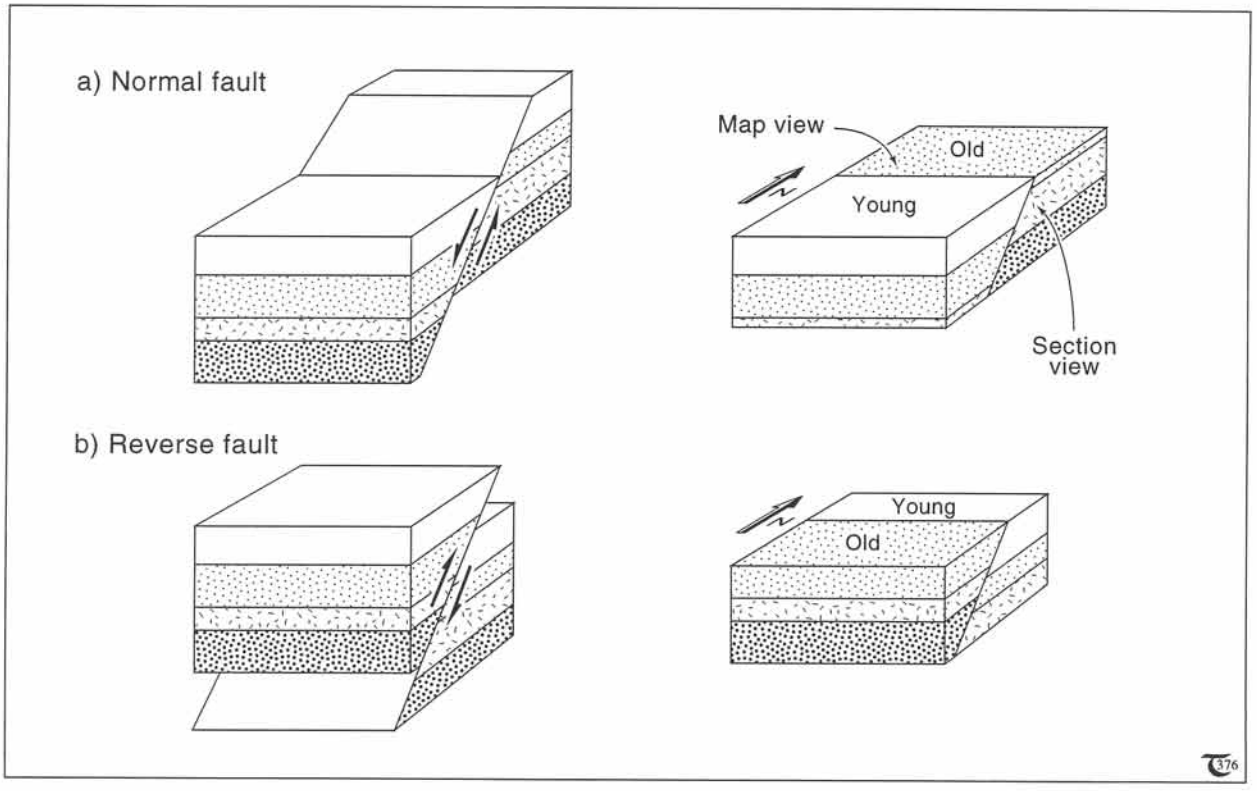

Figure 11-13: *Block diagrams, before and after erosion: (a) normal faulting, and (b) reverse faulting. Hanging walls of normal faults show younger rocks; reverse faults expose older rocks in hanging walls.*

result in map patterns juxtaposing younger rocks against older rocks. Obviously, the older rocks are exposed at the side of the *upthrown block*, after erosion has leveled the upthrown block to the same elevation as the *downthrown block*. Younger rocks are exposed above the downthrown, hanging wall when the fault is normal (Fig. 11-13a). Older rocks are exposed above the upthrown, hanging wall when the fault is reverse (Fig. 11-13b). However, *it is impossible to tell whether a fault is normal or reverse from the map pattern alone if the dip of the fault plane is unknown*; the map patterns of Figures 11-13a and 11-13b are similar after 180° rotation about the vertical axis.

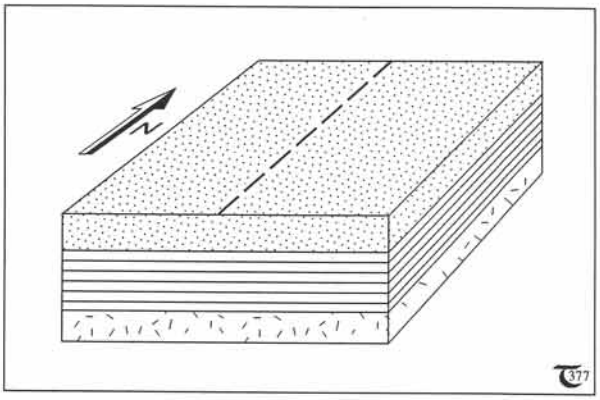

Figure 11-14: *Perspective diagram of subhorizontal strata before faulting. See exercise 11-5.*

☐Exercise 11-5: Consider the block diagram of Figure 11-14, and draw the resultant map patterns after erosional leveling of the ground surface, for (a) an east-dipping normal fault, and (b) a west-dipping reverse fault.

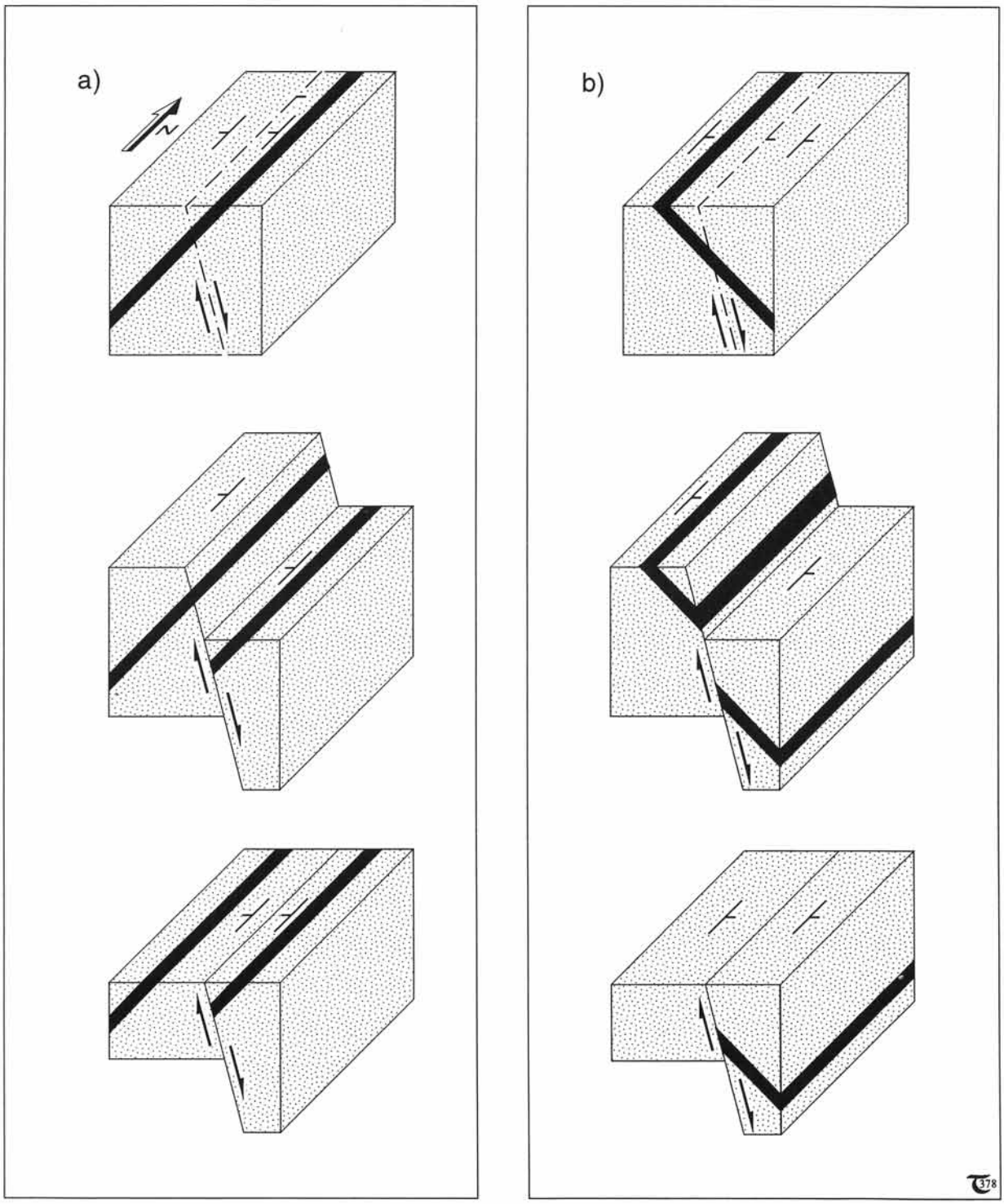

Figure 11-15: *a) & b) Three-stage perspective diagrams (pre-faulting, post-faulting, post-erosional) for normal faulting longitudinal or parallel to the strike of a sedimentary sequence. (a) Dipping opposite to, or (b) dipping in the same direction as the fault plane. Case (a) leads to stratigraphic repetition. Case (b) involves reduction of the stratigraphic section.*

11-4 Dip-slip faulted, homoclinal beds

Strata dipping uniformly may be dislocated by dip-slip faults in two fundamentally different orientations. The dip-slip fault may be either parallel (longitudinal) or oblique (transverse) to the strike of the strata - the latter including the orientation normal to the strike. Each of the two fault types may cause a distinctive disturbance of the map pattern, outlined in turn below.

Longitudinal dip-slip faults

The sequence of block diagrams of Figures 11-15a and 11-15b shows the effect of faulting on the map pattern of inclined strata after leveling of the ground surface by erosion. Figure 11-15a portrays a case where the normal fault is dipping in a direction opposite to that of the beds cut by the fault. The associated final map pattern includes a repetition of the stratigraphic sequence. Figure 11-15b portrays a case where the normal fault is dipping in the same direction as the strata it transects. The final map pattern includes lags (missing strata); the black markerbed is not seen in the map after faulting and erosion.

☐Exercise 11-6: Consider the block diagram of Figure 11-16, and draw the resultant map patterns after erosional leveling of the ground surface, for: (a) a steep, east-dipping reverse fault, and (b) a west-dipping reverse fault. Indicate whether repetition or omissions of parts of the stratigraphic sequence occur. Compare the result with that of the normal faults in Figures 11-15a and b.

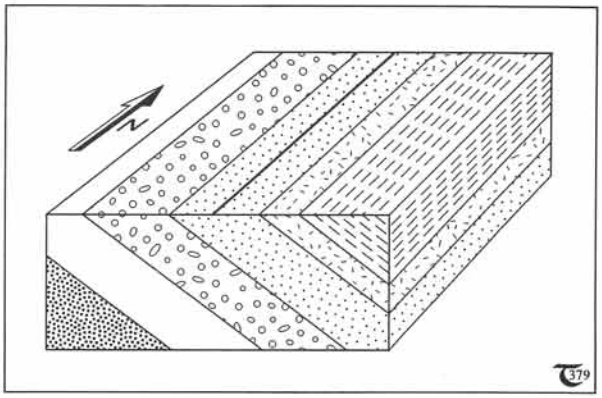

Figure 11-16: *Inclined sedimentary sequence, prior to fault displacement. See exercise 11-6.*

☐Exercise 11-7: Refer to the map of Figure 11-17. a) Complete the cross-section along A-B. b) Interpret the outcrop pattern in a short description of the tectonic history of the map region.

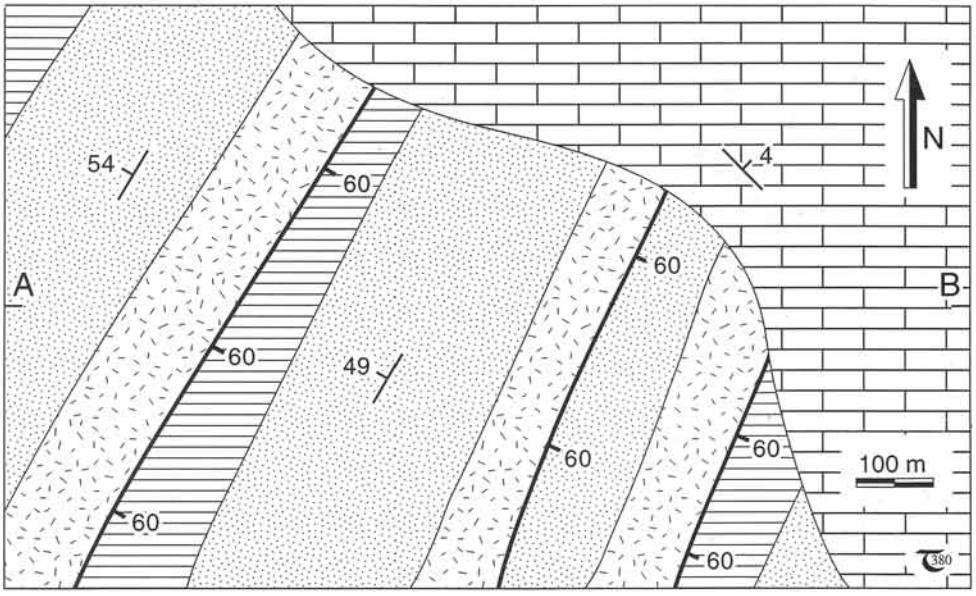

Figure 11-17: *Geological map of a flat area. See exercise 11-7.*

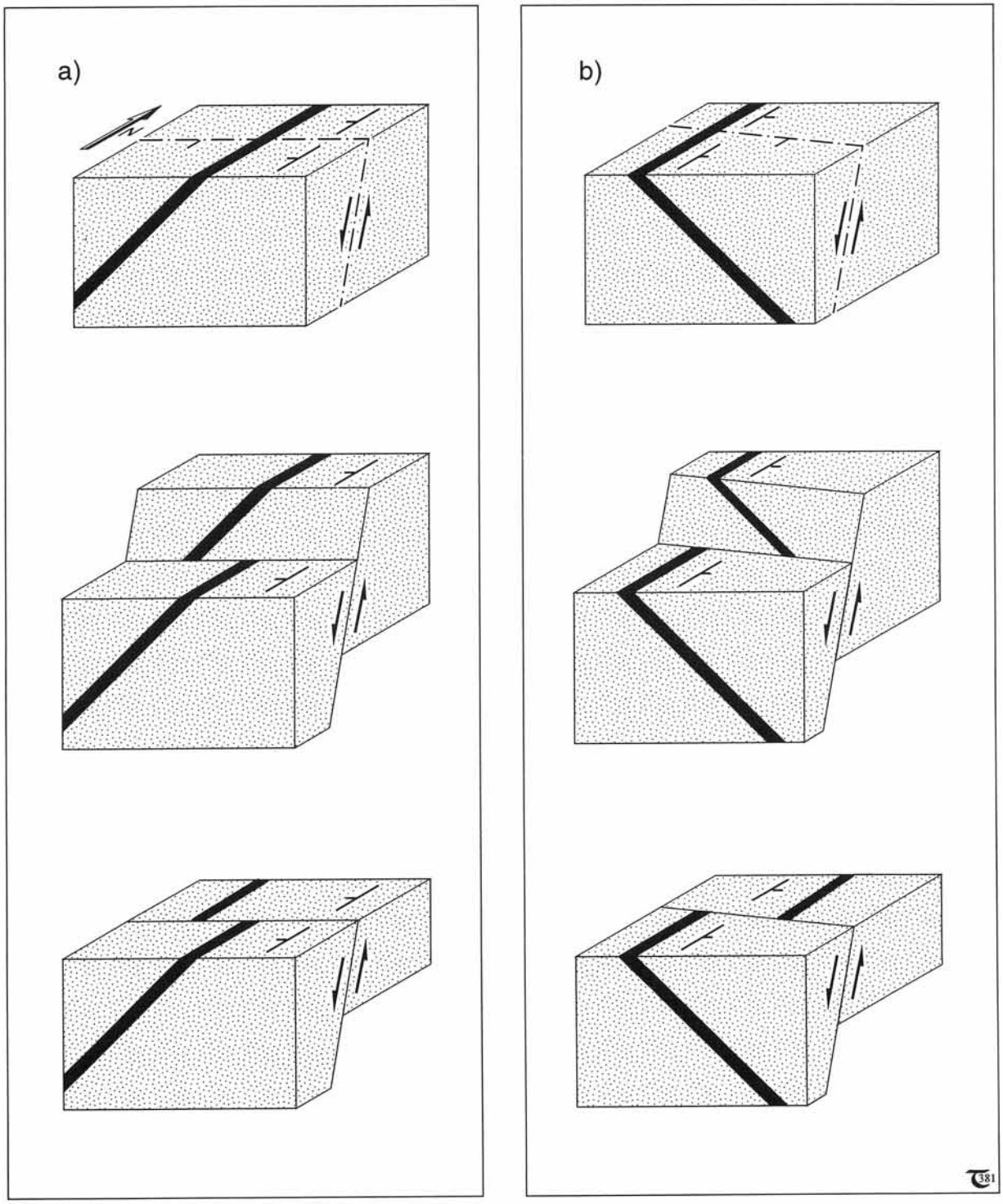

Figure 11-18: *a) & b) Three-stage perspective diagrams (pre-faulting, post-faulting, post-erosional) for normal faulting transverse or oblique to the strike of a sedimentary sequence. The post-erosional diagrams illustrate the apparent strike-slip displacement. The sense of off-set (strike separation) depends upon the initial inclination of the displaced layer(s). Case (a) illustrates apparent left-lateral displacement; case (b) shows apparent right-lateral off-set.*

Transverse dip-slip faults

The sequence of block diagrams of Figures 11-18a and 11-18b shows the effect of faulting on the map pattern of inclined strata after faulting oblique to their strike and subsequent leveling of the ground surface by erosion. The normal fault portrayed cannot lead to either any repetition or omission of the stratigraphic sequence, as exposed at the surface. The strike separation visible on maps alone could be misinterpreted as the result of a strike-slip movement. Yet no component of strike-slip movement is involved; all movement is by dip-slip only. The direction of the strike-slip inferred would be different for layers dipping in opposite directions, as follows from comparing the final outcrop patterns of the models in Figures 11-18a and 11-18b.

Figures 11-18a and b have illustrated that it may be difficult to distinguish *transverse dip-slip faults* from *transverse strike-slip faults*, because their respective map pattern may be similar in regions of uniformly dipping strata. The ambiguity can be avoided if the uniformly dipping beds are cut by another planar feature, e.g., an igneous dike or another, older fault plane (or by determining the dip of the beds and faults in the field). Figure 11-19a to c illustrates such a case and excludes any explanation involving strike-slip alone, because each of the marker units is displaced in opposite directions with different strike separations. Additionally, the horizontal distance between the units at the surface of the eroded, upthrown block is much shorter than in the downthrown block. Such a situation requires an explanation involving a component of dip-slip.

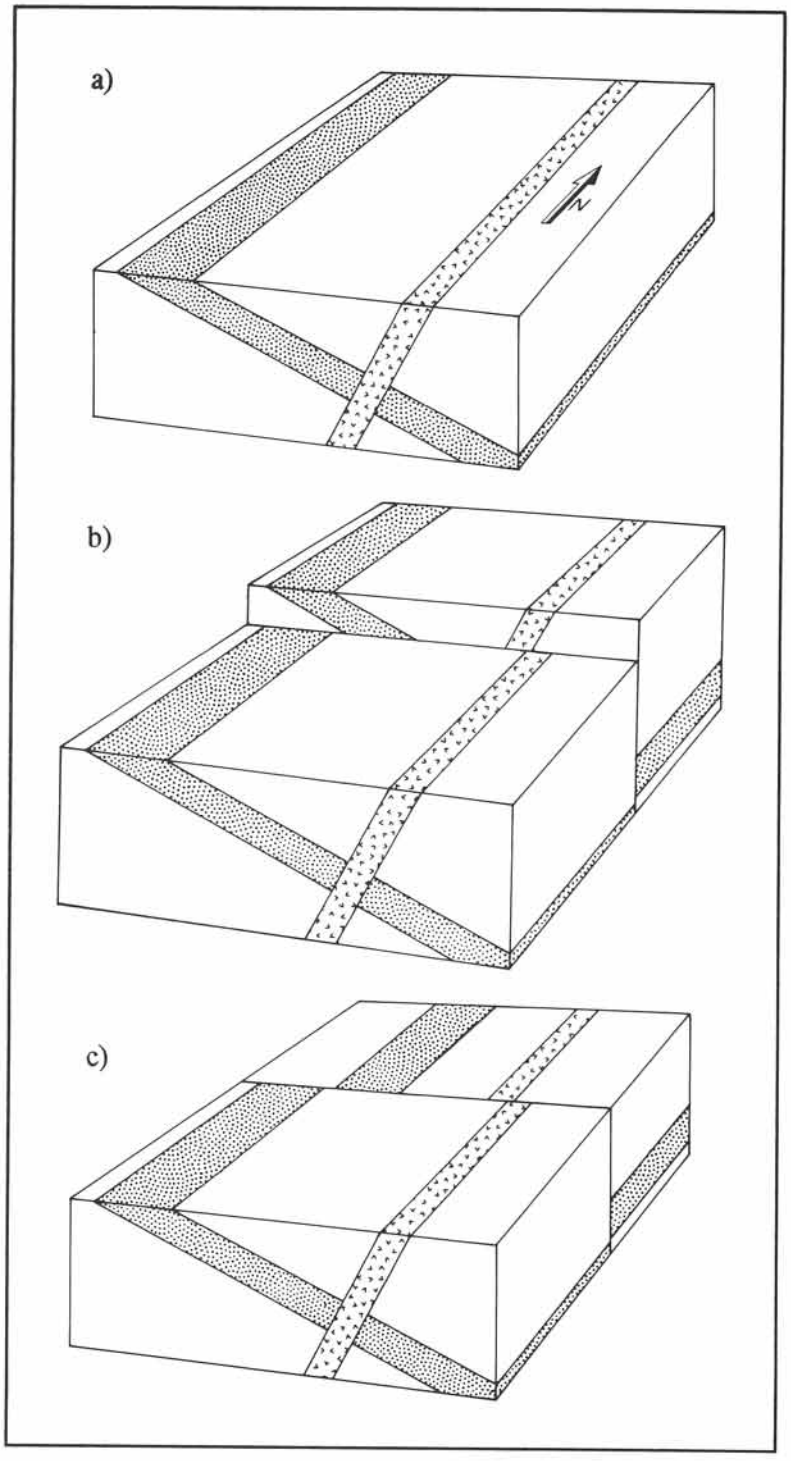

Figure 11-19: *a) to c) Three-stage perspective diagrams (pre-faulting, post-faulting, post-erosional), showing dip-slip movement on a transverse, vertical fault through a sandstone bed and an oppositely-dipping igneous dike.*

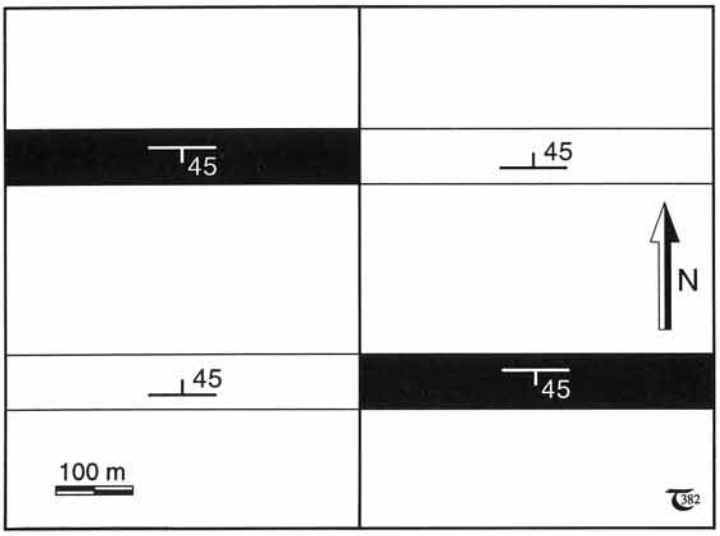

☐Exercise 11-8: Draw a series of three block diagrams, i.e., pre-faulting, pre-erosional, and post-erosional, illustrating how the faulted map pattern of Figure 11-20 can be explained.

Figure 11-20: *Map for exercise 11-8.*

☐Exercise 11-9: Refer to the map of Figure 11-21a. a) Interpret the outcrop pattern in a short description of the tectonic history of the map region. Assume that strike-slip faulting has not occurred at any time. b) Complement and illustrate your story further by completing the cross-section of Figure 11-21b.

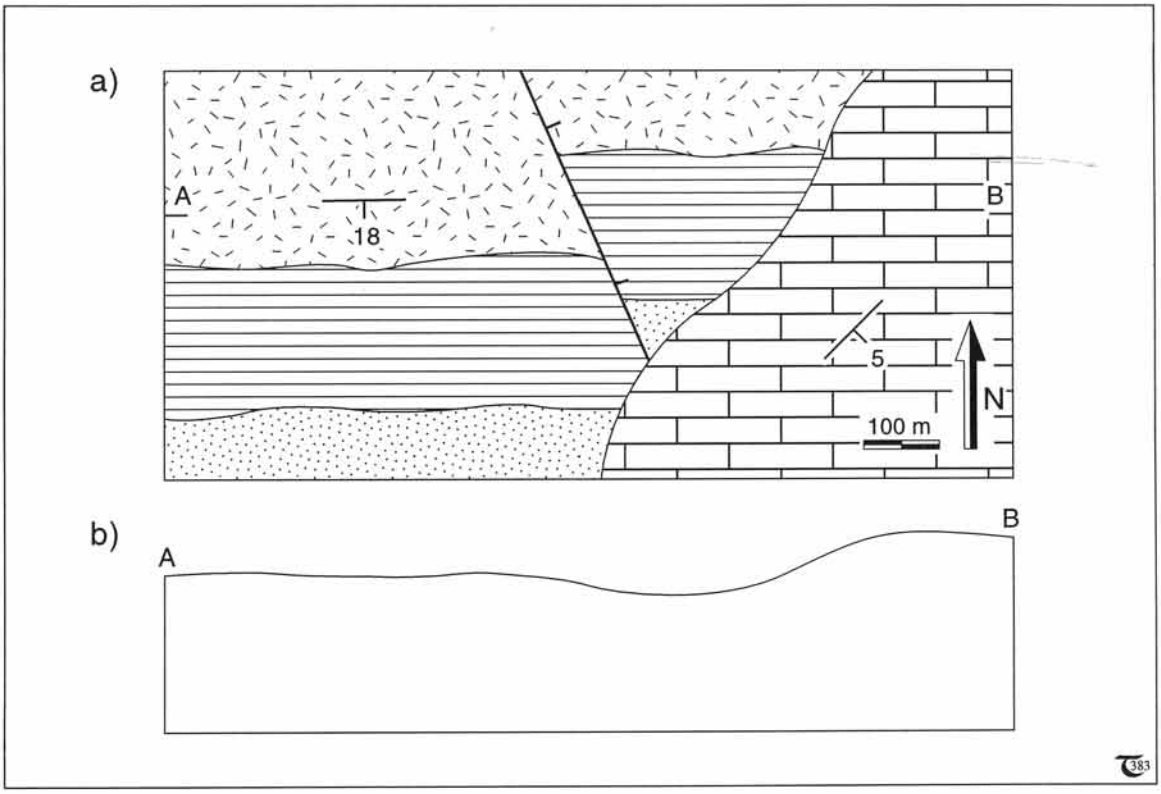

Figure 11-21: *a) & b) Map and cross-section for exercise 11-9.*

☐Exercise 11-10: a) Excluding strike-slip movement, is the central region on the map of Figure 11-22 a graben or a horst? b) Construct an accurate E-W cross-section A-B across the map.

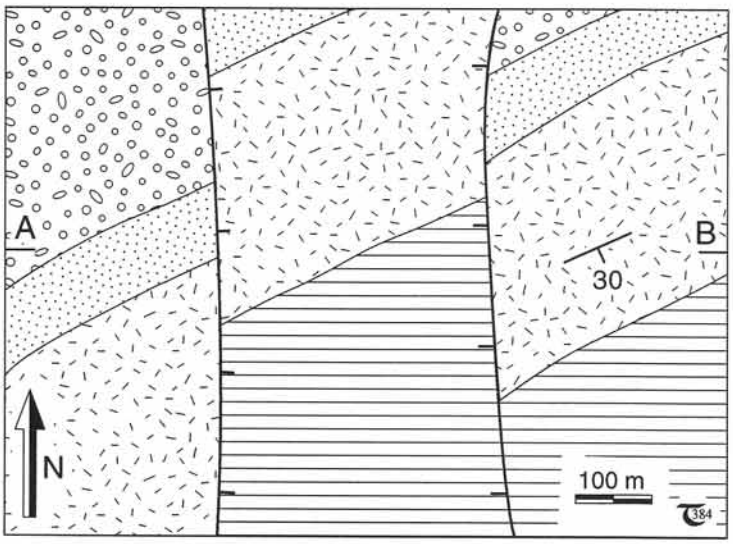

Figure 11-22: Map for exercise 11-10. Assume the area has no topographic relief.

☐Exercise 11-11: Refer to the map of Figure 11-23. Assume only dip-slip faults are involved. a) Interpret the outcrop pattern in a short description of the tectonic history of the map region. b) Complement and illustrate your story further by completing the E-W cross-section A-B across the map of Figure 11-23.

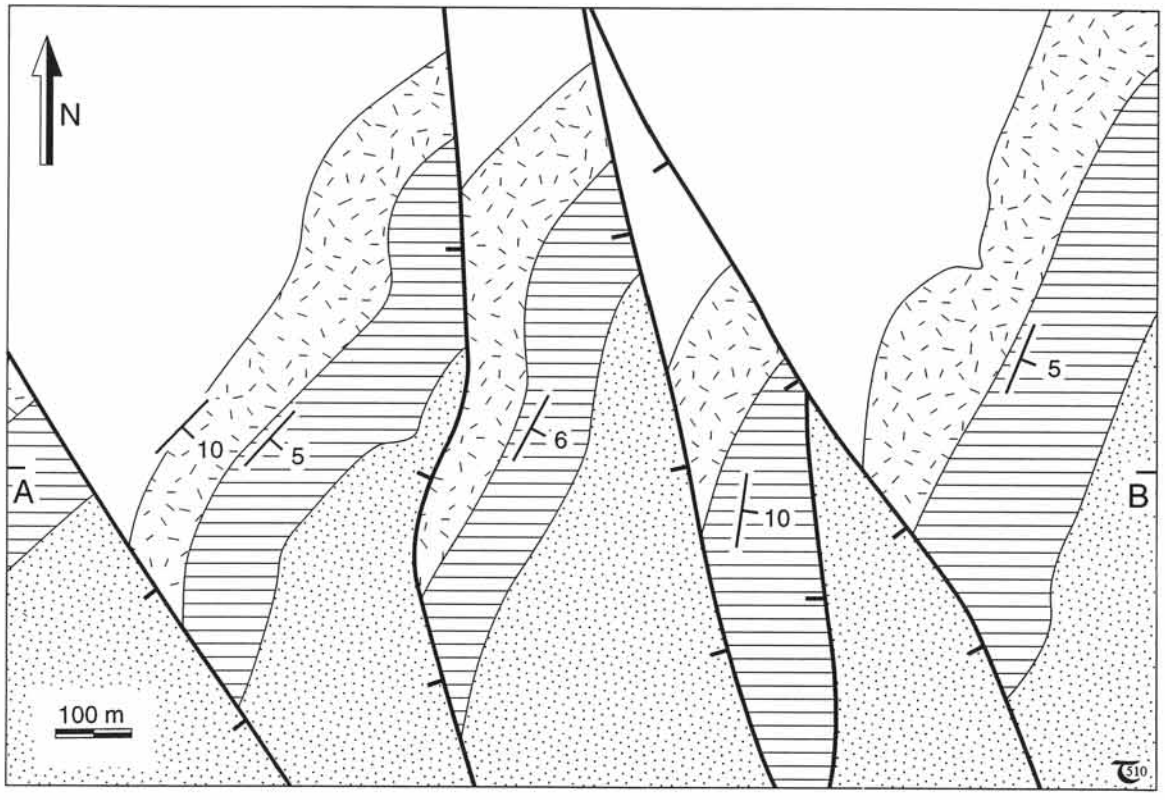

Figure 11-23: Map for exercise 11-11. Assume the area illustrated is a nearly flat terrain.

11-5 Map symbols for fault traces

A variety of geological symbols is used on geological maps to facilitate the interpretation of fault structures. The faults used in most of the figures of this chapter were not marked with any special notation to encourage assessment of the implication of the dislocated outcrop patterns. On professional geological maps, most of the faults have been interpreted for the user by the field geologist, who included special map symbols denoting the nature of the fault. Some of the map symbols, used to characterize faults along their trace, are given in Figure 11-24. It is possible to annotate on the map both the direction and the amount of dip of a fault plane. A bar and ball are used for downthrown blocks if the fault plane is subvertical. Hachures are used to indicate the downthrown block for normal faults. Reverse faults can be marked either by a combination of dip symbols and *U(p)* and *D(own)* markings or by writing an *R* on the upthrown side. Strike-slip faults are marked by a solid line with a conjugate pair of half-arrows, indicating sinistral or dextral sense of shear. Fault breccia, if extensive, may be included on the map as a local rock unit, concentrated along the trace of the fault plane. Finally, thrust faults - a special class of low angle reverse faults, which will be discussed later - are marked with sawteeth on the hanging wall or upper plate.

☐Exercise 11-12: Draw a conjugate pair of half-arrows on either side of a hypothetical strike-slip fault trace, indicating (a) sinistral, and (b) dextral sense of shear.

11-6 Faulted strata in topographic relief

The map patterns, outlined above, considered ground surfaces that were completely leveled by erosion. More complex map patterns of faulted layers arise in terrains of rugged topography. In such cases the true direction of strike and dip of layers and fault planes can be obtained using structure contours, according to the principles

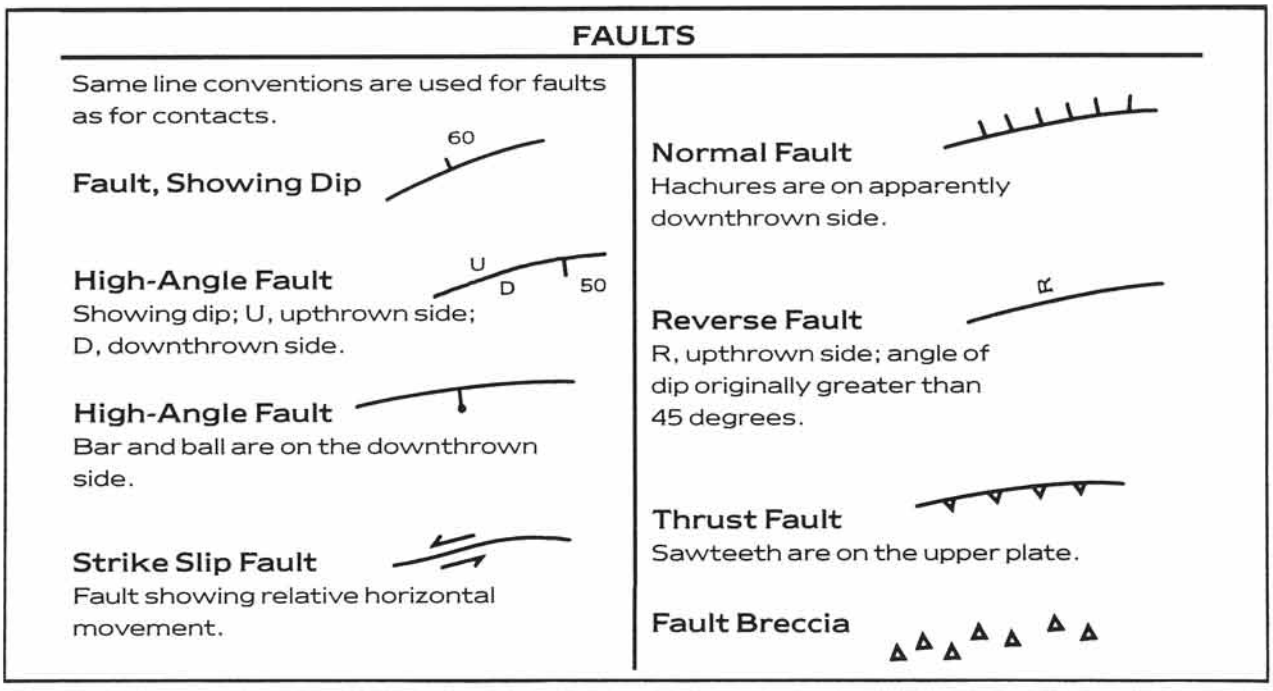

Figure 11-24: Common map symbols for indicating fault elements.

☐Exercise 11-13: Examine the map pattern of Figure 11-25. A NNW-SSE striking fault divides the map into a west and east part. a) Concentrate first on the west part of the map, and determine the structure of the sandstone formation. b) What is the dip of the fault plane? c) Determine the azimuth and dip of the sandstone formation to the east of the fault. d) Determine the dip separation of the fault (see, also, section 11-2 and Fig. 11-12). e) Assuming only dip-slip has occurred, did the east wall move up or down relative to the west wall? f) Determine the strike separation. g) Assuming only strike-slip occurred, is the sense of shear sinistral or dextral?

discussed in chapter five. Figure 11-25 is a map of a sandstone formation, transected by a fault. For this simple structure, the exact amount of fault separation can be determined by the construction of structure contours, as elaborated in exercise 11-13. However, if no further information is available, the same fault separation can be due to either dip-slip alone, strike-slip alone, or a combination of both in oblique slip.

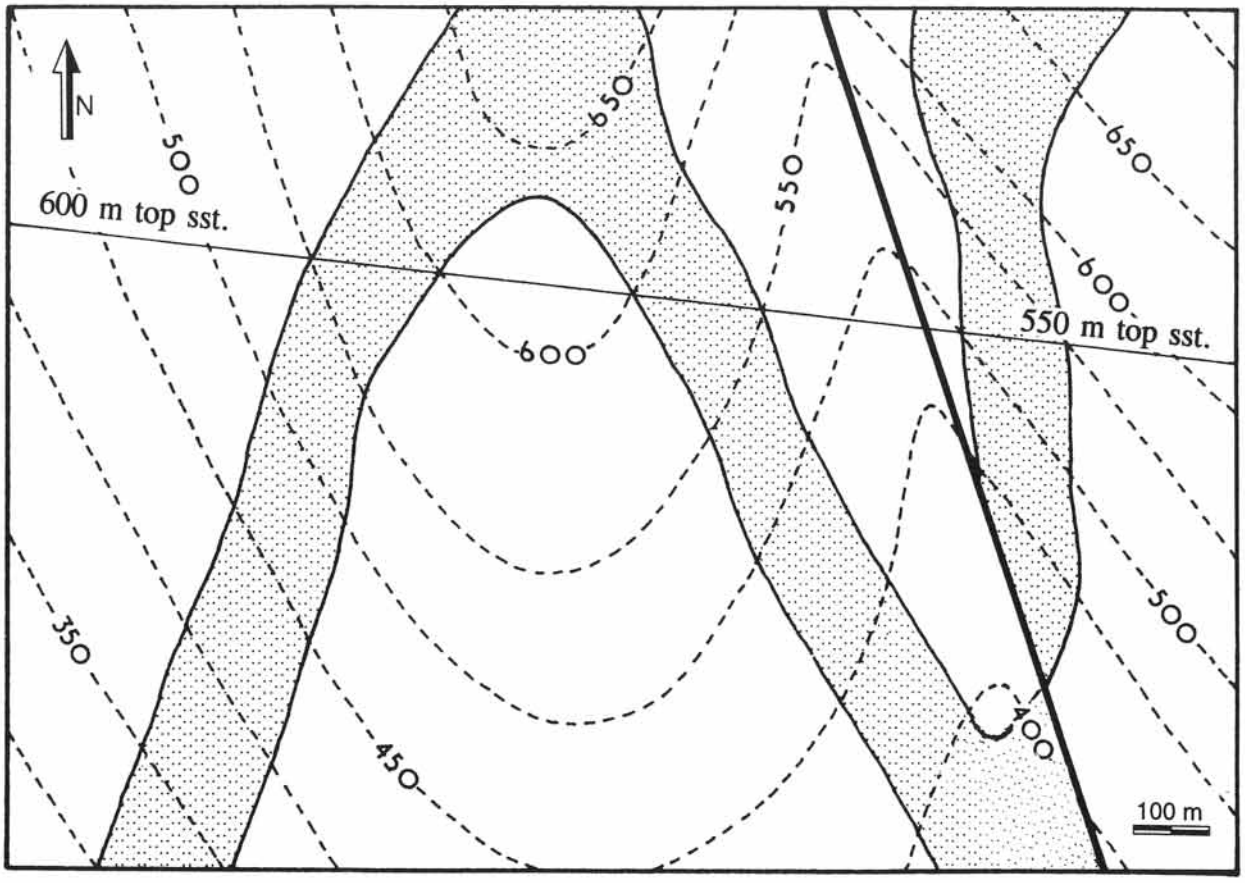

***Figure 11-25:** Outcrop pattern of faulted sandstone formation on topographic base map. See exercise 11-13.*

Chapter 12: Maps of Faulted Folds

THE MAP patterns of faulted planar strata have been outlined in chapter eleven, both for horizontal and for uniformly inclined beds. The map pattern of folded sequences may be quite complex, even in the absence of disruption by any faults, as previously discussed in chapters seven and eight. This chapter illustrates how the map pattern of folds may be further complicated by faulting. Any fault slip commonly causes displacement of fold closures in mappable units so that the effect can be seen on geological maps. The amount and direction of slip involved in such displacements can sometimes be reconstructed from the map pattern.

Contents: Map patterns of upright horizontal folds, disrupted by dip-slip faults, are discussed in section 12-1. The effect of faulting on the map appearance of upright, plunging folds is considered in section 12-2. Map patterns of strike-slip and oblique-slip faults are outlined in section 12-3. The use of displaced fold hinges in the assessment of oblique slip faults is explained in section 12-4. The analysis of faulted folds in terrains of rugged topography, which requires the use of structure contours, is addressed in section 12-5. Shear zones are introduced in section 12-6.

12-1 Dip-slip faulted, horizontal folds

Similar to the distinction made in section 11-4, dip-slip faults may be either parallel (longitudinal) or normal (transverse) to the strike of the folded strata. Transverse faults are discussed first, followed by a brief outline of faults longitudinal to the strike of the folded sequence.

Transverse, dip-slip faults

The sequence of block diagrams of Figures 12-1a to c illustrates the effect of transverse faulting on the map pattern of a synform with a vertical axial surface and a horizontal hinge line. After leveling of the ground surface by erosion, the exposure width of the rocks in the *synformal core*

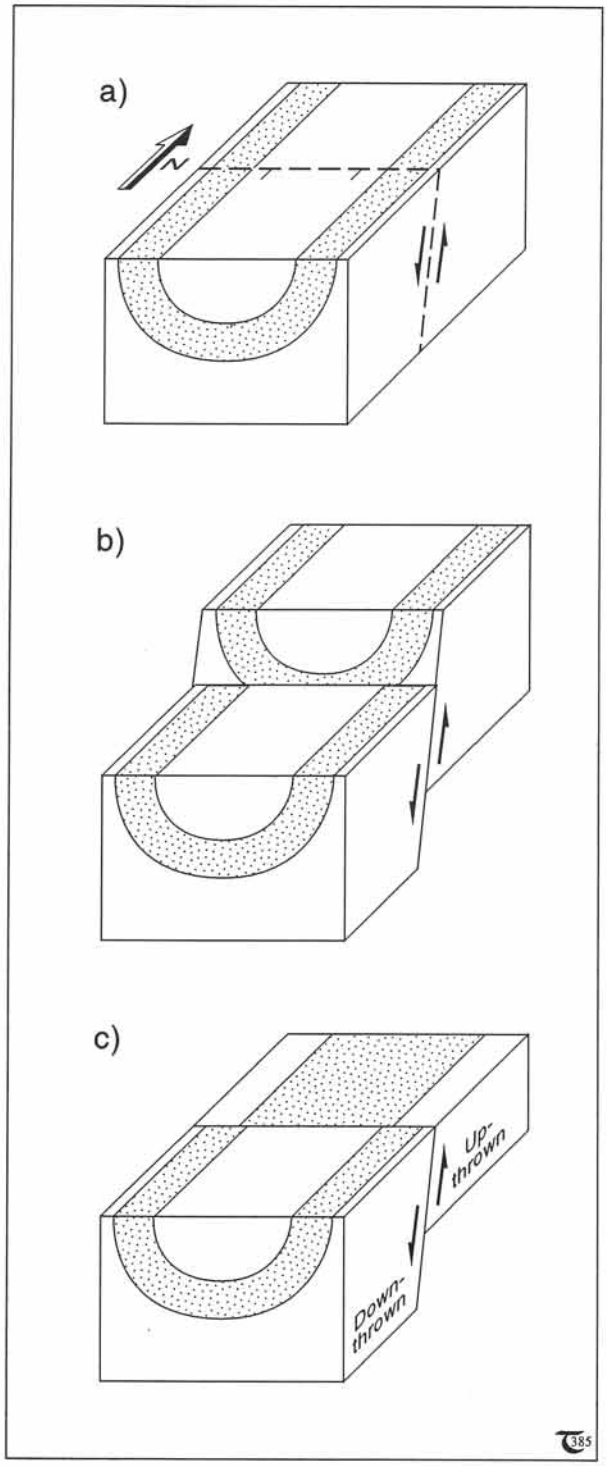

Figure 12-1: *a) to c) Three-stages of transverse, dip-slip faulting of an upright, horizontal synform: pre-faulting, post-faulting, and post-erosional.*

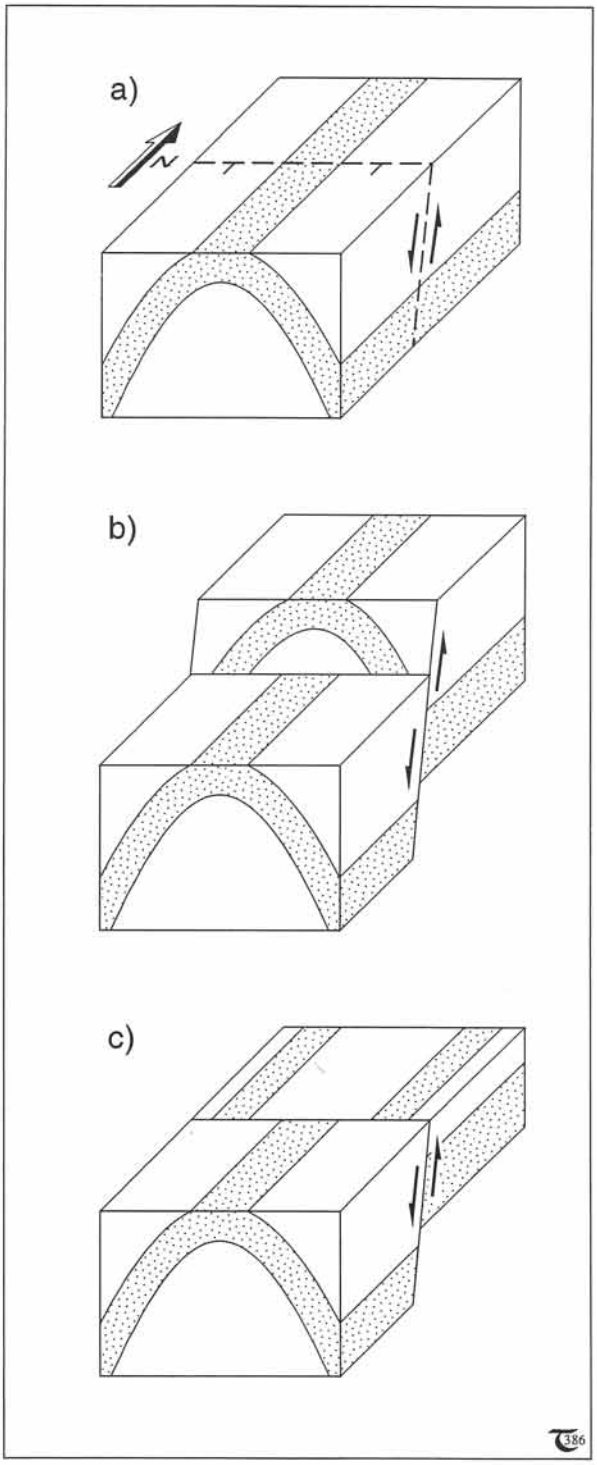

Figure 12-2: *a) to c) Three-stage perspective diagrams of upright, horizontal antiform, displaced by transverse, dip-slip fault.*

of the downthrown block is larger than that exposed on the surface of the upthrown block (Fig. 12-1c). Consequently, the change in width of the outcrop pattern of synformal fold closures across transverse faults reveals which of the two fault walls has been downthrown.

In the analysis of fold closures displaced by faults, it is important to establish first whether the affected closures are antiformal or synformal. Contrary to what is observed for dip-slip faulted synforms, the exposure width of rocks in the core of an *antiform is smaller in downthrown blocks* (as compared to the corresponding width on the surface of the eroded upthrown block) (Fig. 12-2a to c). The sequences portrayed in Figures 12-1 and 12-2 show the effect of steep, *normal*, transverse faulting upon the fold pattern. The effect of a steep, *reverse* fault would be similar. Downthrown blocks increase the stratigraphic section exposed in the core of faulted synforms, whether due to normal or reverse faulting. Conversely, in the case of faulted antiforms, it is always the upthrown blocks that expose the deeper layers in the fold core.

☐Exercise 12-1: Interpret the map pattern of Figure 12-3a. a) Indicate any axial plane traces, the upthrown and downthrown blocks, and any other discontinuities. b) Complete section A-B in Figure 12-3b. c) Discuss the geological history of the area.

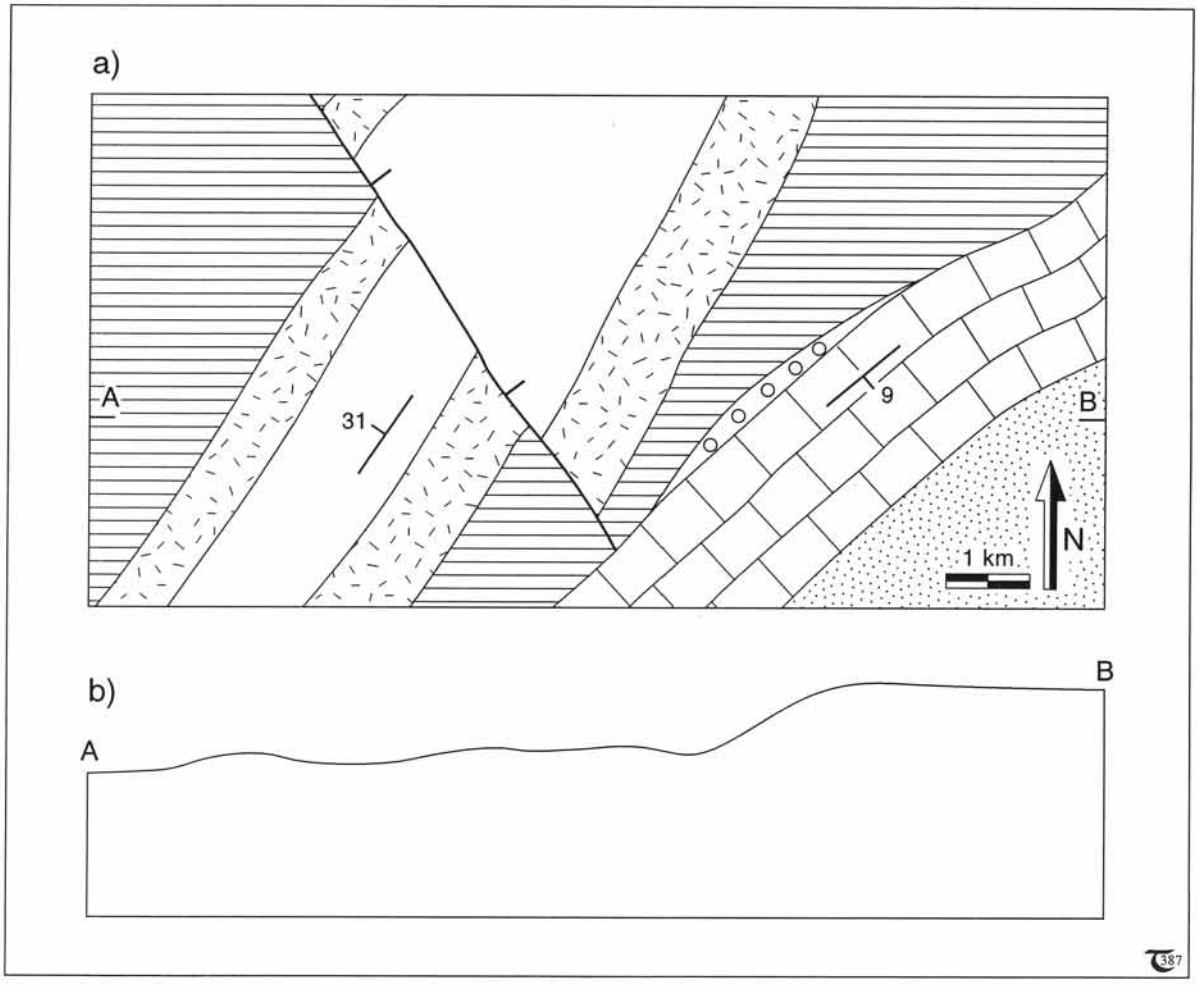

Figure 12-3: *a) & b) Geological map and cross section for exercise 12-1.*

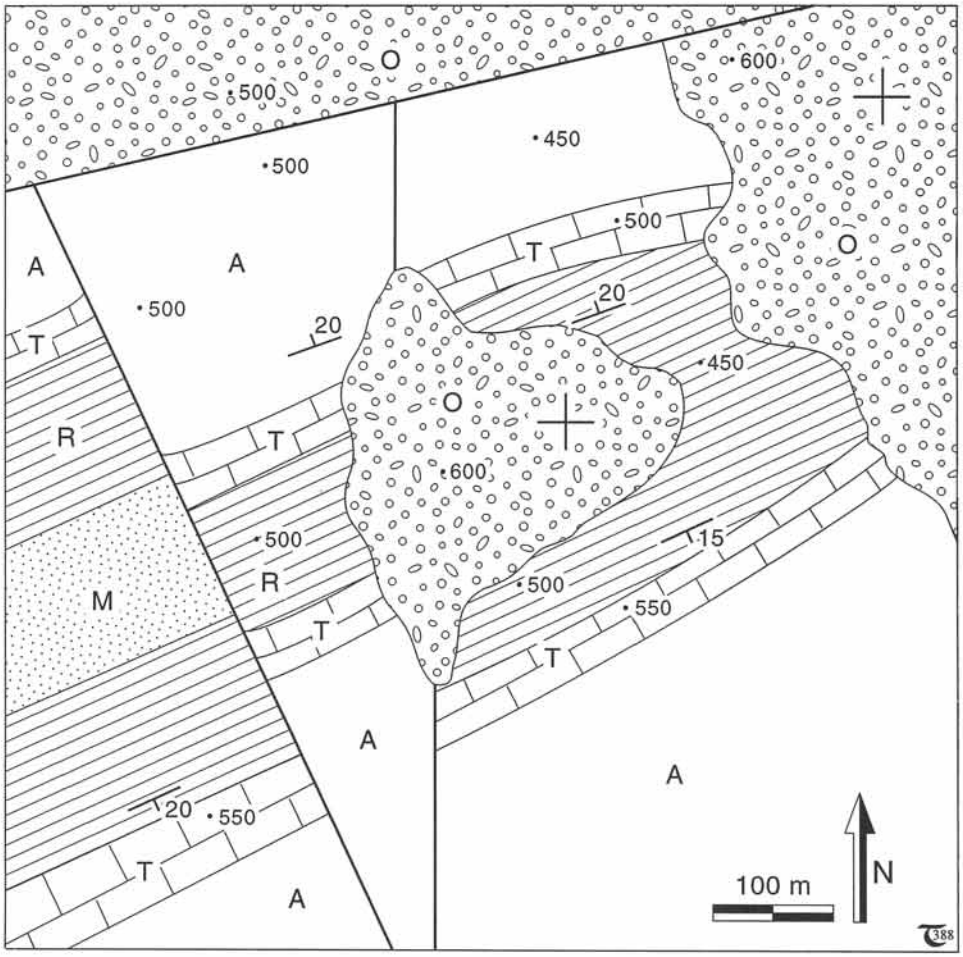

☐Exercise 12-2: The map of Figure 12-4 exposes normal faults. a) Use hachures to indicate the downthrown blocks. b) Rank the various lithological units (A, T, R, M, and O) from old to young. c) Discuss the geological history of the area. d) Where are the oldest rocks exposed? e) Assume hydrocarbons are trapped in the fold core. Mark the best drill location.

Figure 12-4: *Geological map for exercise 12-2. Elevations indicated are in meters.*

Longitudinal, dip-slip faults

The disruption of the map pattern of upright, horizontal *synforms* by longitudinal faulting is illustrated in Figure 12-5a to c. The effect of any longitudinal faulting, whether by normal or reverse dip-slip, is a *reduction of the stratigraphic section* in the core of synforms. The youngest rocks of the stratigraphic sequence will be found in the downthrown wall of the synform, near the fault trace (Fig. 12-5c).

Conversely, longitudinal dip-slip faulting of upright, horizontal *antiforms* results in an *increase of the stratigraphic section* near the fault trace (Fig. 12-6a to c). The oldest strata will be found in the upthrown wall of the antiform near the trace of the dip-slip fault (Fig. 12-6c). The sequences portrayed in Figures 12-1 and 12-2 show the effect of steep, *normal*, longitudinal faulting upon the map patterns of folds. The effect of a steep, *reverse* fault would be similar.

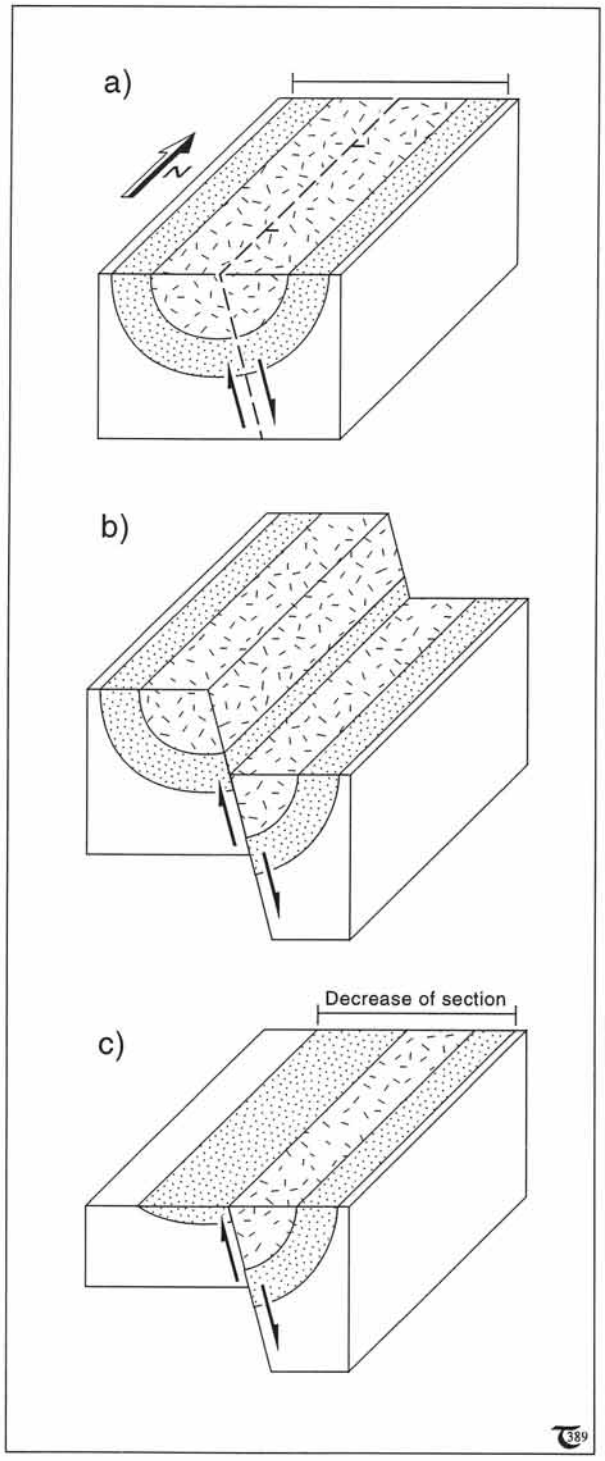

Figure 12-5: *a) to c) Three-stage perspective diagrams of upright, horizontal synform, displaced by longitudinal, dip-slip fault.*

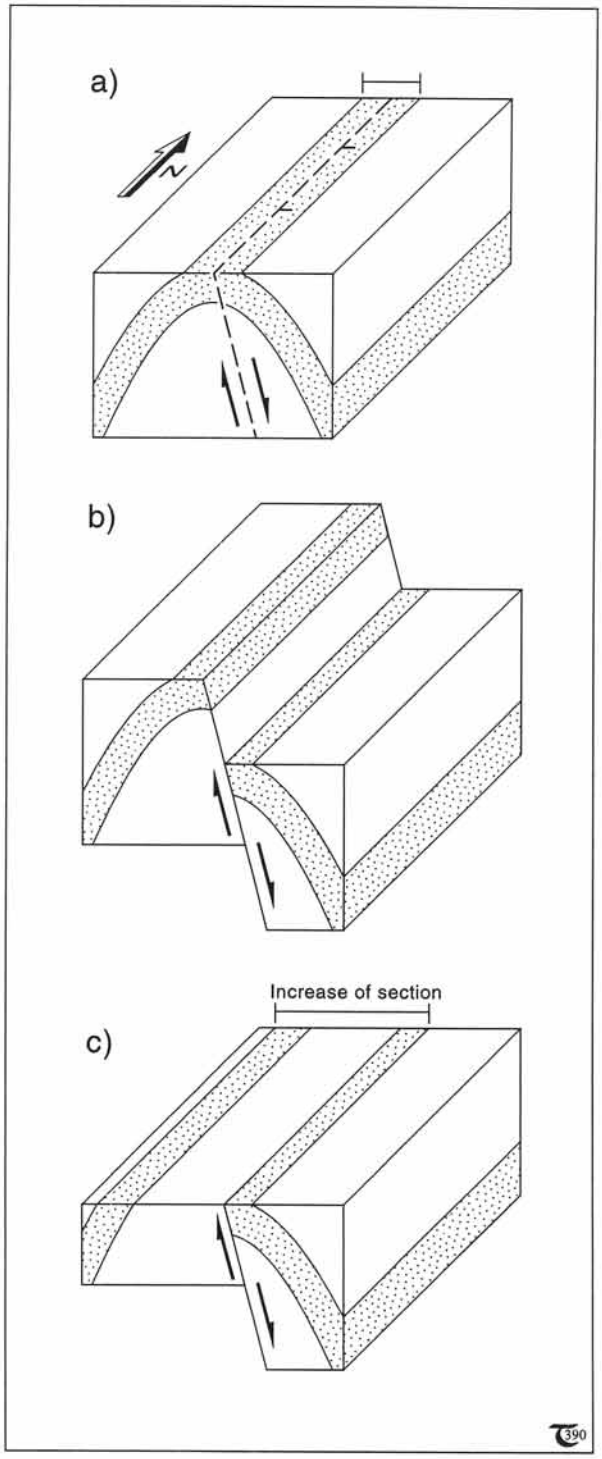

Figure 12-6: *a) to c) Three-stage perspective diagrams of upright, horizontal antiform, displaced by longitudinal, dip-slip fault.*

☐Exercise 12-3: Interpret the map pattern of Figure 12-7. a) Indicate any axial plane traces, the upthrown and downthrown blocks, and any other discontinuities. b) Complete cross-section A-B. The profile of the ground surface can be approximated using the elevation data indicated on the map. c) Discuss the geological history of the area.

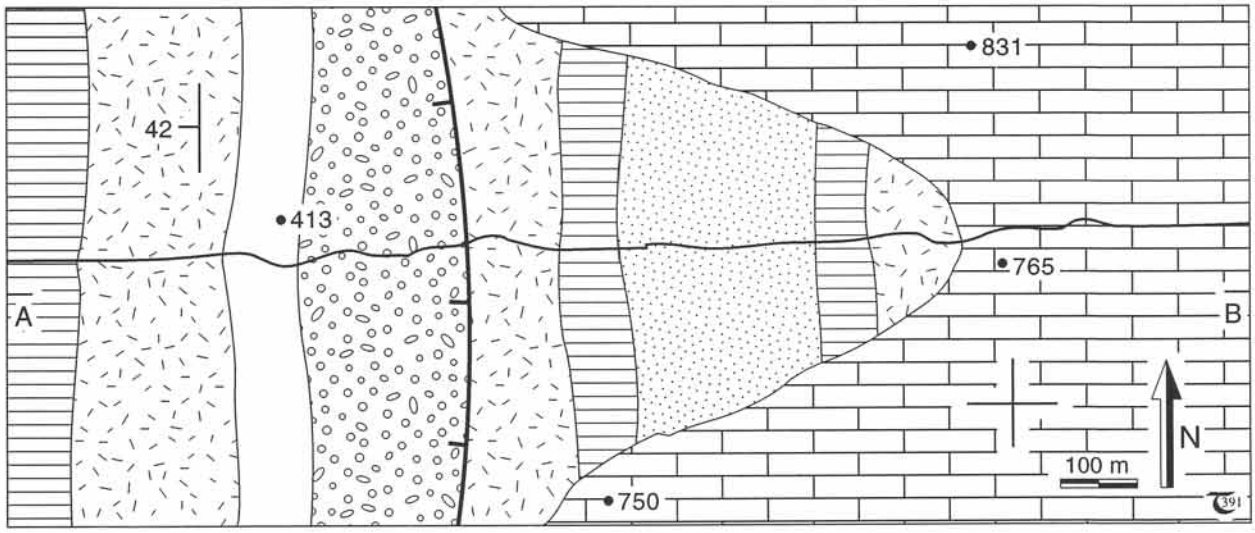

Figure 12-7: *Geological map for exercise 12-3. Elevations indicated are in meters.*

☐Exercise 12-4: The map of Figure 12-8 traverses a region of folded and faulted strata. The symmetry in the stratigraphic succession in the central part of the map indicates the presence of a synform. The location of two longitudinal faults is obvious from the omission and repetition of strata. a) Construct an east-west cross section along the southern margin of the map. b) What is the relative movement of the central block - upward or downward?

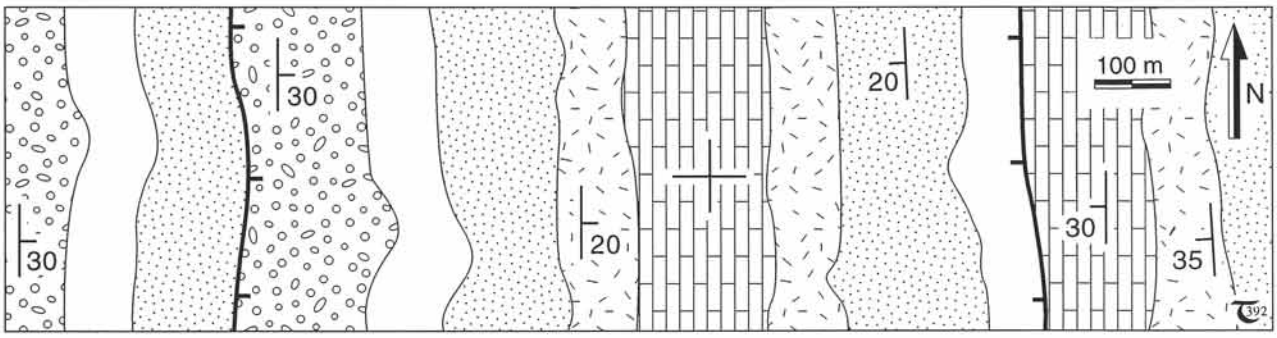

Figure 12-8: *Geological map for exercise 12-4. The ground surface is relatively flat.*

12-2 Dip-slip faulted, plunging folds

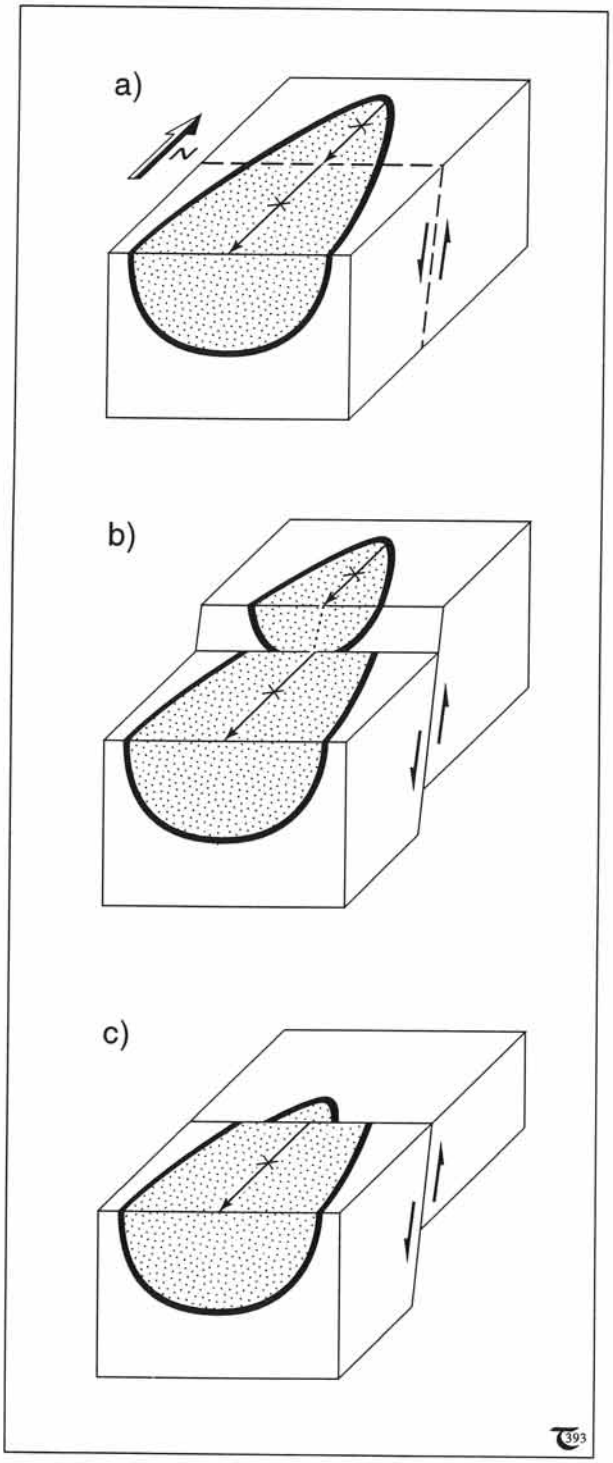

Figure 12-9: a) to c) Three-stage perspective diagrams of upright, plunging synform, displaced by transverse, dip-slip fault.

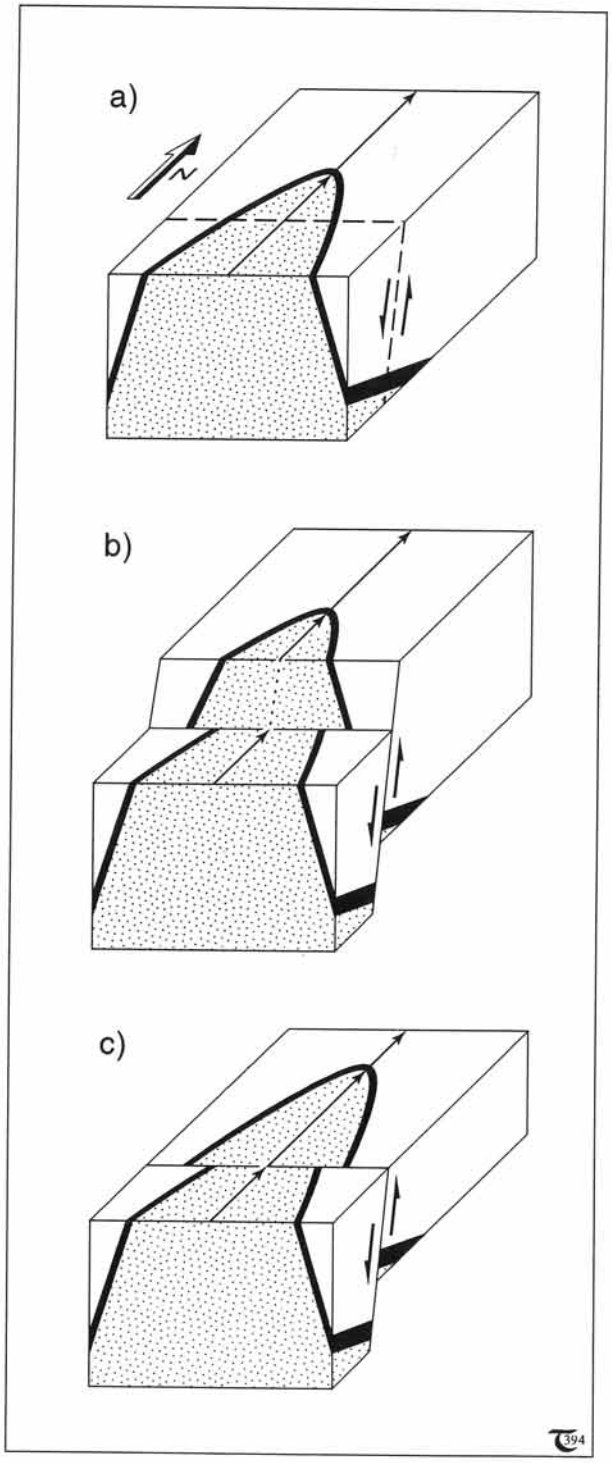

Figure 12-10: a) to c) Three-stage perspective diagrams of upright, plunging antiform, displaced by transverse, dip-slip fault.

Transverse faults

Fold closures of plunging synforms in mappable units tend to disappear in the upthrown block of transverse dip-slip faults (Fig. 12-9a to c). The effect is similar for normal and reverse faults. However, if the northern block in Figure 12-9a to c were to be downthrown instead of being upthrown, then repetition of the plunging synform-hinge occurs in the downthrown block, after leveling of the ground surface by erosion.

The fold hinge of plunging antiforms is repeated in the upthrown block of transverse, dip-slip faults (Fig. 12-10a to c). The effect is, again, similar for normal and reverse faults. But if the northern block of Figure 12-10a to c were to be downthrown instead of being upthrown, the antiformal closure would be omitted in the downthrown block, after leveling of the ground surface by erosion (not illustrated).

☐Exercise 12-5: a) Determine whether the NW-block of the map in Figure 12-11 is upthrown or downthrown. b) Complete section A-B. Fault dip is unknown; assume the fault to be subvertical.

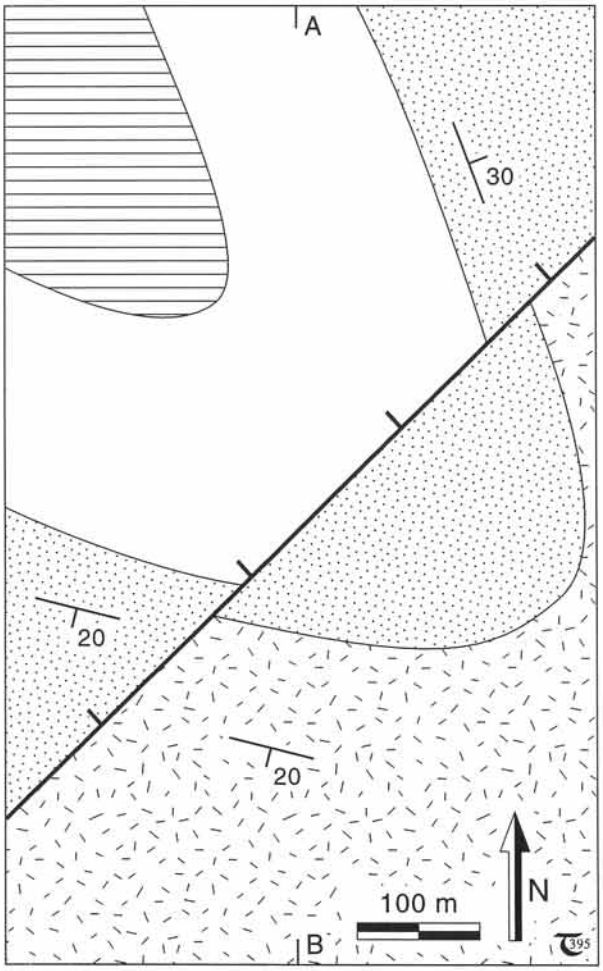

Figure 12-11: *Geological map for exercise 12-5. Assume the area is a flat terrain.*

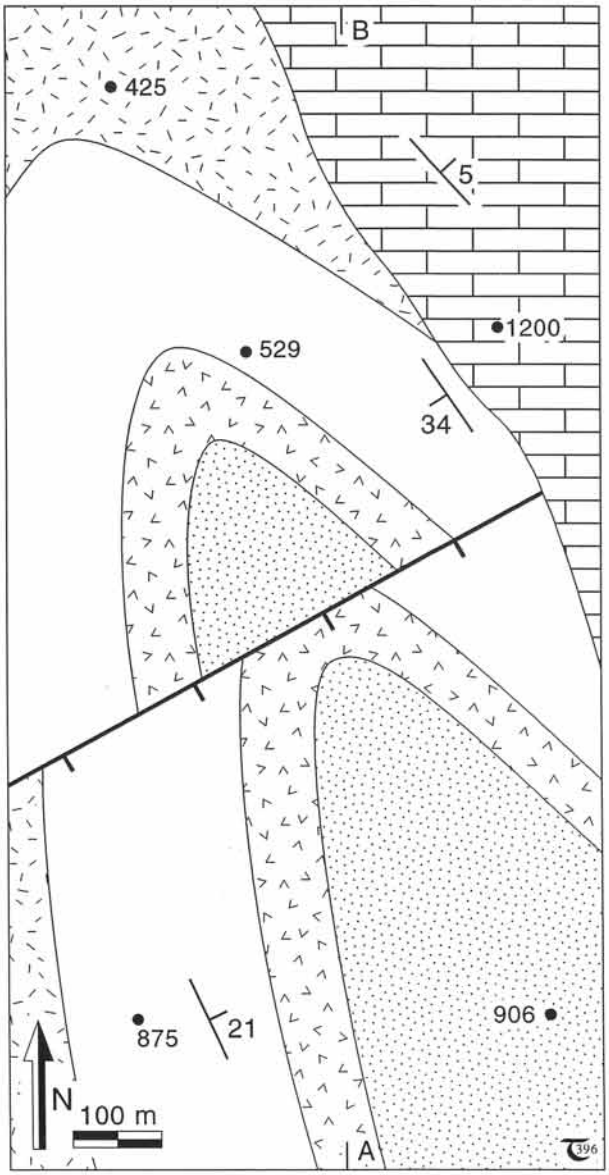

Figure 12-12: *Geological map for exercise 12-6. Local elevations are in meters.*

☐Exercise 12-6: Interpret the map pattern of Figure 12-12. a) Indicate any axial plane traces, antiform and synform symbols, the direction of the fold plunge, the upthrown and downthrown blocks, and any other discontinuities. b) Complete section A-B; assume that the map area is that of a flat terrain. c) Discuss the geological history of the area.

☐Exercise 12-7: The map pattern of Figure 12-13 shows plunging folds in a flat area, cut by transverse, dip-slip faults. a) Indicate any axial plane traces, antiform and synform symbols, the direction of the fold plunge, and the upthrown and downthrown blocks. b) Complete section A-B. c) Discuss the geological history of the area.

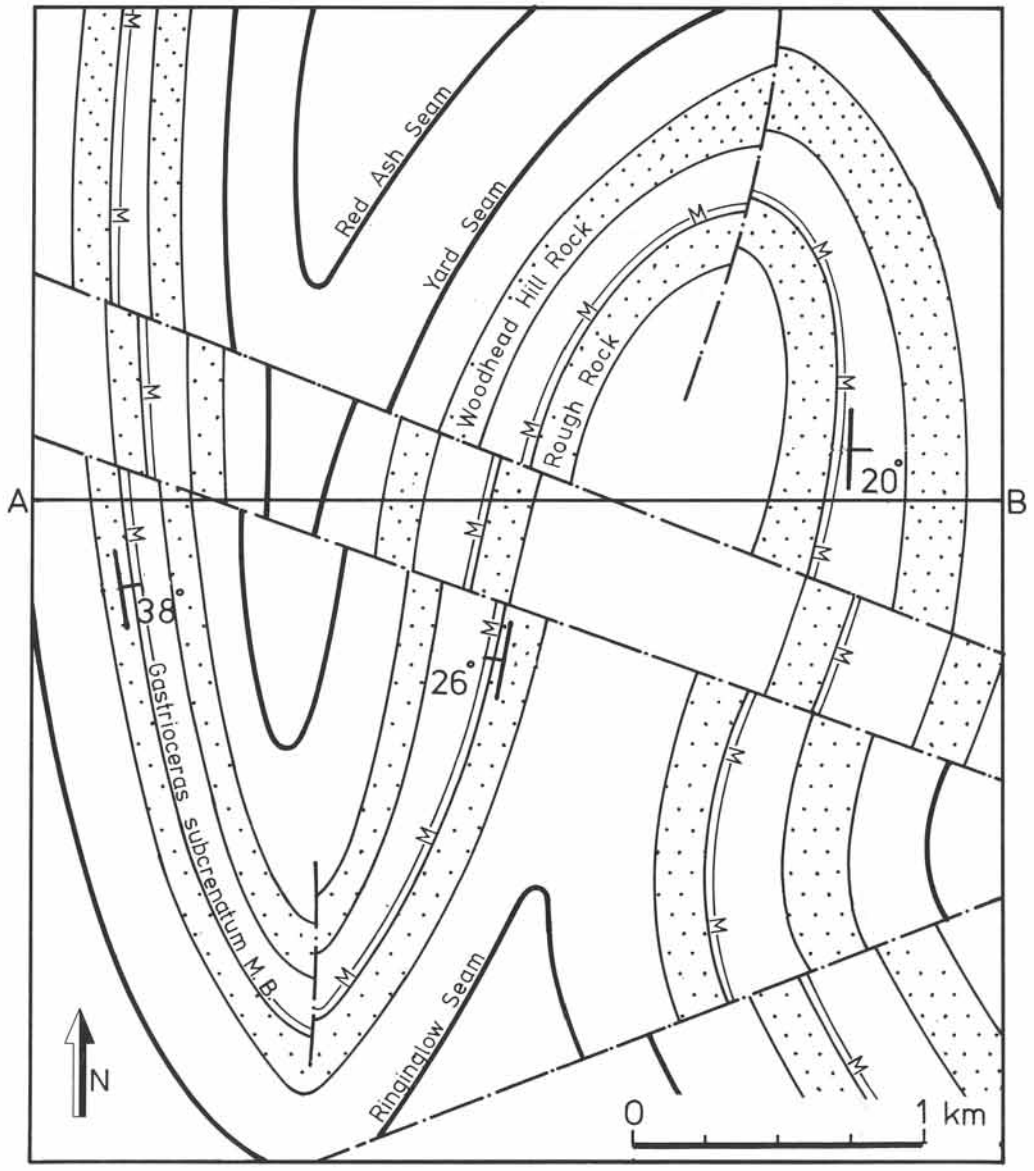

Figure 12-13: Geological map for exercise 12-7.

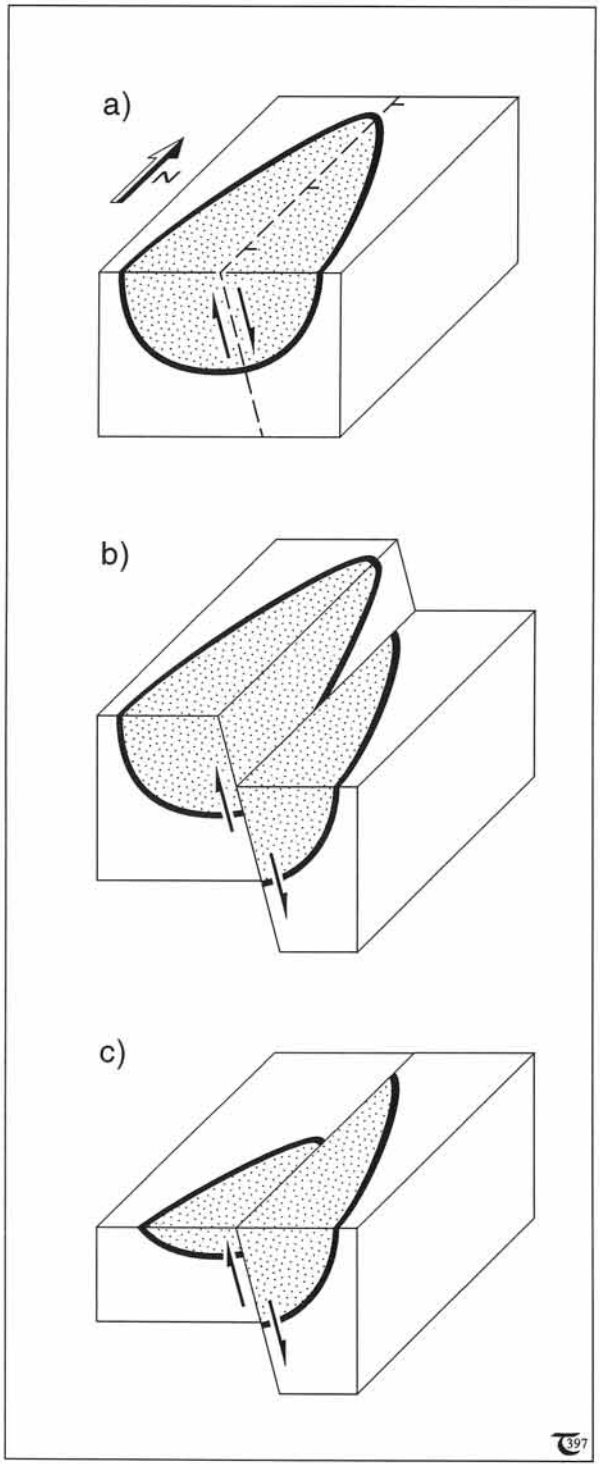

Figure 12-14: *a) to c) Three-stage perspective diagrams of upright, plunging synform, displaced by longitudinal, dip-slip fault.*

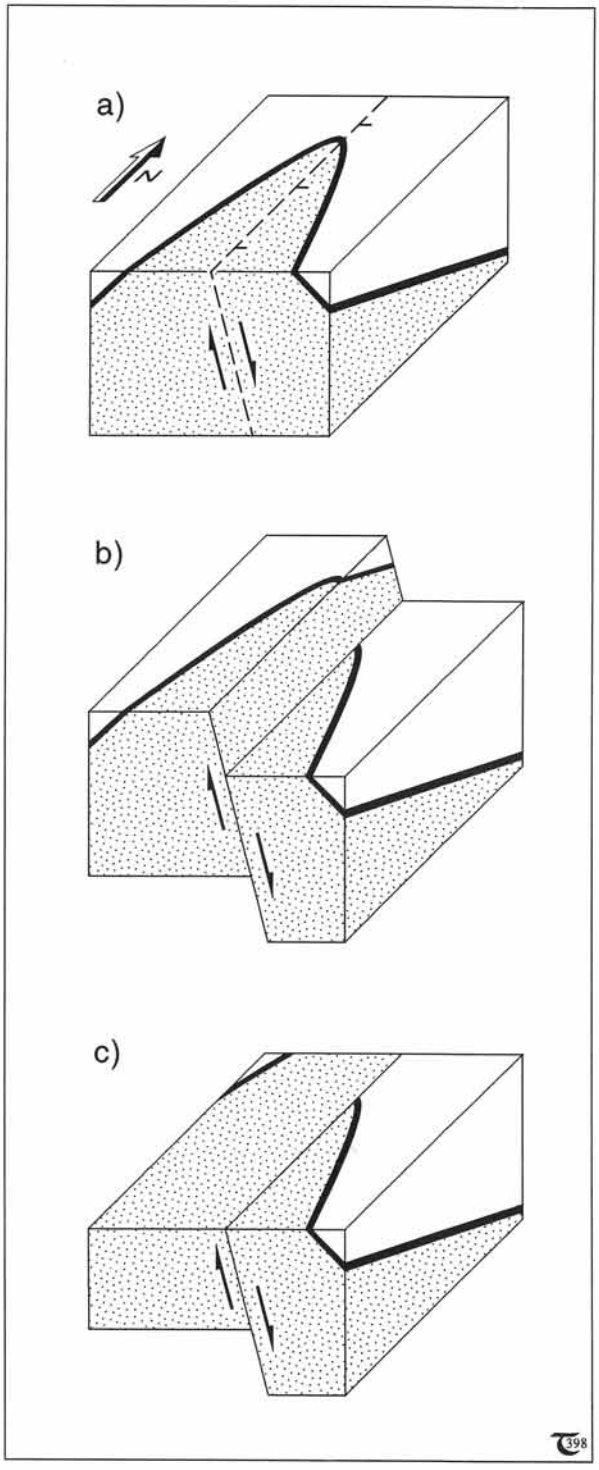

Figure 12-15: *a) to c) Three-stage perspective diagrams of upright, plunging antiform, displaced by longitudinal, dip-slip fault.*

Longitudinal faults

The map pattern of plunging fold closures, disrupted by longitudinal, dip-slip faults, typically display strike separation of the fold hinge (Figs. 12-14 and 12-15). This strike separation may easily be (mis)interpreted as a result of strike-slip movement, but such slip is not necessarily required to explain the map pattern.

The map pattern of Figure 12-16a shows a doubly plunging synform, displaced by longitudinal normal faults. The outcrop pattern of the southern limb of the synform is repeated three times in the map pattern, due to the normal faulting. In order to understand this map better, solve excercise 12-8.

□Exercise 12-8: Study the map pattern of Figure 12-16a. a) Indicate any axial plane traces, antiform and synform symbols, the direction of the fold plunge, and the upthrown and downthrown blocks. b) Complete section A-B given in Figure 12-16b. c) Discuss the geological history of the area.

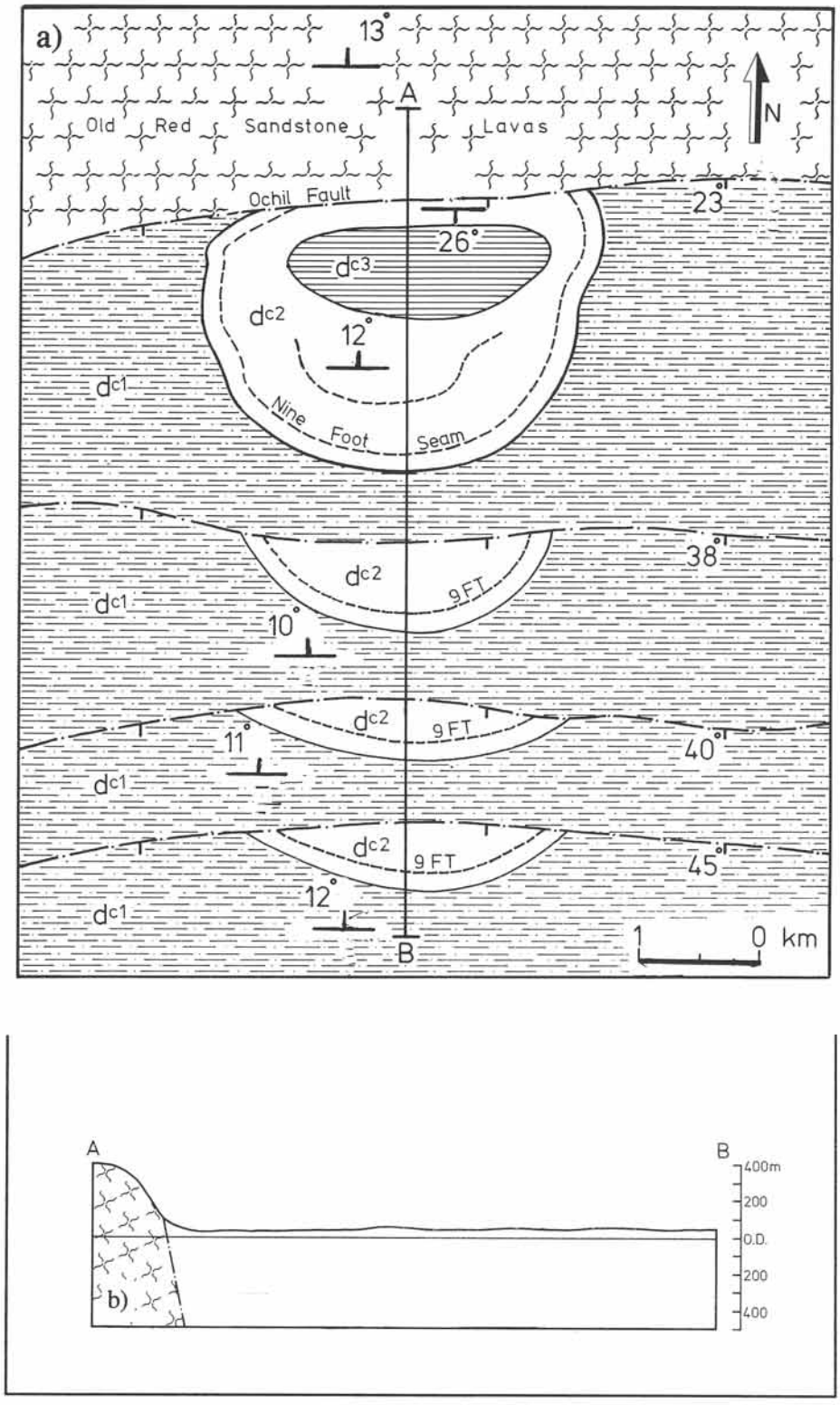

Figure 12-16: a) & b) Geological map and cross-section for exercise 12-8.

12-3 Strike-slip faults

So far, our attention has been focussed on the disruption of fold patterns by dip-slip faults. Strike-slip faults that are longitudinal to plunging folds result in map patterns similar to those illustrated in Figures 12-14c and 12-15c. Without detailed field observations (not explained here), the respective map patterns of fold hinges longitudinally faulted by dip-slip faults and strike-slip faults cannot be distinguished.

Generally, the interpretation of transverse faults is less ambiguous than that of longitudinal faults. Transverse, *strike-slip* faults cause lateral transfer of outcrop patterns and displace the fold-limbs and the trace of the axial plane, all with the same amount of strike separation (Fig. 12-17a & b). This is in contrast to the disruption by dip-slip faulting, which displaces the outcrop pattern of the fold limbs in opposite directions without any strike separation of the axial plane trace (Fig. 12-17c & d). This assumes the faulted folds are upright. Some displacement of the axial plane trace would occur in inclined folds, if cut by transverse, dip-slip faults.

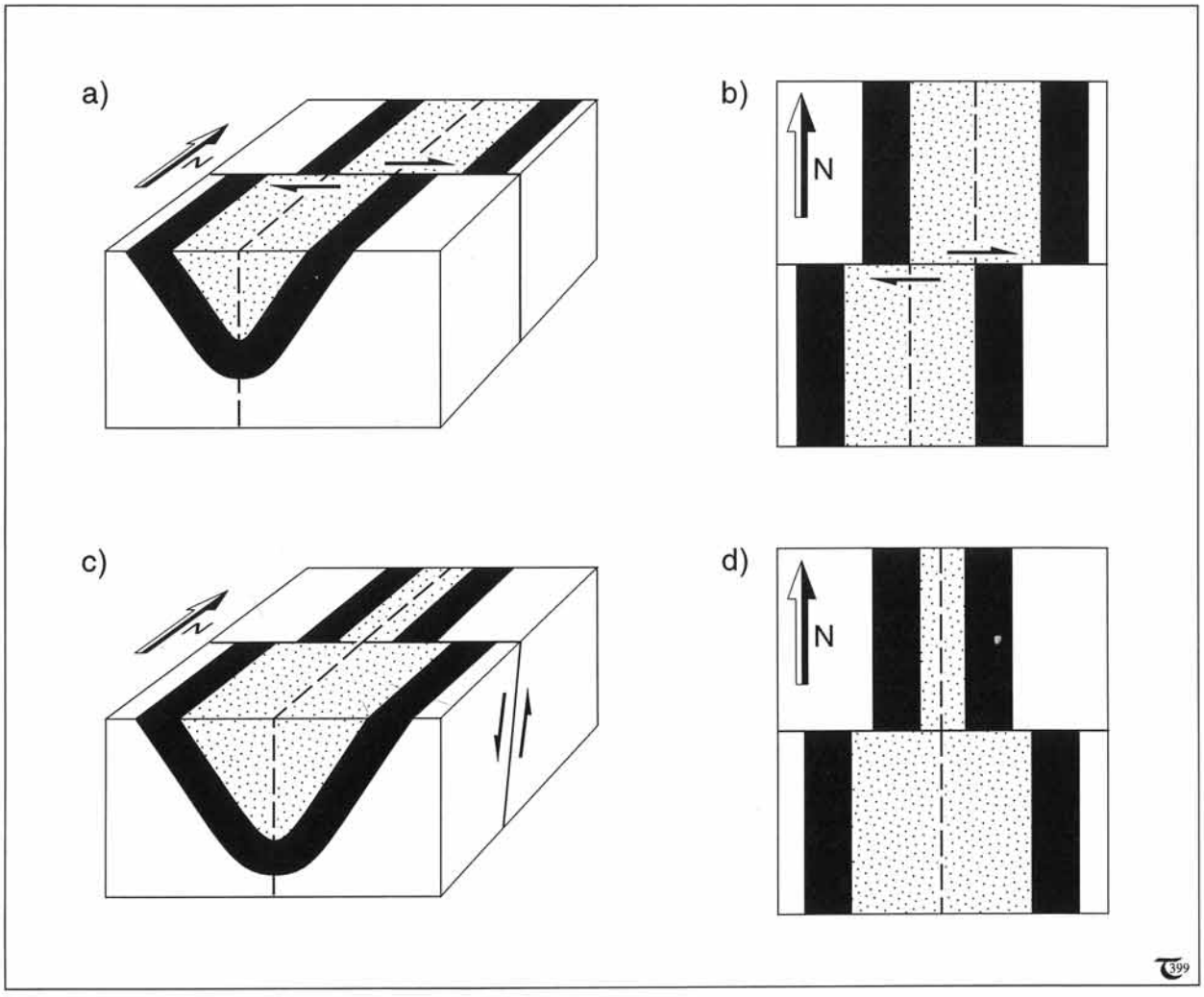

Figure 12-17: *a) to d) Perspective diagrams and map views of right-lateral, strike-slip fault (a & b) and steep, dip-slip fault (c & d).*

12-4 Oblique-slip faults

Faulted folds are particularly interesting when it comes to interpreting strike separations resulting from oblique fault slip. Faulted folds provide one of the few easily recognized linear features (fold closures in specific stratigraphic units) available in geology. Thus, one can sometimes determine the actual fault slip from the displacement of a fold hinge line (Fig. 12-18). The actual slip can be determined using structure contours, provided the dip of the fold limbs is everywhere known. The basic concept of structure contours for solving map problems involving undisrupted, folded layers, has been outlined in chapter eight.

The map pattern of Figure 12-19 illustrates a faulted, upright, horizontal fold. The strike separations seen in this map cannot be explained by either dip-slip or strike-slip alone. The map pattern must be the result of oblique slip and, thus, includes the combined effects of dip-slip and strike-slip displacement (see exercise 12-10).

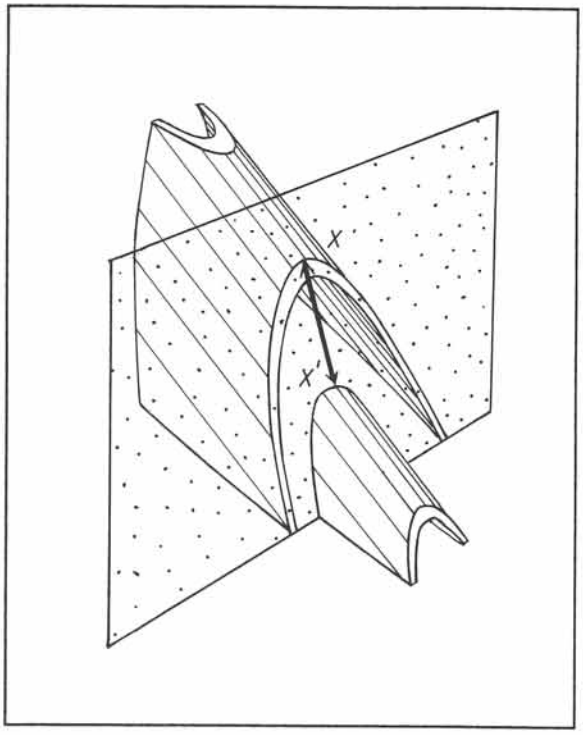

Figure 12-18: *Faulted, upright, plunging antiform. The orientation of the oblique slip vector and the amount of slip can be determined from the displaced hinge line of the fold.*

☐Exercise 12-9: The details of the map pattern in Figure 12-19 can be interpreted in two different ways, depending upon whether the displaced fold is an antiform or synform. Consider each of the two possibilities, and indicate whether the southern block was downthrown or upthrown.

☐Exercise 12-10: Assume that the fold cut in Figure 12-19 is a chevron type synform with both limbs dipping at 45°. Use structure contours to establish the amount of net slip on the fault plane, which itself is subvertical.

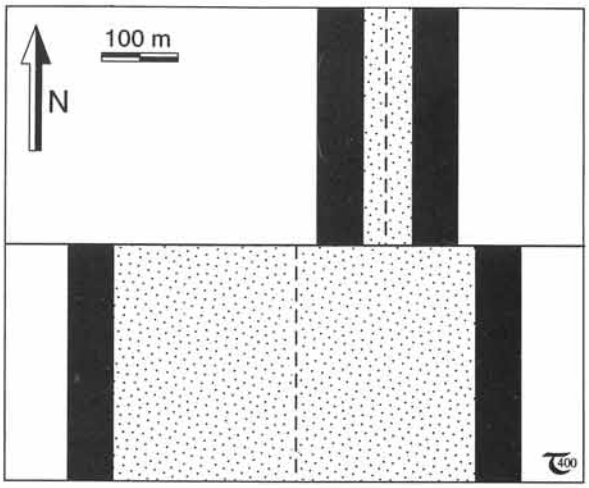

Figure 12-19: *Map pattern for exercises 12-9 and 12-10.*

☐Exercise 12-11: Interpret the displacements seen in the maps of Figures 12-20a and b.

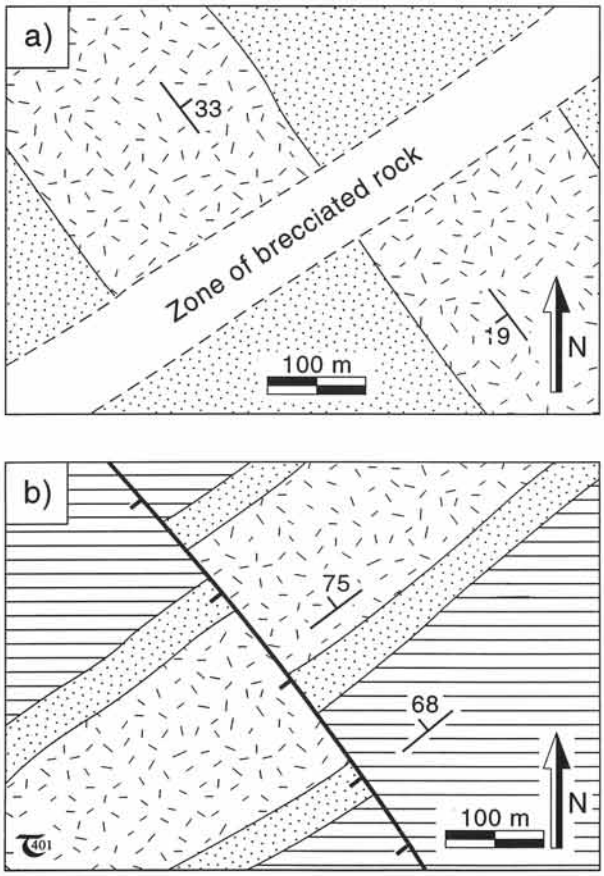

Figure 12-20: *a) & b) Geological maps for exercise 12-11.*

12-5 Faulted folds in topographic relief

The above discussion considered the effect of fault dislocations upon the outcrop patterns of folds. The ground surface was assumed to be completely leveled by erosion. This kept the analysis relatively simple, because the outcrop pattern was not distorted by any topographic relief. When interpreting map patterns of terrains with rugged topography, one needs to take into account the visual distortion of the map pattern caused by the irregular incision of the terrain. Figure 12-21 shows an example of a detailed geological map that includes topographic contours. The true trend of the fold limbs and the fault planes in such terrains can be obtained, making use of structure contours (exercise 12-12).

12-6 Shear zones

The disruption and displacement of rock units may occur along a narrow, discrete surface of failure (Fig. 12-22a). This type of localized deformation commonly occurs when faults are formed at shallow depths, where the rock cannot deform by ductile distortion. However, in deeply eroded rocks, uplifted in orogenic belts and cratons, a much more diffuse type of localized distortion is encountered, termed *shear zones*, resembling the geometry illustrated in Figure 11-22b. If a shear zone involves ductile deformation only, the displaced reference beds are distorted

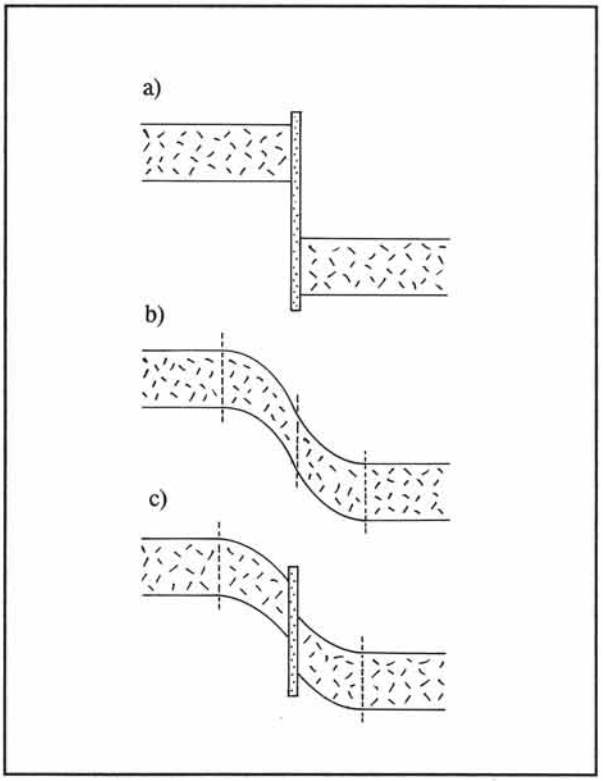

Figure 12-22: *a) to c) Various types of localized deformations: (a) brittle fault, (b) ductile shear zone, and (c) brittle-ductile shear zone.*

☐Exercise 12-12: Examine the map pattern of Figure 12-21. A N-S striking fault divides the map into an east and a west part. a) First concentrate on the fault plane itself; construct structure contours to determine the azimuth and dip of that fault plane. b) Continue your analysis by constructing structure contours for the sandstone layer in the hanging wall; determine the azimuth and dip of the layer. c) Next, concentrate on the outcrop pattern of the sandstone layer in the foot wall; construct stratum contours, and determine the orientation of the fold hinge line (plunge/trend). d) Determine the orientation of the fold limbs (azimuth/dip). e) Construct an E-W section along line A-B across the map. f) With the understanding of the map pattern thus derived, it is possible to establish whether the fault is a reverse or a normal fault.

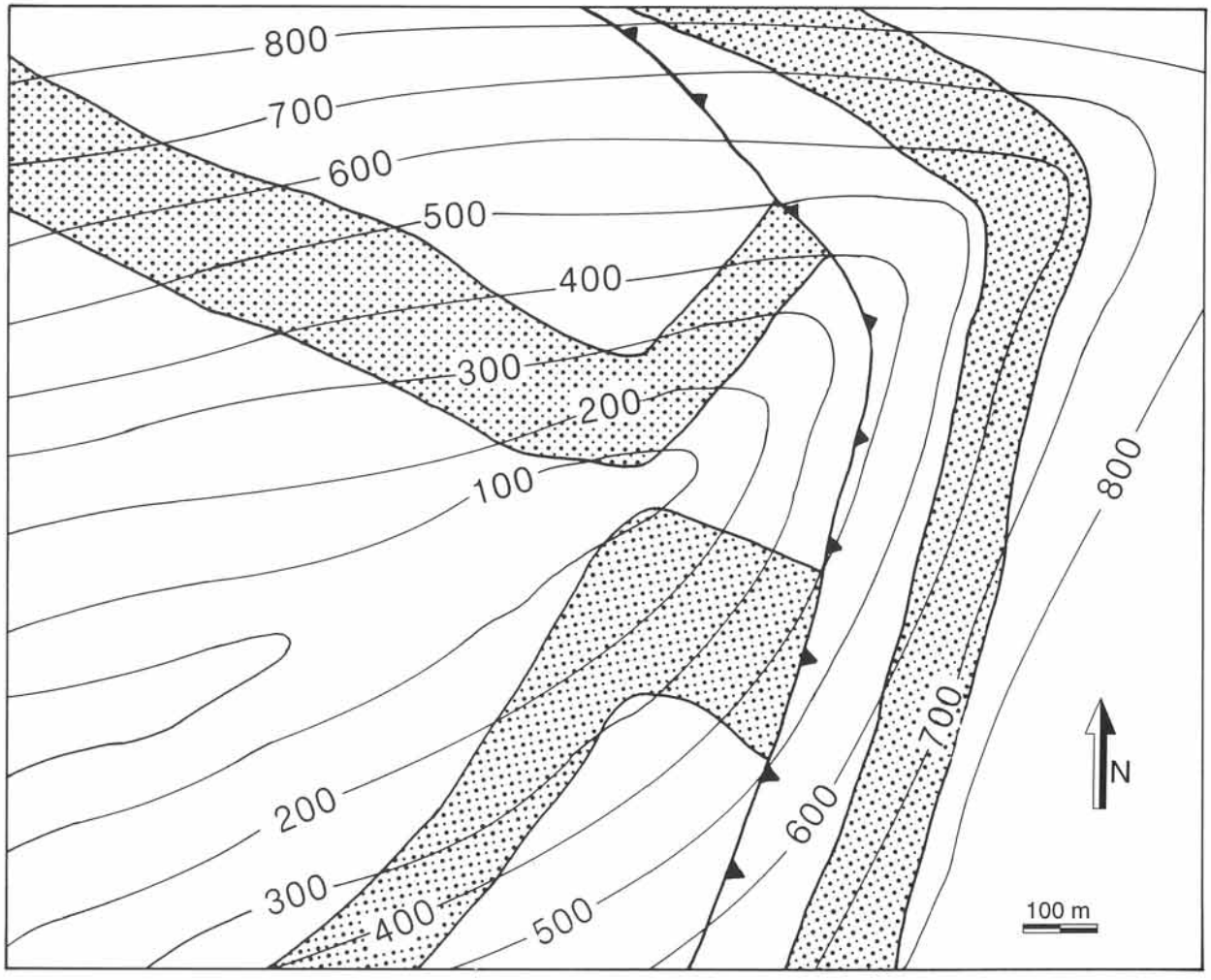

Figure 12-21: *Outcrop pattern of a faulted sandstone formation on a topographic base map. See exercise 12-12.*

by the shear but remain continuous (Fig. 12-22b). But some shear zones involve a discrete disruption surface and, therefore, are termed brittle-ductile shear zones (Fig. 12-22c).

Figure 12-23 illustrates the map pattern of the Palomares shear zone, southeast Spain. A strike-slip fault, in the central part of this brittle-ductile shear zone, displaces the Alhamilla anticline left-laterally. The horizontal strike-slip on the central fault amounts to some 50 kilometers. The proper interpretation of shear zones requires detailed ground studies and good understanding of techniques of strain analysis, beyond the scope of basic map interpretation methods outlined here. These techniques are treated elsewhere (see, for example, the companion textbook, *Principles of Rock Mechanics*).

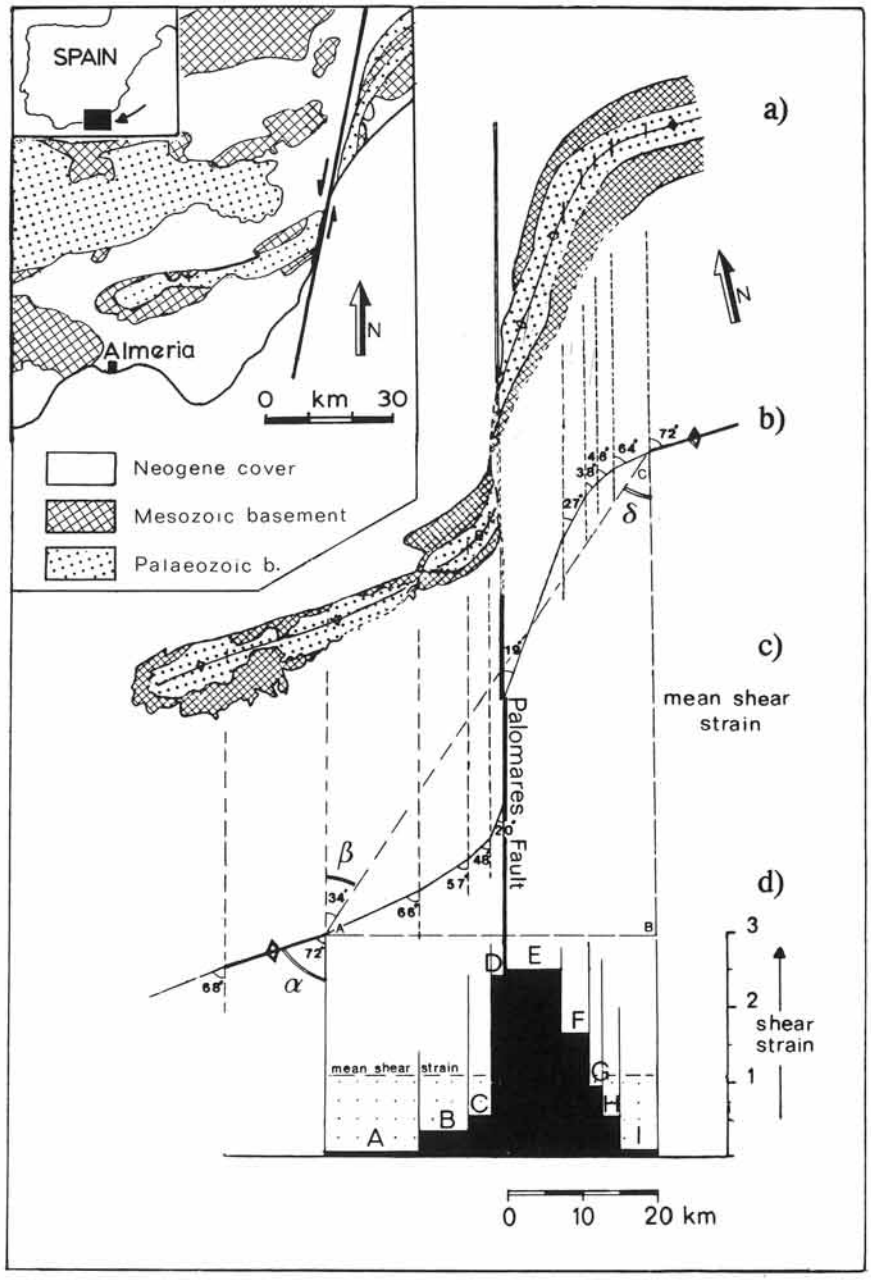

Figure 12-23: *Palomares brittle-ductile shear zone. a) Outcrop pattern of the deflected and disrupted Alhamilla anticline. b) Angular deflection of the fold axis. c) Mean shear strain across the shear zone. d) Strain-distance histogram across the Palomares shear zone.*

Chapter 13: Maps of Intrusive Igneous Structures

IGNEOUS INTRUSIONS may have a large variety of shapes and sizes. They occur principally at plate boundaries and follow fracture zones or force aside the country rock in diffuse shearing. Eventually, igneous intrusions may crop out at the ground surface after removal of the overlying rock units by erosion. This chapter illustrates some of the principal features seen on geological maps of igneous terrains. The tectonic setting and various processes involved in the generation and emplacement of igneous intrusions are, also, briefly explained.

Contents: The geological setting of igneous rocks is outlined in section 13-1. Their various shapes are illustrated in section 13-2. Zoned plutons, nested plutons, and mantled gneiss-domes are addressed in sections 13-3 and 13-4.

13-1 Geological setting of igneous rocks

Igneous rocks originate from magma, produced by partial melting at depth. Most of the partial melting sites occur beneath modern, evolving plate boundaries and are associated with anomalies of pressure, temperature, and water-content in the crust and mantle. The solidifying melt is emplaced within the crust either along fracture zones or by forcing aside the country rock in diffuse shearing. Magmatism is particularly abundant in mature rift zones, along active continental margins, and at subduction island arcs. Each of these magmatic sites is briefly outlined in turn below.

Continental and oceanic rift zones

The extensional thinning and incipient failure of continental crust by rifting are commonly accompanied by the intrusion of large tabular or sheet-like bodies into fractures. These bodies, termed igneous dikes, are predominantly of basic, rather than acidic, composition. The Great Dyke of Zimbabwe, Africa, has long been considered the world's largest single dike feature. This gabbroic body is about 480 kilometers long with an average width of six kilometers (Fig. 13-1a). However, detailed field investigations have revealed that the Great Dyke is comprised of

horizontal cumulus layers (Fig. 13-1b), intruded into the Archean greenstone-granodiorite terrane of the Zimbabwe craton about 2.5 billion years ago. The horizontal gabbro sheets were fed by steep dikes, much thinner than the six-kilometer-width seen on Figure 13-1a. The walls of the Great Dyke are merely faulted contacts of a central graben, formed posterior to the emplacement of the gabbro. The Zimbabwe craton, also, hosts the nested *plutons*, discussed in section 13-4.

Indeed, rather than emplacing a huge volume of igneous rock into one single fissure, *swarms* of subparallel, smaller dikes are more common in many parts of the world with formerly rifted, continental crust. The early Tertiary basic dike swarm of the British Isles is a good example of failed rifting (Fig. 13-2). The rifting ceased in an early stage, but, if the rifting continues, the continental crust may fail altogether and separate to give way to newly formed oceanic crust (Fig. 13-3). The ocean floor is composed of gabbro intrusions, overlain by basalt flows.

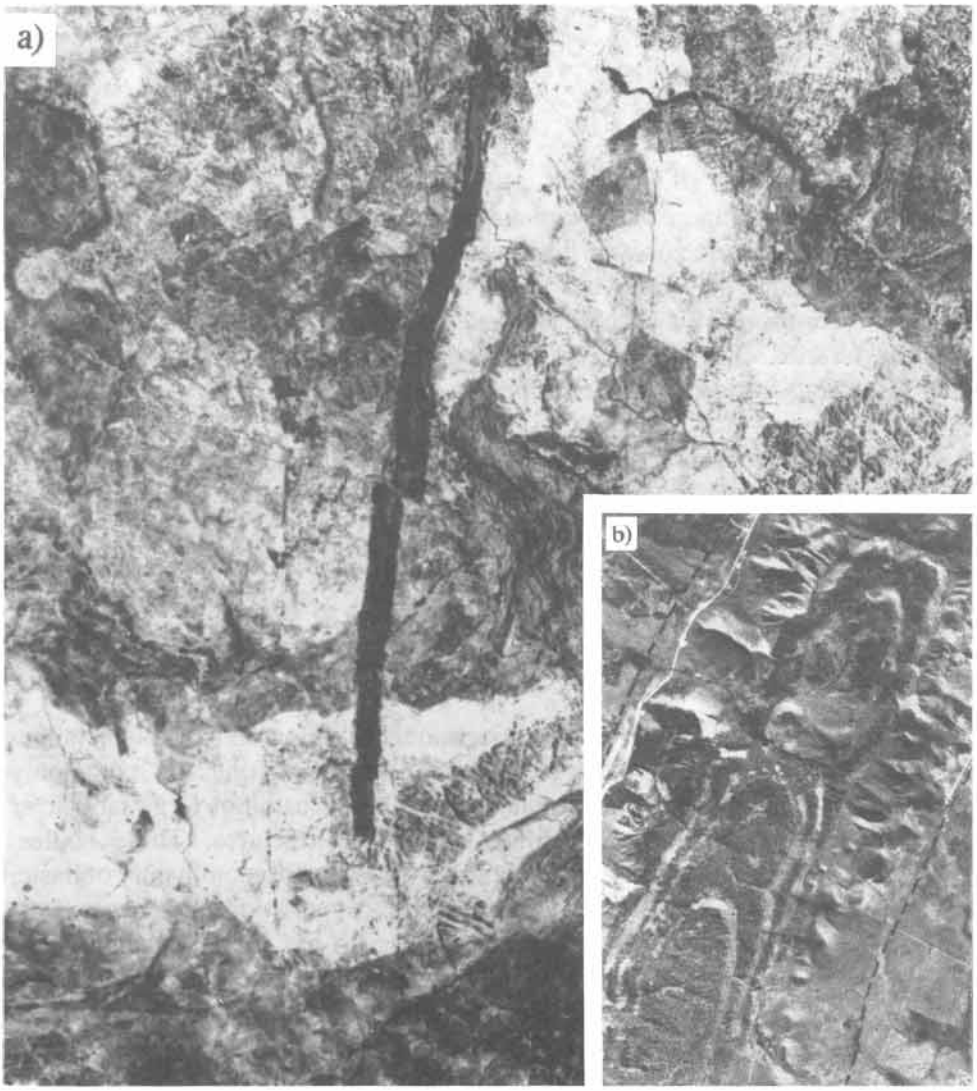

Figure 13-1: *a) Landsat image of six-kilometer-wide graben, containing the Great Dyke, Zimbabwe. b) Aerial photo, revealing erosion-pattern of horizontal cumulus layers now trapped in the central graben.*

Much of the ocean floor's internal structure remains inaccessible, because the oceanic lithosphere is normally subducted back into the mantle when colliding with another plate. But, occasionally, segments of the subducting oceanic plate may be flexured or may become less dense so that they are *obducted* or thrust onto the continental margin. Consequently, the structure and composition of the oceanic crust, generalized in Figure 13-3, can be studied in detail in such obducted *ophiolites*, which crop out along many major collision sutures (e.g., in Oman). It is important to remember, however, that the oceanic crust preserved in ophiolite complexes was ini-

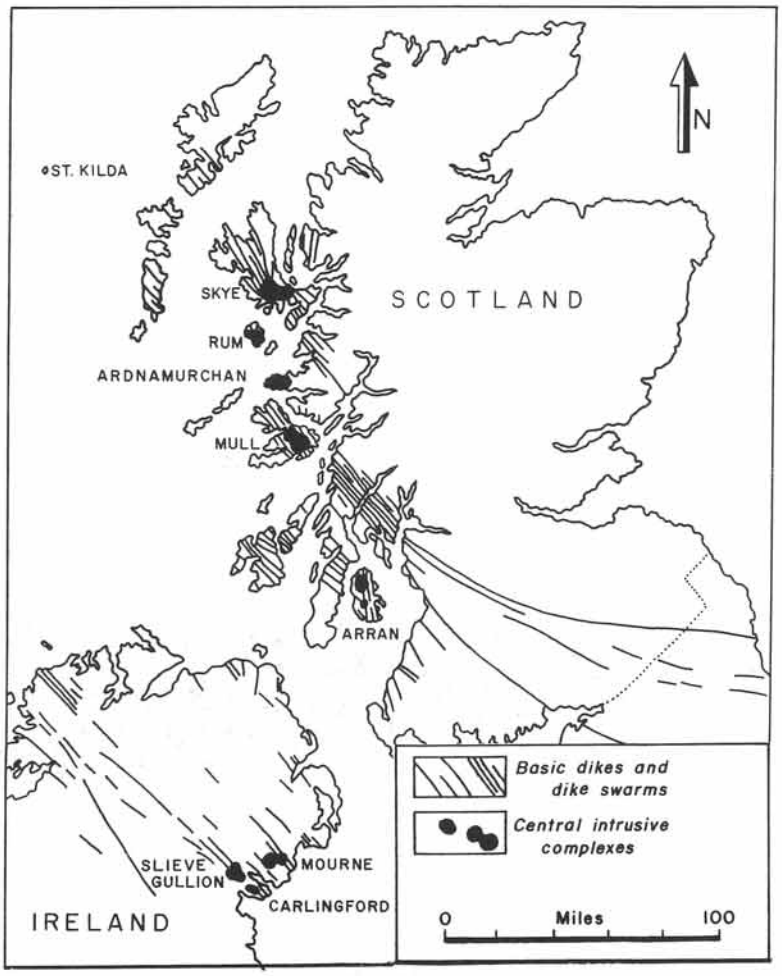

Figure 13-2: *NW-SE trending Tertiary basic dike swarm and central intrusive complexes of the British Isles and northern Ireland (Skye, Rum, Ardnamurchan, Mull, Arran, Mourne, Slieve, Gullion, and Carlingford).*

tially formed by rifting and spreading, rather than by the shortening involved in its emplacement onto the continental crust.

Iceland, perhaps, is one of the most unique locations for unravelling the internal structure and active growth of oceanic crust. It is located on the mid-Atlantic spreading ridge and is entirely made of modern oceanic crust. Figure 13-4 illustrates fresh 1988 lava and normal faults in the central rift zone near the Krafla field of Iceland. The time-averaged spreading rate across the rift zone is about five centimeters per year.

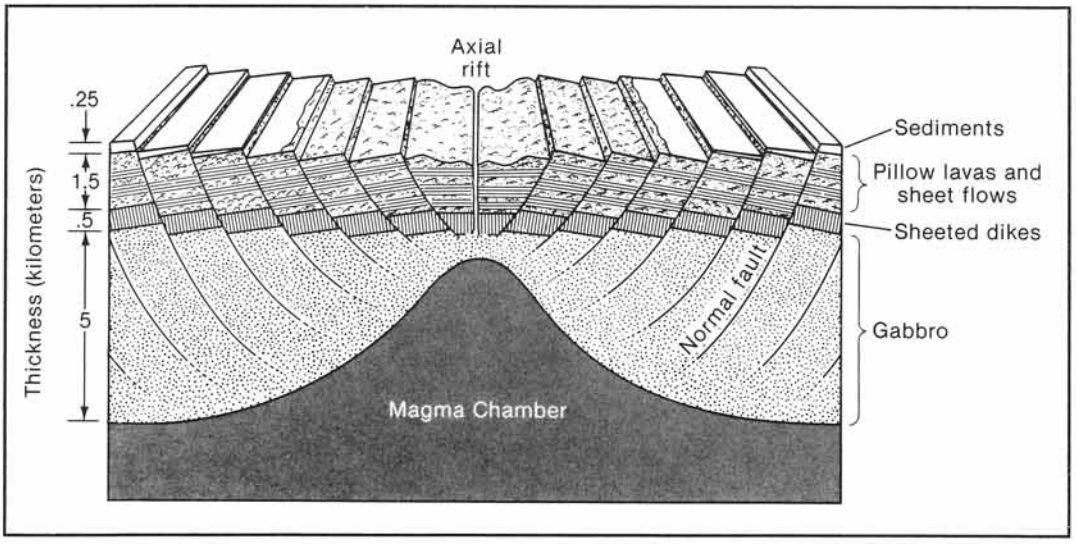

Figure 13-3: *Idealized cross-section of oceanic crust near a mid-oceanic spreading ridge.*

Continental collision zones

The convergence of tectonic plates and the associated subduction causes *partial melting* in the interaction zone between them. It is, therefore, common to find huge acidic or granitic intrusions stoped inside the mountain ranges formed at collision zones (Fig. 13-5a). Some of the plutons rise so close to the ground surface that they may feed large, volcanic *eruption centers*. In the core of eroded mountain ranges, these plutons form batholith complexes that may become exposed at the surface after erosion. A batholith is a large, generally discordant, plutonic mass that has more than one hundred square kilometers of surface exposure and no known floor. Individual plutons within the floor of batholiths often dominate the landscape as barren monoliths, protruding from the ground surface after removal of the surrounding rock units in which they were initially emplaced (Fig. 13-6). Batholiths are found in the core of all major fold belts. They may form at active collision zones of oceanic-continental lithosphere. They are, also, found in the thrust belts of mountain ranges, formed when two continents ultimately collide after subduction of the intermediary oceanic lithosphere that drove them together. "Batholith" literally means "rock that came from the deep." The various emplacement mechanisms of batholiths are the subject of continual investigations and are beyond the scope of the present book.

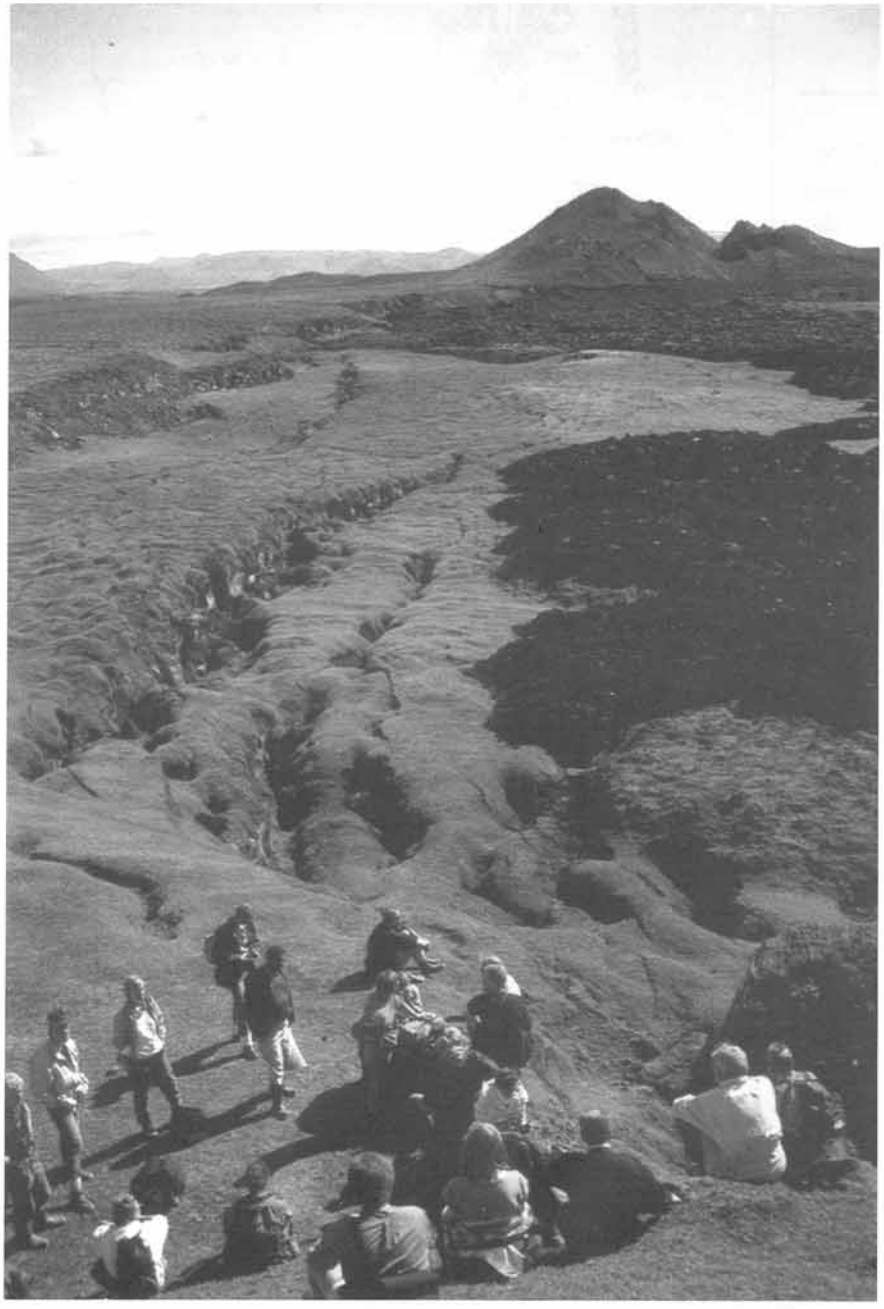

Figure 13-4: *Central rift zone near the Krafla field, Iceland. Looking due south, the North American plate, right, meets the Eurasian plate in the left of the image.*

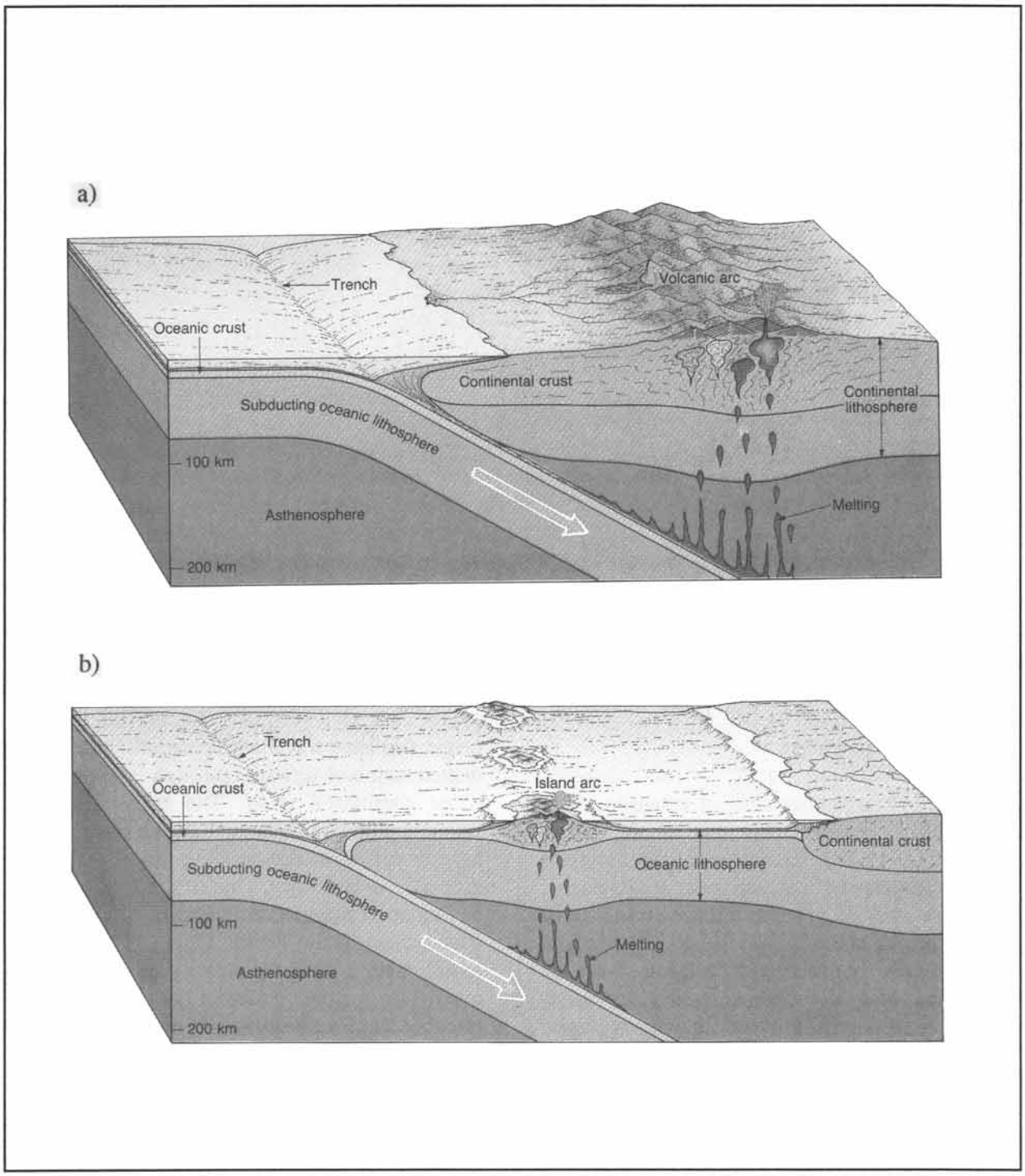

Figure 13-5: *a) Emplacement of plutons in proto-orogen on active continental margin. b) Formation of volcanic island arc in the overriding plate of an active oceanic-oceanic plate collision.*

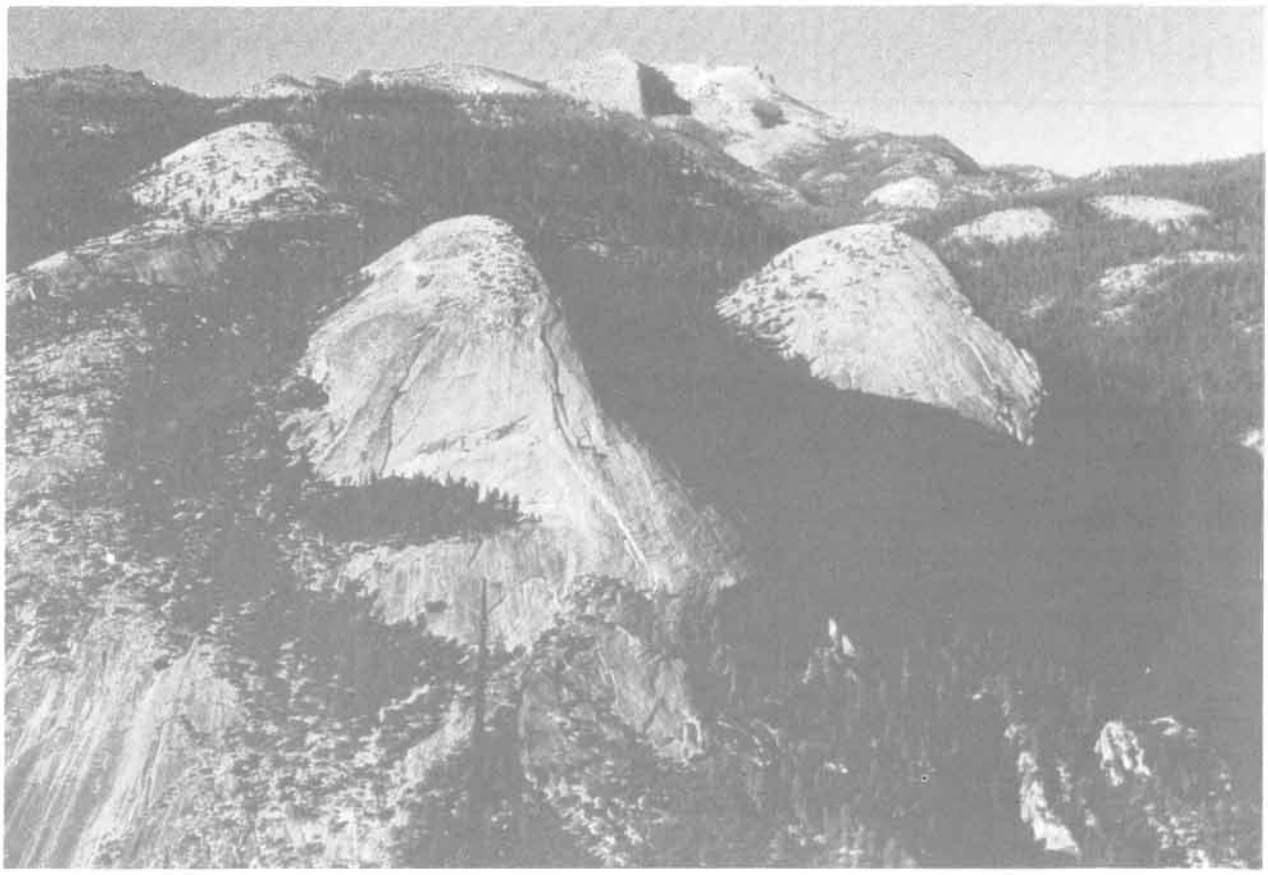

Figure 13-6: *Exhumed plutons of the Sierra Nevada batholith, Yosemite National Park, California.*

Subduction island arcs

Island arcs are other sites of extensive magmatic activity, formed where two oceanic plates collide (Fig. 13-5b). Examples are the Aleutians and the Indonesian and Japanese archipelagos, which are sites of granitic intrusions associated with extensive andesitic volcanism. Such island arcs naturally connect with volcanic belts on continental margins, because volcanoes form, also, where a continent overrides oceanic plates. For example, Mount Katmai is an active volcano on the continental margin of the Alaskan Peninsula that lines up with similar volcanoes on the oceanic island arc of the Aleutians (see next chapter, section 14-7).

Another type of magmatic emplacement occurs above *hot-spots*. These are parcels of deep mantle origin that have travelled through the mantle and melted their way upwards through existing oceanic or continental crust. The buoyant hot-spot material probably escapes from the unstable D''-layer (pronounce "dee-double-prime layer") at the core-mantle boundary. One of the best examples of hot-spot magmatism created the Hawaiian island chain in the Pacific Ocean. This volcanic island chain is nowhere near a plate boundary. It grew from episodic pulses of hot mantle magma, piercing from the mantle into the northwestward moving Pacific plate (Fig. 13-7).

☐Exercise 13-1: Consider regions of modern magmatic activity close to your region, and discuss their specific types of tectonic settings.

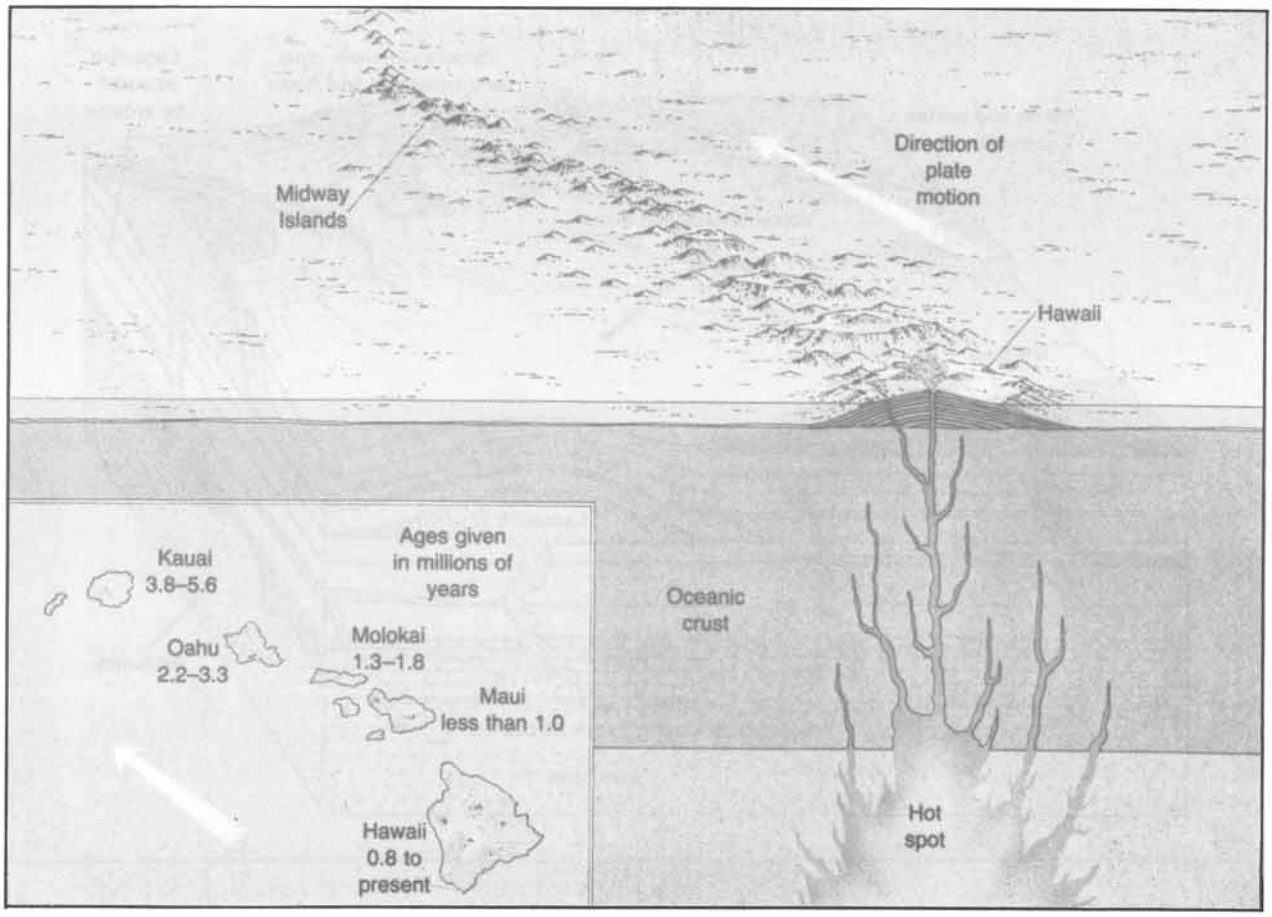

Figure 13-7: *The volcanic island chain, stretching from the Aleutian trench towards Hawaii, is emplaced by magmatic pulses of a stationary hot-spot, which is overridden by the northwest-moving Pacific plate.*

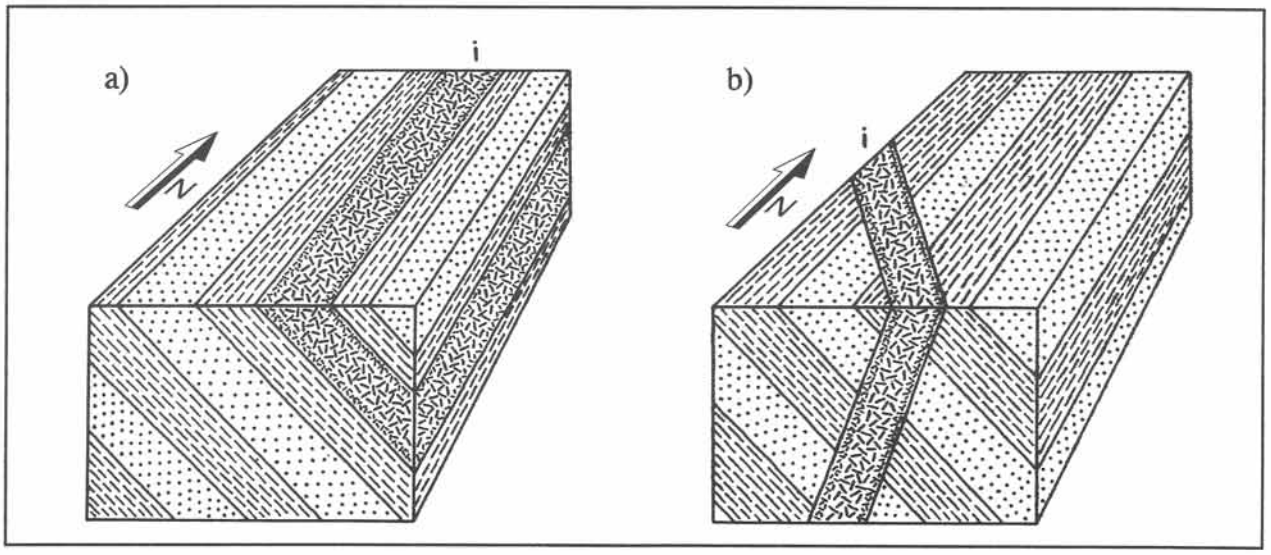

Figure 13-8: *Igneous dikes (i) intruded: a) concordantly, and b) discordantly, with respect to the layering of the host rock.*

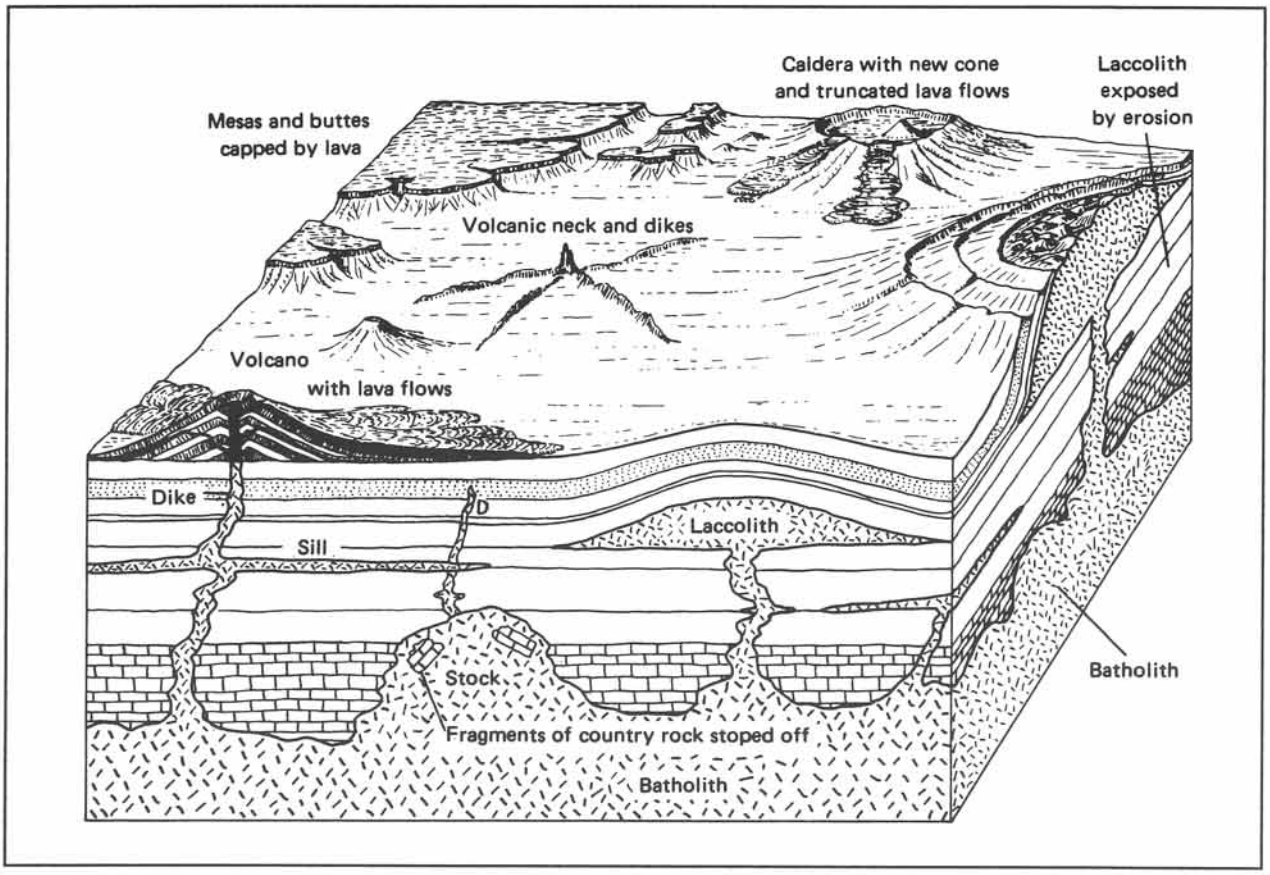

Figure 13-9: *The geometry of a magmatic complex, including: stock, dike, sill, and laccolith in the subsurface, and lava flows, neck, and caldera at the surface.*

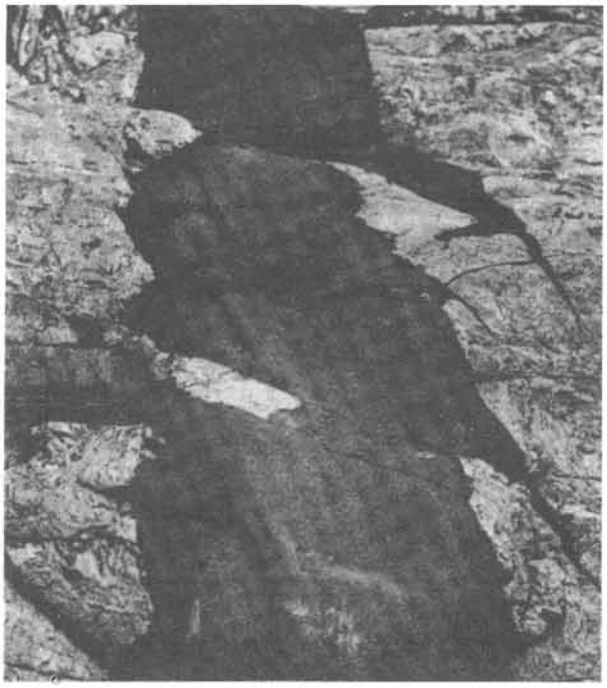

Figure 13-10: *Two-foot-wide diabase dike with apophyses intruded into host rock of rhyolitic tuffs, Rye, New Hampshire.*

13-2 Shape of igneous intrusions

Magmatic intrusions may cut across the lithological contact between pre-existing rock structures or may force their way parallel to pre-existing surfaces. Intrusions that cut across such contacts are termed *discordant*; those injected along existing contacts are termed *concordant* (Fig. 13-8). Figure 13-9 is a block diagram of a hypothetical region with a subhorizontal sedimentary sequence, intruded from below by a massive *magma chamber*, occupying a large volume in the subsurface. It fingers upward into smaller protru-

Figure 13-11a: *Gabbroic sill in subhorizontally-foliated Proterozoic rocks of Bank Island, Northwest Territories, Canada. The sill steps discordantly across the layering in the central part of the picture.*

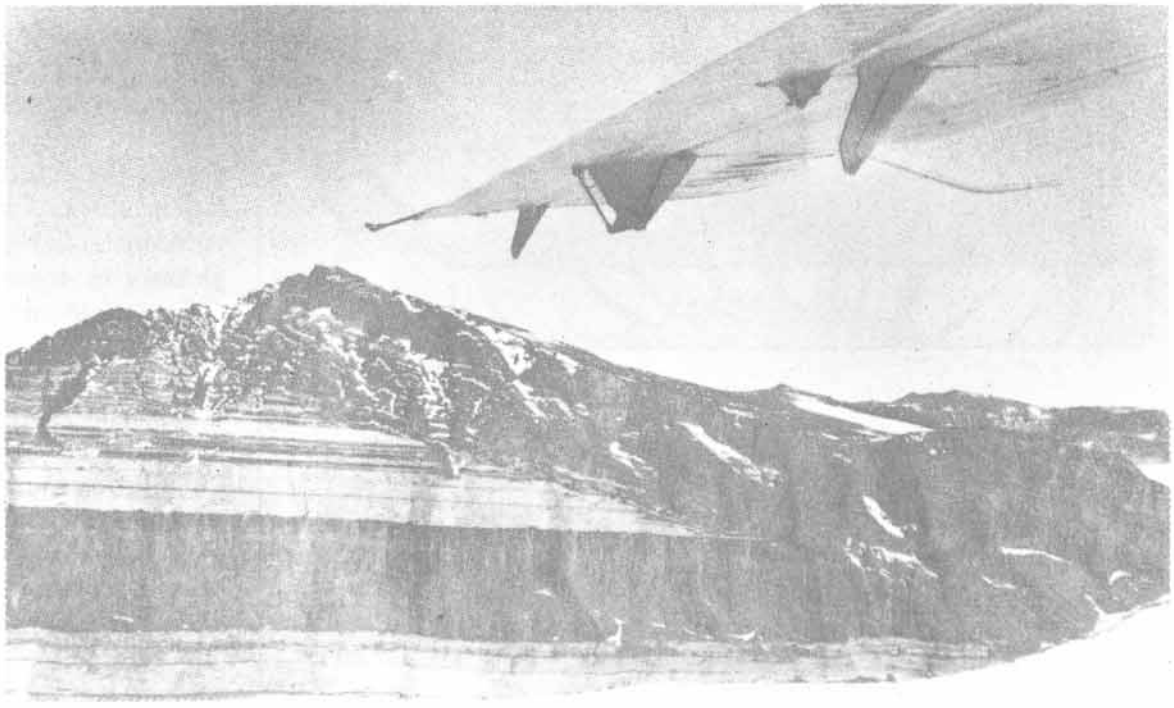

Figure 13-11b: *White-toned Carboniferous sandstones intruded by a concordant diabase sill. Both are truncated by a discordant diabase sheet, sloping to the right of the picture, Victoria Land, Antarctica.*

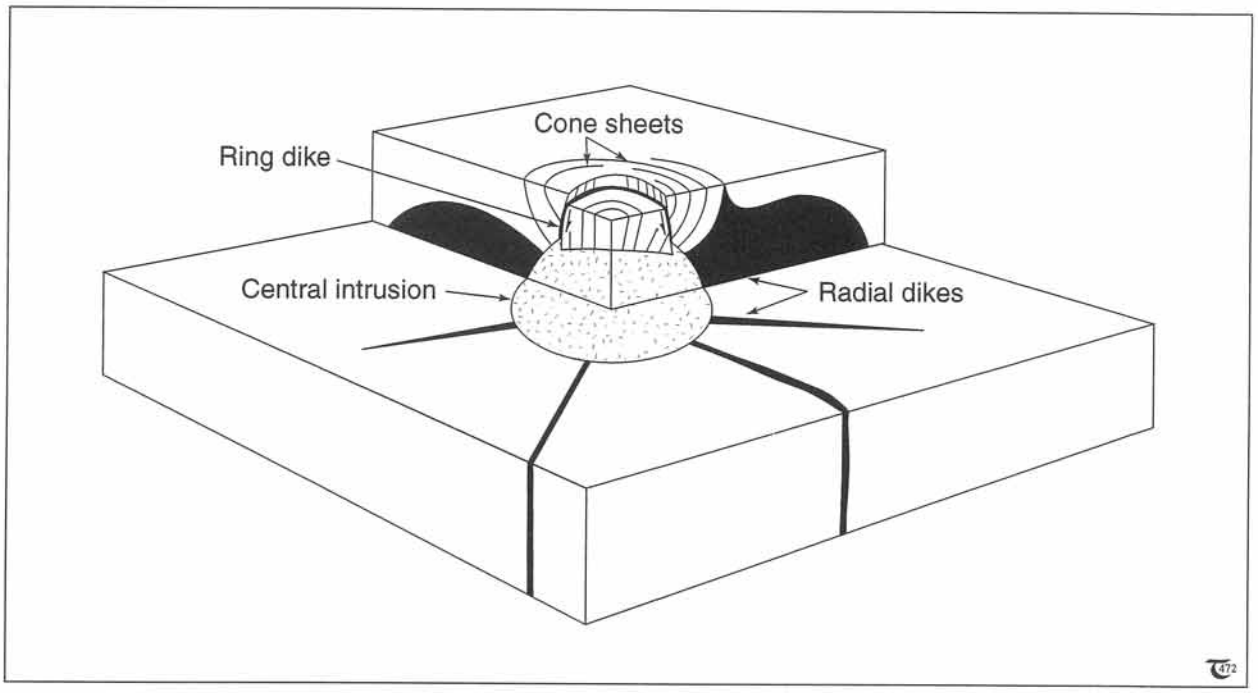

Figure 13-12: *Subsurface structure of a central subvolcanic complex. Shown are radial dikes, ring dikes, and cone sheets around the central magma chamber beneath the volcanic complex.*

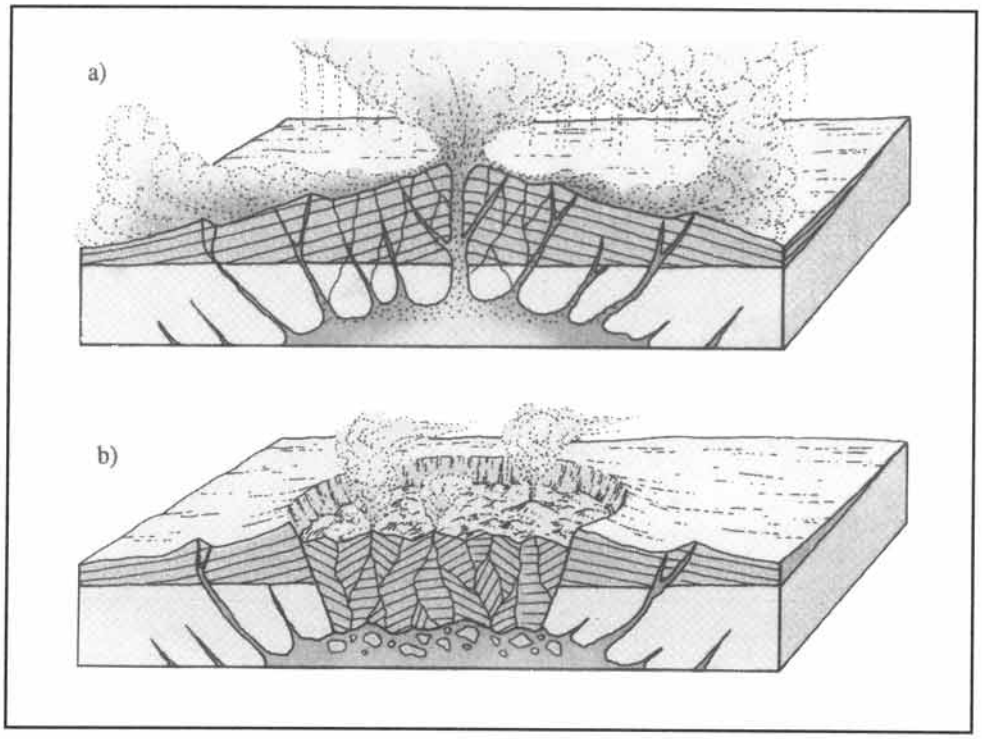

Figure 13-13: *Formation of a caldera. a) Build-up of a central volcano. b) Subsidence of the caldera floor, following a cone-sheet surface.*

sions, termed *stocks*. The stocks themselves feed narrower systems of magmatic injections, including *dikes*, *sills*, *laccoliths*, *necks*, and *volcanic cones* (see glossary in *Appendix C* for definitions).

Figure 13-10 shows a diabase dike, a discordant body, here about sixty centimeters wide, intruded into metamorphic rhyolite tuffs. Sills and laccoliths classify as concordant bodies, because they always closely follow the sedimentary bedding

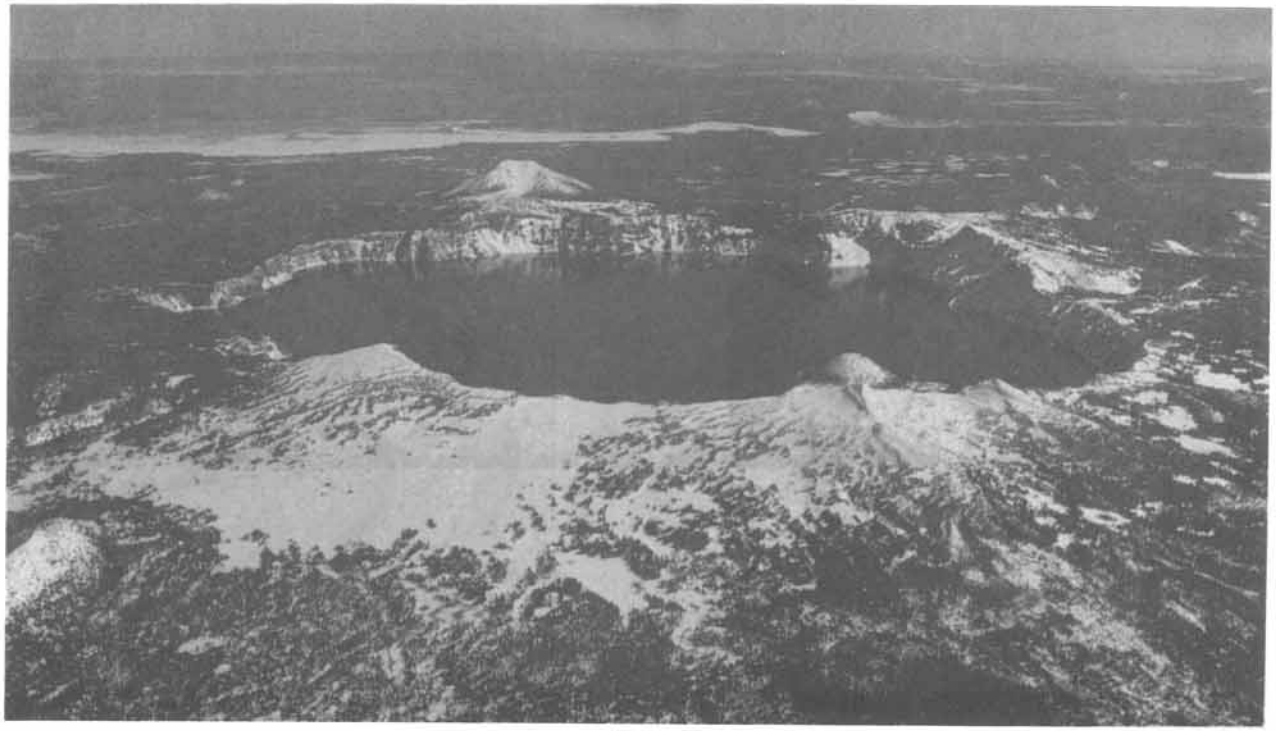

Figure 13-14: *Water-filled caldera of Crater Lake, ten kilometers across, with Wizard Island near the crater rim in the foreground, Oregon.*

or tectonic schistosity of the host rock. Sills and laccoliths are both tabular igneous bodies, that are commonly subhorizontal. The size of sills may range from several centimeters up to several hundred meters (Fig. 13-11a). Sills are more or less planparallel. Laccoliths differ from sills in that they cause updoming of the overlying strata (Fig. 13-9). The general term *igneous sheets* refers to tabular bodies, including both sills and dikes (Fig. 13-11b).

Figure 13-12 shows the generalized subsurface structure, as occurring beneath many major volcanoes. The so-called *subvolcanic complex* includes *radial dikes*, sub-circular *cone sheets*, and full circular *ring dikes* immediately above the central stock. The high pressure of the magma chamber and some thermal expansion elevate a central region, bounded by ring dikes. Alternatively, decompressed magma chambers may sometimes cause *cauldron subsidence*, a collapse of the central overburden into the underlying magma chamber, following the ring dikes as a surface of potential failure (Fig. 13-13). The resulting surface depression, termed a *caldera*, may be up to ten kilometers in diameter. Crater Lake, Oregon - which reaches that dimension - was formed 7000 years ago by the collapse of a former volcano, Mount Mazama. Subsequently, a smaller eruption from the caldera floor created a cinder cone, which emerges above the water surface - Wizard Island (Fig. 13-14). Other examples of calderas are outlined in the final section of chapter fourteen.

Plutons in map view may enclose isolated exposures of *cupolas* and *roof pendants* (Fig. 3-16). Cupolas are upward extensions of an igneous intrusion into its roof. Roof pendants are downward extensions of country rock into an igneous intrusion.

☐Exercise 13-2: The maps of Figures 13-15a and b outline in black the ring dikes, hosted in an igneous complex. Draw simple cross-sections M-N and O-P to illustrate the appearance of the ring dike at depth. Assume the ground surface has been leveled by erosion.

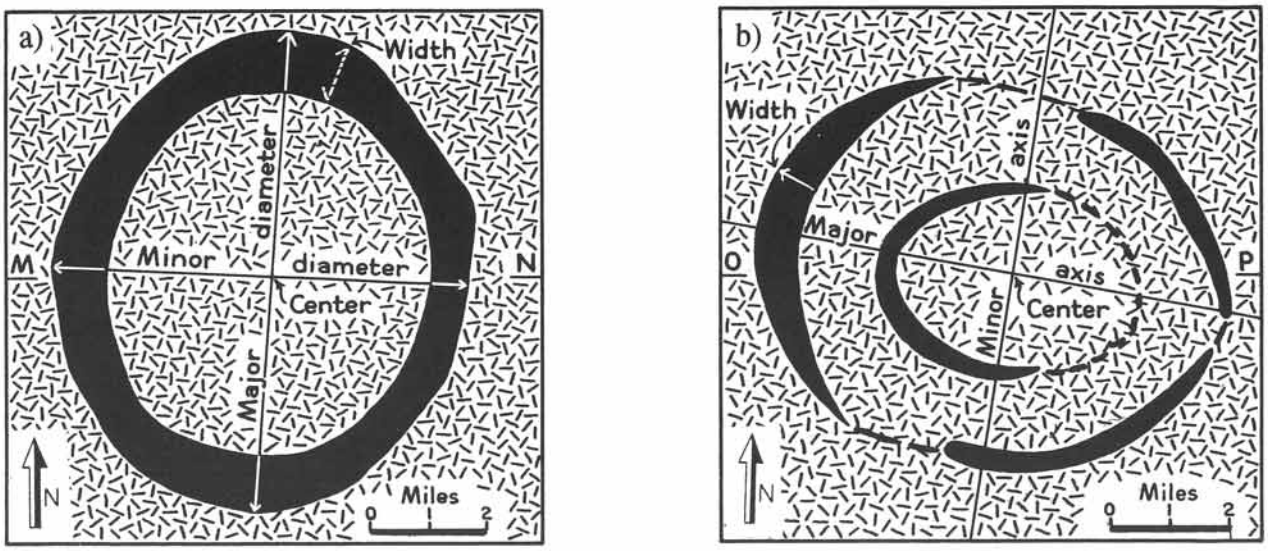

Figure 13-15: a) & b) Geological maps for exercise 13-2.

☐Exercise 13-3: Complete section Q-R across the map of Figure 13-16 to illustrate the subsurface extension of the central intrusion.

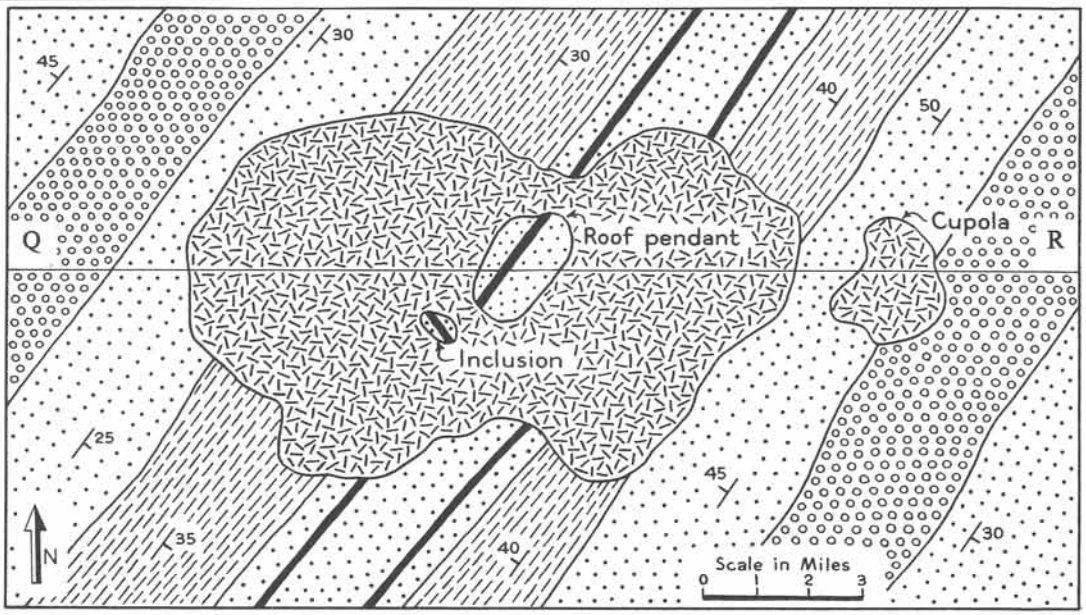

Figure 13-16: Geological map for exercise 13-3.

☐Exercise 13-4: The map of Figure 13-17 outlines the orientation of four basic dikes on a topographic base map. Complete section X-Y to clarify the extent of the dikes at depth.

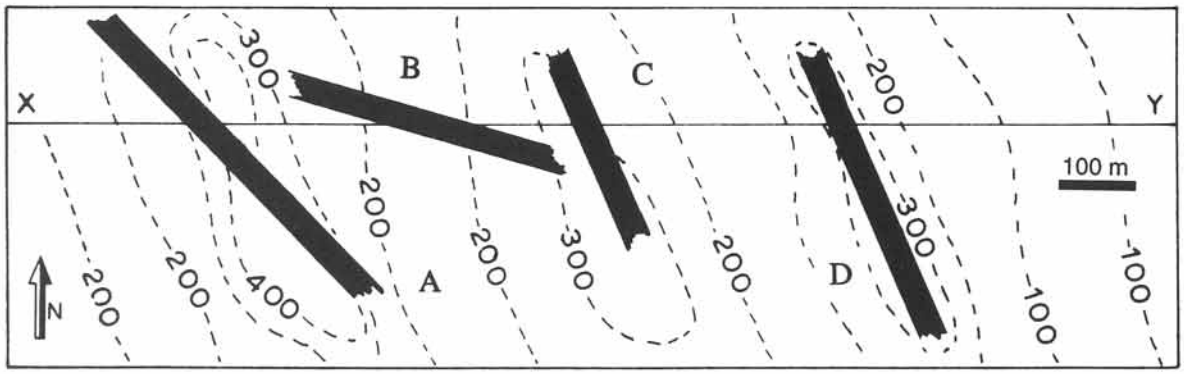

Figure 13-17: Outcrop pattern of igneous dikes on topographic base map. See exercise 13-4.

13-3 Zoned plutons and ring dike complexes

Plutons are bodies of intrusive igneous rocks, solidified from a cooling magma. A batholith is formed by a collection of plutons. The final appearance of plutons and batholiths depends on a variety of physical quantities and conditions and, thus, displays a range of possible shapes and sizes. Plutons are commonly of acid composition and intrude into relatively cold country rock from below, with internal temperatures of 700° to 900° centigrade. Contact metamorphism bakes the wall-rock into hornfelses, forming metamorphic aureoles of up to three kilometers thick around the igneous intrusion. The pluton itself is cooled by the country rock during the emplacement, and this may lead to *magmatic fractionation* and *differentiation*. The map of the Loch Doon pluton, southwest Scotland, illustrates the compositional zonation, mapped at the modern ground surface (Fig. 13-18). The *zonation* reflects the magmatic differentiation that took place either during the emplacement of the batholith or in the magma chamber before the emplacement of the successive magma batches that constitute the pluton. The core of the pluton is of granitic composition, and the margins are dioritic. The map of Figure 13-19 illustrates another *zoned pluton* from central Peru. The internal zonation of such igneous bodies is essentially formed during a single magmatic episode.

In other regions, patterns of intersecting cone sheets and ring dikes suggest that the emplacement of parts of igneous complexes occurred in distinct pulses. The map of the Tertiary ring dike complex on the island of Mull, Scotland, shows several distinct generations of ring dikes (Fig. 13-20). Similarly, the *subvolcanic complex* of Ardnamurchan involves ring dikes and cone sheets of, at least, three successive centers of magmatic activity (Fig. 13-21). It is possible that the underlying pluton was emplaced in a single *magmatic episode*, but that the subsequent intrusion of ring dikes and subsidence of cone sheets occurred during several episodes of volcanic outburst, associated with the slow degassing and settling of a *magma chamber*, cooling in the subsurface.

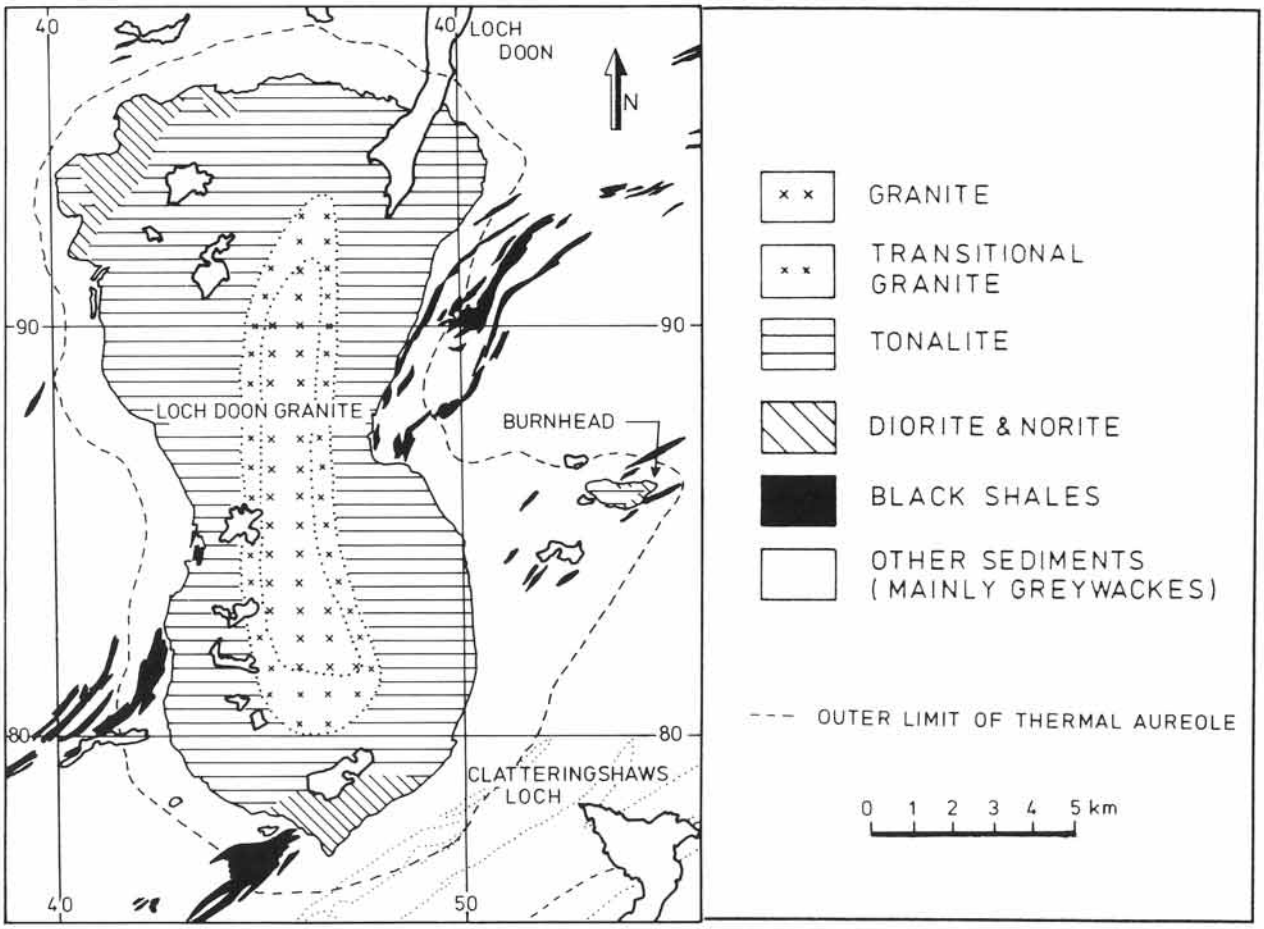

Figure 13-18: *Zoned pluton of Loch Doon, southwest Scotland.*

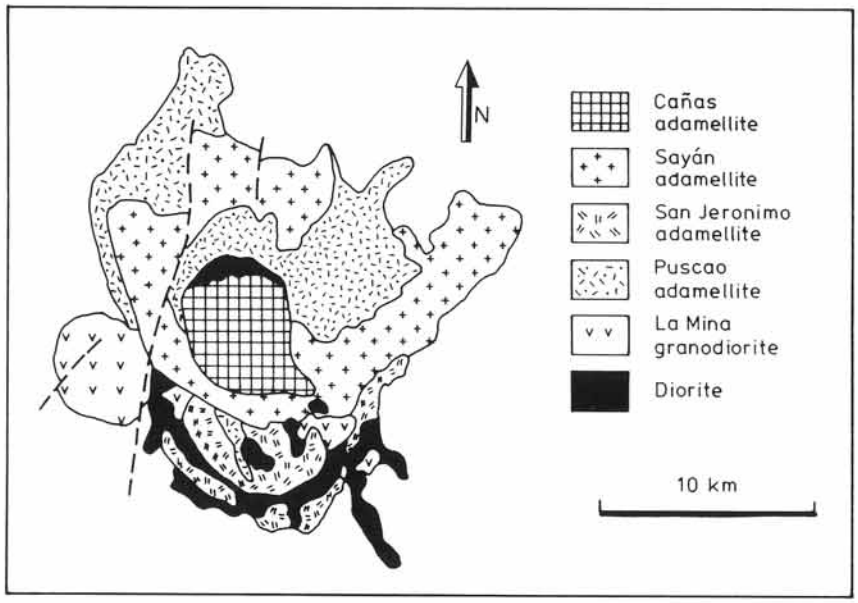

Figure 13-19: *Zoned pluton, central Peru.*

Figure 13-20: Geological map of Tertiary ring dikes and igneous complex of Mull, Scotland. For location see Figure 13-2.

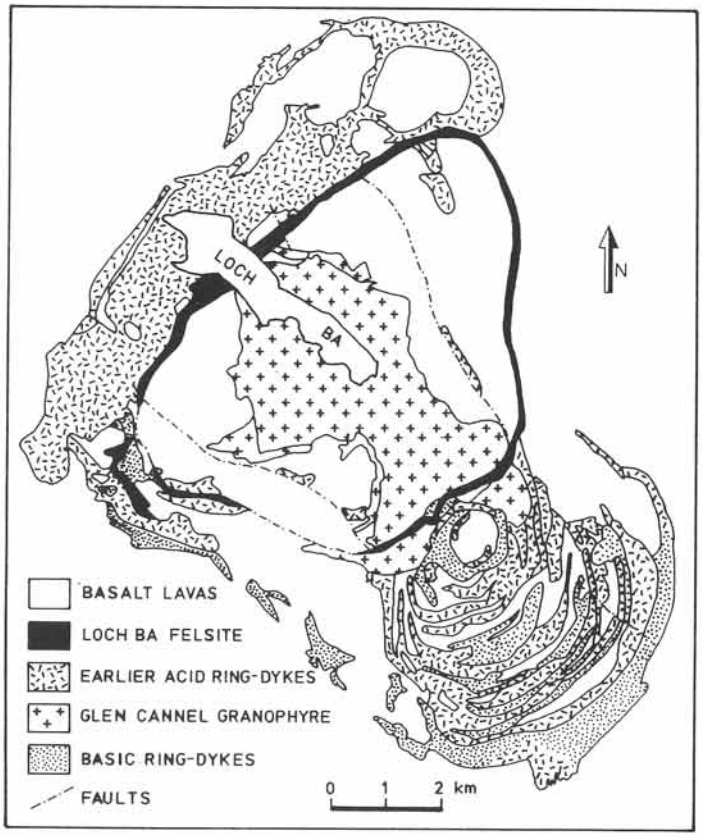

☐Exercise 13-5: Study the map of Figure 13-20, and distinguish intrusion centers and their sequence, similar to the distinction made for the central intrusive complex of Ardnamurchan in Figure 13-21.

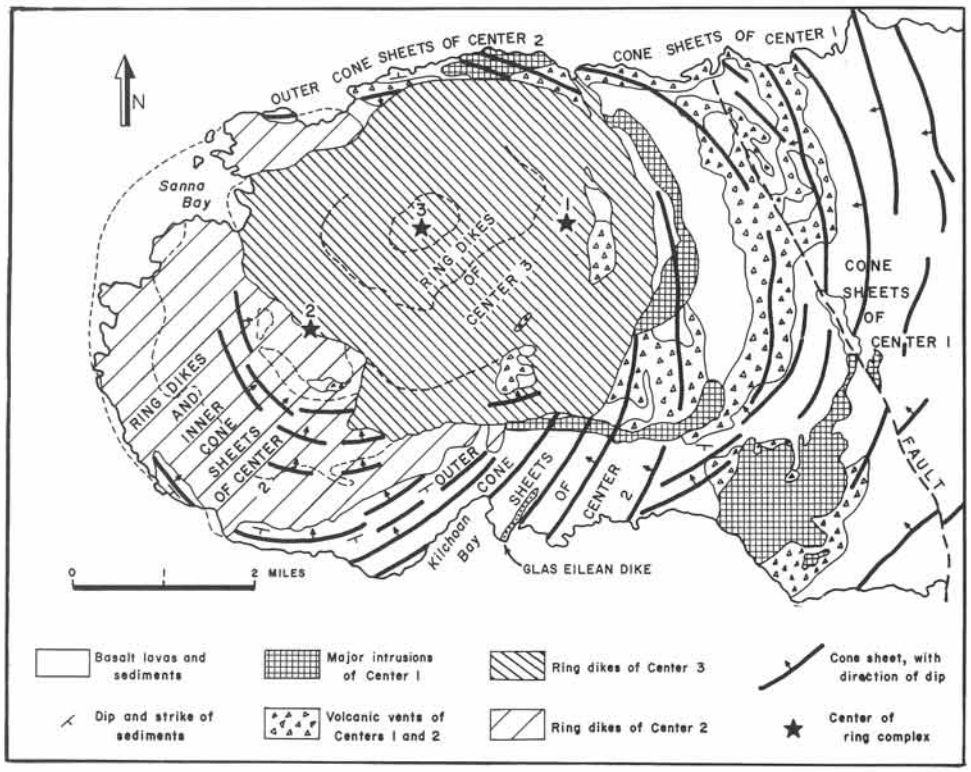

Figure 13-21: Geological map of the Tertiary central intrusive complex of Ardnamurchan, Scotland. For location see Figure 13-2.

13-4 Nested plutons and mantled gneiss-domes

Many plutons are emplaced in the core of orogens, formed along active continental margins. The plutons may be numerous and tend to coalesce at depth to define a *magmatic belt* of interconnected plutons. Such magmatic belts are found in the interior of the Himalayas, Alps, Pyrenees, Andes, and Rocky Mountains. The magmatic belts create batholiths, that commonly cut across the folded layering of the country rock and represent an advanced stage in the formation of a mountain range. For example, Figure 13-22 illustrates the coalescence or nesting of several plutons in the core of the Sierra Nevada, in the heart of the North American Cordillera. These plutons are *syntectonic*, which means that they were emplaced during the orogenic episode that involved folding of the country rock. The plutons partly cut across existing fold trends but, also, follow the grain of the fold belt, which locally wraps around the plutons.

Most Precambrian terrains are characterized by the occurrence of so-called *mantled gneiss-domes*. These are pluton-shaped masses of granite-gneiss, nested in overlying layered metasediments or supracrustals. Mantled gneiss-domes differ from the ordinary nested plutons by their higher degree of metamorphism and by the consistently concordant relationship of their boundary with structures in the host rocks. The map of Figure 13-23 illustrates gneiss domes mantled by supracrustals, from the Canadian Precambrian shield region near Halliburton-Bancroft. The form lines, outlined by the foliation within these gneiss-domes, remain subparallel with the contact surface of the host rock, suggesting that the *foliation* formed coeval with the dome

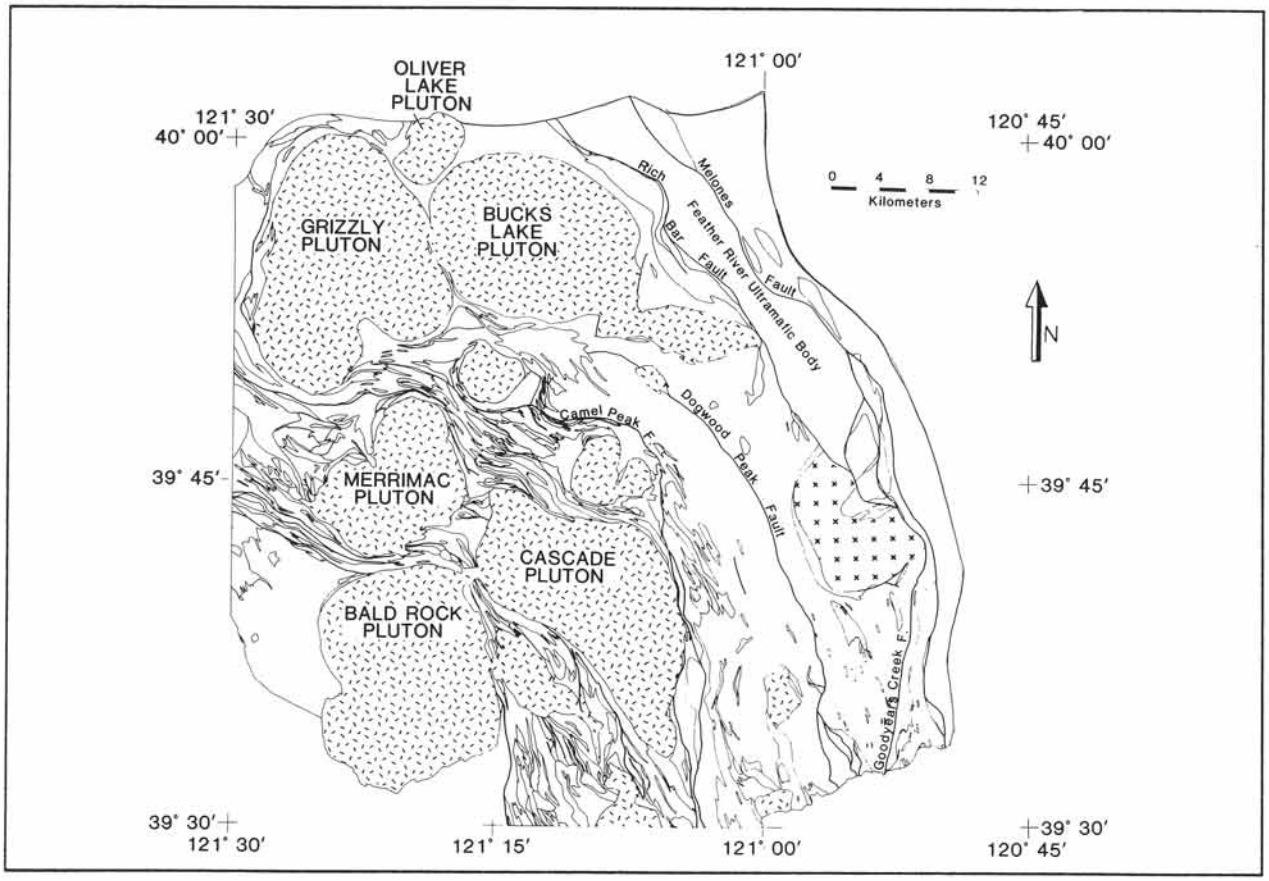

Figure 13-22: *Geological map of nesting plutons in the central part of the Sierra Nevada, California.*

emplacement. Some of the best-known, mantled gneiss-domes occur in the Archean greenstone-granodiorite rocks of the Zimbabwe craton, Africa (Fig. 13-24). The plutons are enveloped in strongly folded and foliated greenstone schists, concordant with the intrusive contacts. The interior of the plutons may still possess an igneous or magmatic texture, but their marginal zones are plastically deformed under metamorphic conditions, that commonly created an internal fabric or *gneissosity*.

Perhaps the most complex map patterns occur in geologic terrains, exposing deeply eroded gneiss-domes. The map of Figure 13-25 illustrates a region of the Proterozoic shield rocks in west Greenland. The form lines, that follow the gneissic foliation and compositional layering, outline a pattern of interconnected domes and basins. A more detailed map of the same area and a block diagram of the Tovqussap dome are illustrated in Figure 13-26a and b.

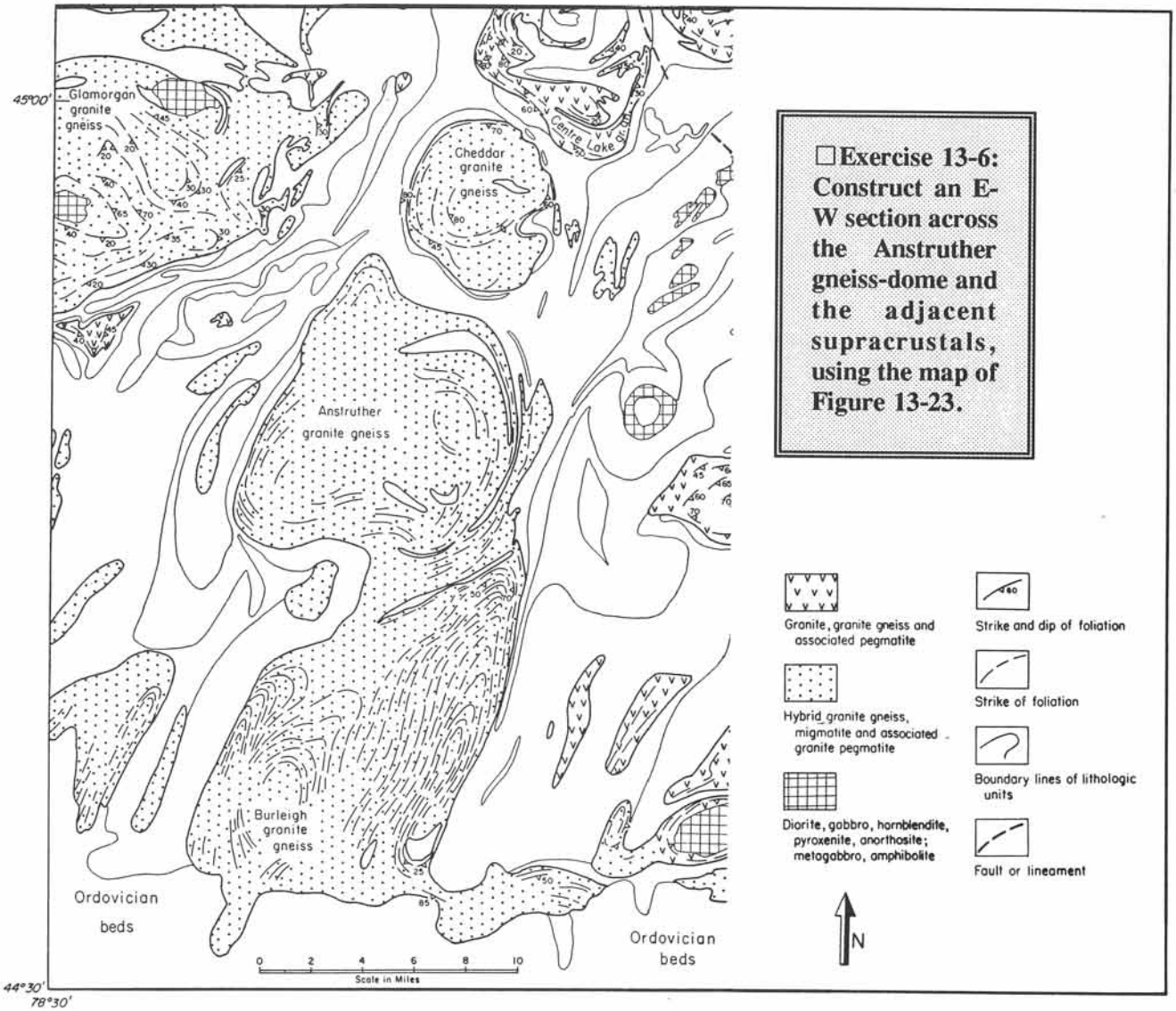

Figure 13-23: *Geological map of mantled gneiss-domes in Precambrian shield of Halliburton, Bancroft area, Canada.*

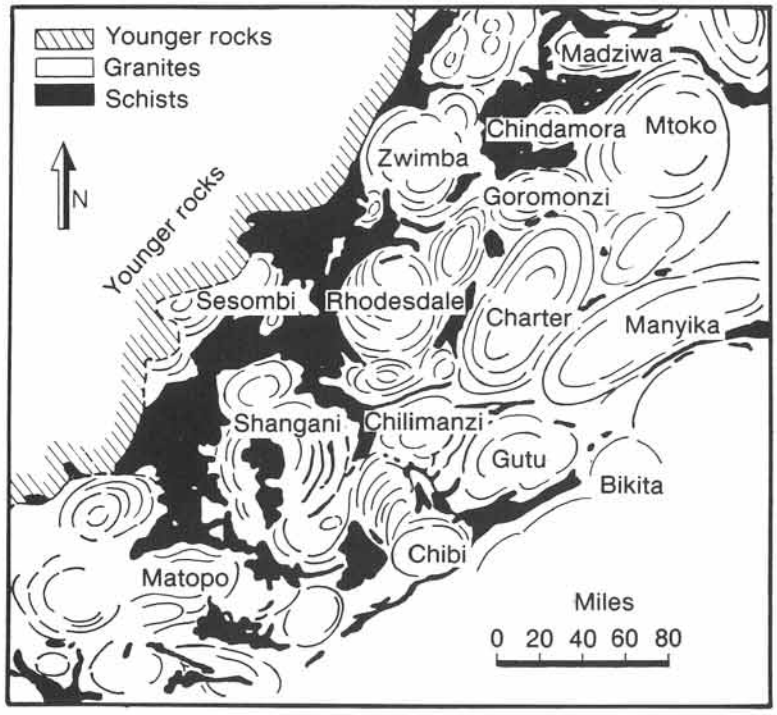

Figure 13-24: Mantled gneiss-domes of the Archean Zimbabwe craton, Africa.

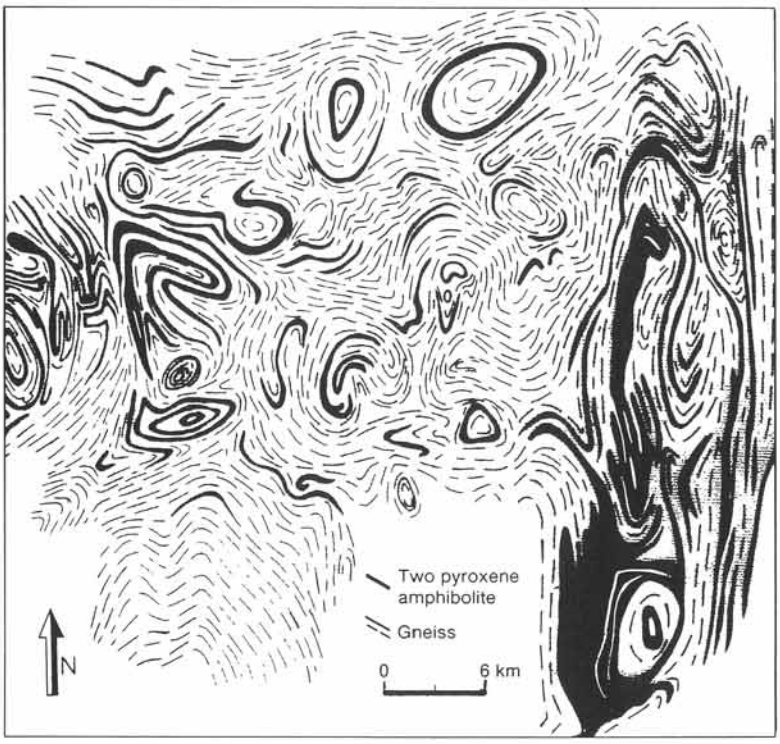

Figure 13-25: Deeply eroded gneiss-domes of Proterozoic shield in Fiskefjord region, west Greenland.

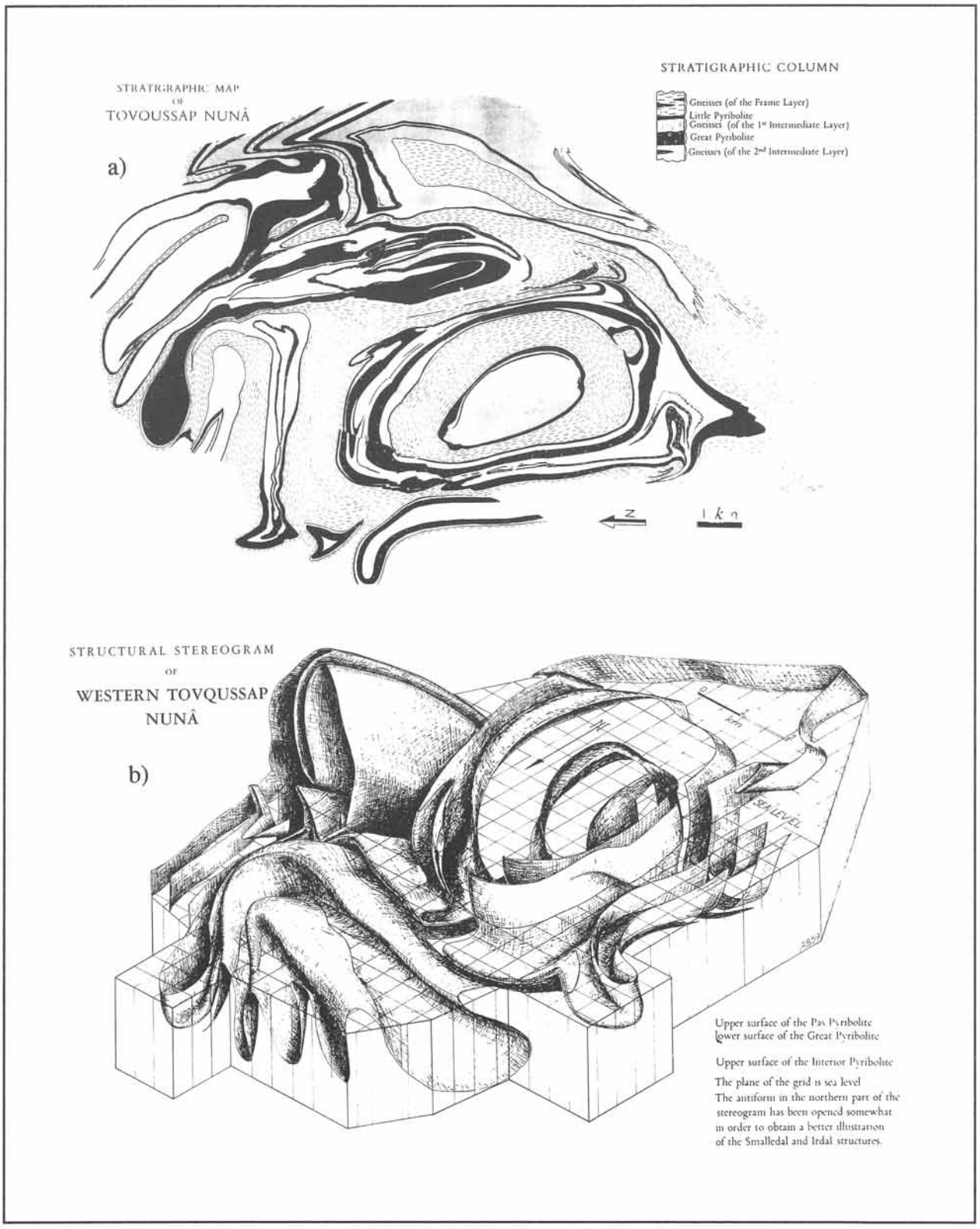

Figure 13-26: *a) & b) Map and perspective diagram of the Tovqussap gneiss-dome, west Greenland.*

☐Exercise 13-7: The Landsat image of Figure 13-27 covers the Archean granite-greenstone terrain of the Pilbara block in the Precambrian shield of northwest Australia. Construct a simple, form-line contour-map of the basic features in this terrain of mantled gneiss-domes.

Figure 13-27: *Landsat image of granite plutons (light albedo) and surrounding supracrustals (dark) of the Archean Pilbara block, NW Australia. Image is 100 kilometers wide.*

Chapter 14: Maps of Volcanogenic Structures

EXTRUSIVE IGNEOUS rocks reach the surface through vents in the Earth's crust, which conduct the eruption of gases, volcanic bombs, ashes, and hot lava. Geological maps of volcanic fields document the spatial distribution of individual lava flows, mudflows, and pyroclastic and epiclastic deposits. Field investigations have revealed that many extrusion vents follow fissure systems, sometimes marked on the ground by an array of closely spaced cinder cones aligned over the fissure zones. Other extrusions built up large shield volcanoes and stratovolcanoes by episodic eruption through subcircular vents. Renewed eruption of such volcanoes commonly involves explosive fracturing and gravity collapse and may create craters and calderas. This chapter includes examples of geological maps of volcanogenic structures and deposits and explains some of the basic features necessary for an elementary understanding of such maps.

Content: Some exploitation purposes of volcanic deposits are discussed in section 14-1. The structure of the ocean floor is illustrated in section 14-2. Flood basalts, shield volcanoes, and stratovolcanoes are outlined in sections 14-3 through 14-5. The map patterns of mudflows and glowing avalanches are illustrated in sections 14-6 and 14-7. Craters, calderas, and eroded volcanic landforms are discussed in section 14-8 and 14-9.

14-1 Exploitation of volcanic rocks

Volcanic eruptions may occur quite unexpectedly, and various estimates suggest that such eruptions have killed, at least, a quarter million people over the past millenium. Much of the destruction is caused, not by the ejected material, but by secondary effects. These effects include: flood waves (tsunamis), caused by the collapse of marine volcanoes; famine due to the spoilage of crops after ashfall; and mudflows, released either by melting of ice sheets on high volcanic cones or by the emptying of crater lakes.

Although volcanoes pose an awesome hazard to man and his construction, they do provide some

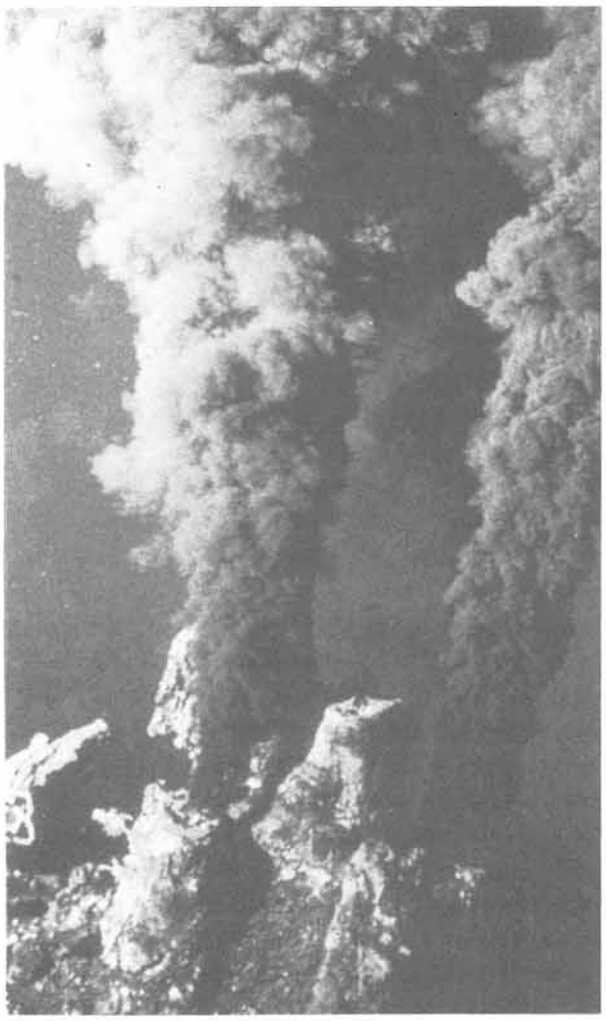

Figure 14-1: "Black smoker" or submarine geyser pours 350° centigrade water, saturated with metallic sulfides, into the cold Pacific waters 2.5 kilometers below sea level. Image taken by French submersible Cyana, 1982, at 13° NL on the mid-Pacific ridge axis.

beneficial products. Extrusive igneous rocks have been used by ancient man for the construction of hunting tools (obsidian), cement, and building stones. Pumice is used as a bathing stone for removing excess callus from footsoles and handpalms. Basalt provides massive masonry. For example, the extensive network of sea dikes in the Netherlands is reinforced with heavy basalt blocks, imported from abroad. The national heritage city of Cappodocia, Turkey, is a magnificent landscape of small conical hills of differentially eroded volcanic ashflows, that were excavated to host houses. The gigantic heads of Easter Island, stoically staring out over the ocean, consist of volcanic pyroclastics. They were sculpted by a people vanished long ago. Volcanic ashes commonly fertilize agricultural land, and the 1912 eruption of Katmai-Novarupta, Alaska, has been quoted as "the best thing that ever happened to Kodiak." Many fine French wines and champagne come from vineyards situated on volcanic soils.

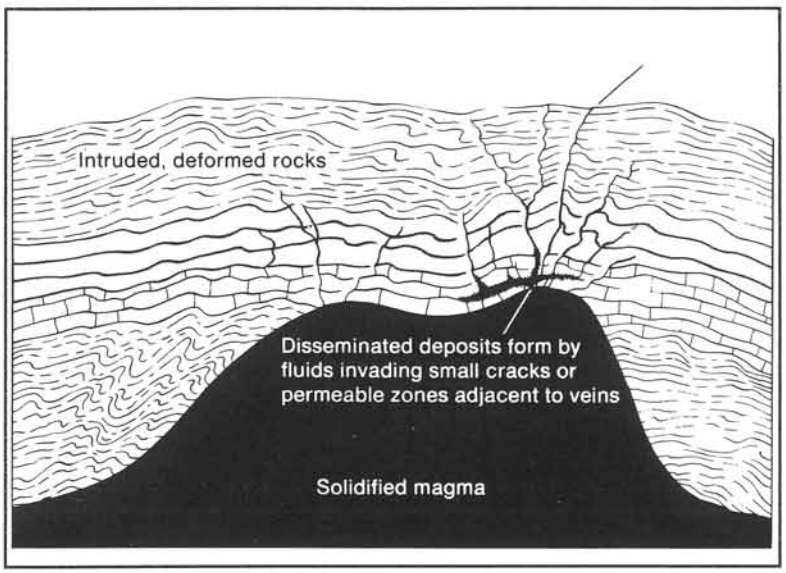

Modern interest in volcanic terrains partly stems from the search for mineral and energy resources. Economic mineral deposits of galena, sphalerite, pyrite, gold, silver, zinc, uranium, and diamonds all are associated with volcanic rocks. Metal-rich sulfide deposits have been formed and are forming today from saturated

Figure 14-2: Pegmatite veins intrude into fissures, emanating from a magma chamber. Other hydrothermal deposits accumulate in the rocks, fractured by the pressure of the central batholith.

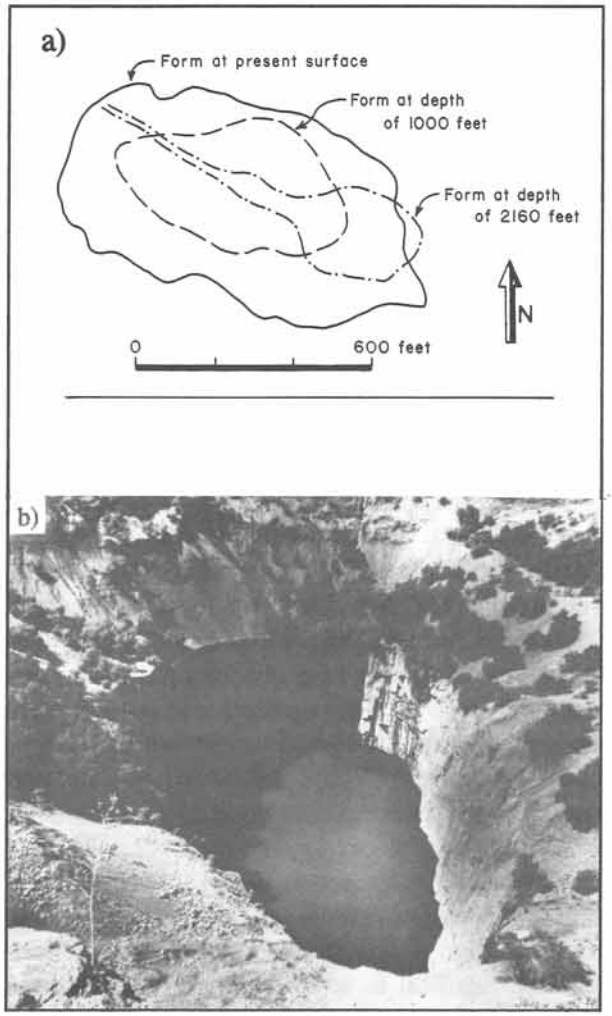

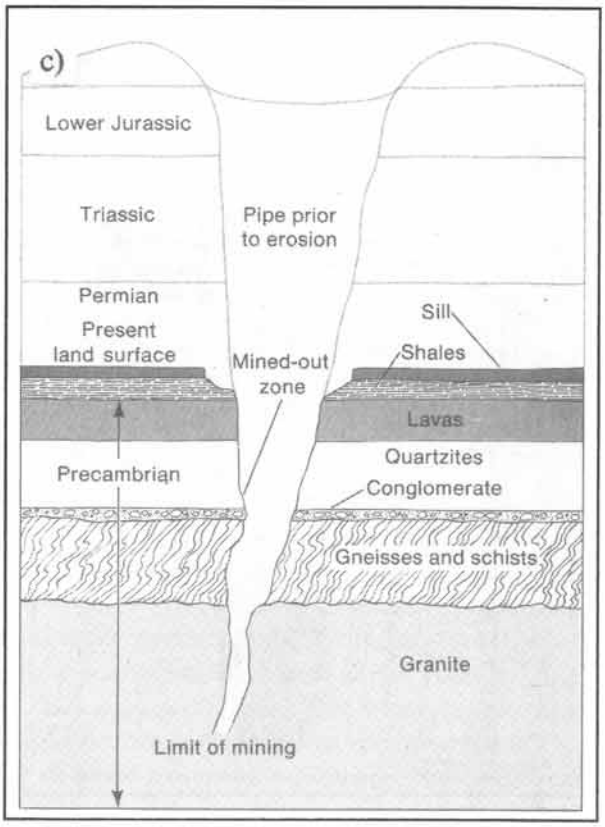

Figure 14-3: *Magma pipe of diamond-bearing kimberlite at Kimberley, South Africa. a) Map projection of pipe outline at three different levels. b) Oblique view into the mined magma pipe. c) Schematic cross-section of the magma pipe up to three kilometers below the ground surface.*

thermal water, rising in "*black smokers*." These are submarine geysers, occurring along the axial fracture zone of active mid-oceanic ridges, ejecting hot water that precipitates massive sulfide deposits upon mixture with the ambient, cold sea water (Fig. 14-1).

Other important ore bodies are found near subvolcanic complexes, formed by hydrothermal fluids, rising through fractures in the host rock. The solutions scavenge particular elements from the country rock to precipitate elsewhere in lead, zinc, and gold-bearing quartz veins (Fig. 14-2). Subvolcanic stocks of ultrabasic, high-pressure magmas or *kimberlites* carry up diamonds from over 200 kilometers deep and are mined extensively in South Africa. The prototype diamond pipe at Kimberley, South Africa, was mined to over one-kilometer depth.It follows a fissure in the subsurface but concentrates into a funnel shape of subcircular plan-section near the surface (Fig. 14-3a & b). The upward widening suggests that pressure was such that, on approaching the surface, an extensive blow-out occurred to form a conical pipe and pyroclastic deposits. Steep-sided pipes of igneous origin are, also, called *stocks*, *plugs*, *necks*, or *diatremes*. Deep circular surface depressions associated with blow-outs are termed *maars* (Fig. 14-3c).

The residual *geothermal energy* in the subsurface of recent and subrecent volcanic regions has

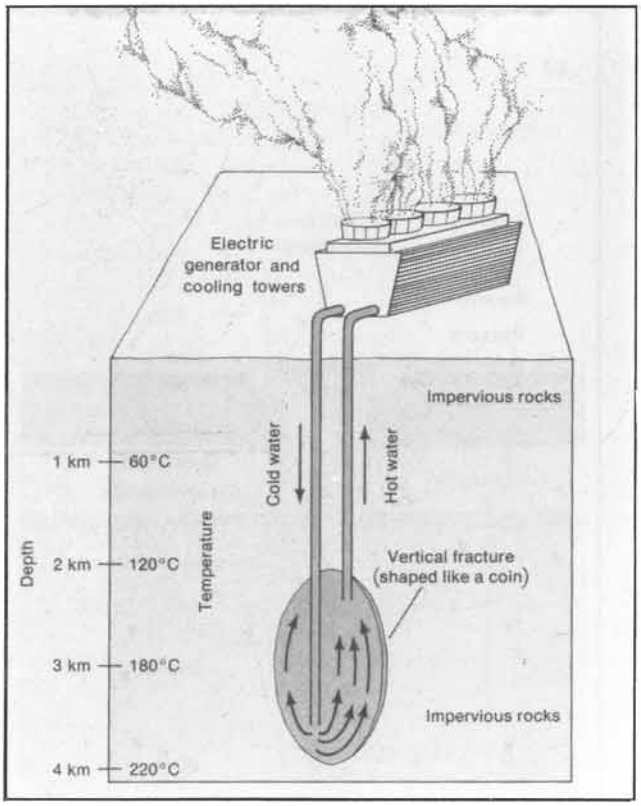

Figure 14-4: *Fractures in hot igneous rocks can be injected with water to extract geothermal energy for heating purposes and the generation of electricity. Illustrated is a region with a steep geothermal gradient of 60° centigrade per kilometer.*

been exploited in ancient times by the Romans and Arabs for the heating of elaborate public bath houses. The natural steam eruptions or geysers of Iceland and Old Faithful in Yellowstone National Park, Wyoming, are major tourist attractions. Modern man extracts geothermal energy for municipal waterworks on a grand scale (Fig. 14-4). For example, all of Iceland's houses, offices, schools, and greenhouses (for its domestic banana production and consumption) are heated by geothermal steam and hot water pipes. Large extractions, also, occur in Italy, New Zealand, Kenya, and Hawaii, with much room for expansion in other developing countries, such as the Philippines and Indonesia.

14-2 Ocean floor

Geoscientists have pieced together a picture of plate tectonic evolution, involving the breakup, dispersal, and renewed aggregation of *supercontinents*. Presently, at least a dozen major plates are distinguished. This book concentrates on the methods of geological map interpretation and avoids a detailed treatment of plate tectonics, which is already covered in other texts. But the movement of tectonic plates continually renews our ocean floors, which are covered with extensive basalt flows.

The tectonic plates are formed by dispersal of the continental fragments and accretion of new oceanic lithosphere. Pangea, the Earth's youngest single supercontinent, broke up about 200 million years ago. The age distribution of the ocean floor is outlined in Figure 14-5 in transverse Hammer-Aitoff projection. This projection gives an overview of the oceanic spreading pattern in a single map by placing the South Pole in the central node and the north polar axis at the top.

The rifting and tearing apart of continental crust continues at present, as the mid-oceanic rift of the Indian Ocean propagates northward into the Red Sea arm to separate further the Arabian plate from the African plate. The opening of new oceans is compensated for by the closure of other oceans. The global production and consumption of oceanic lithosphere occurs at rates ranging between 2.4 and 3.5 centimeters per year. The mid-Atlantic ridge spreads at a time-averaged rate of about three centimeters per year.

Iceland is located on the mid-Atlantic spreading ridge - the western half is part of the North American plate and the eastern half part of the Eurasian plate. Volcanic eruptions, associated with the growth of the island, are extremely frequent. The Surtsey volcano formed between 1963 and 1967 close to the southwest coast of Iceland by an outpouring of one cubic kilometer of ash and lava (Fig. 14-6). Surtsey is the southwesternmost of the Vestmann Islands, which all lie along a branch of the mid-Atlantic rift zone.

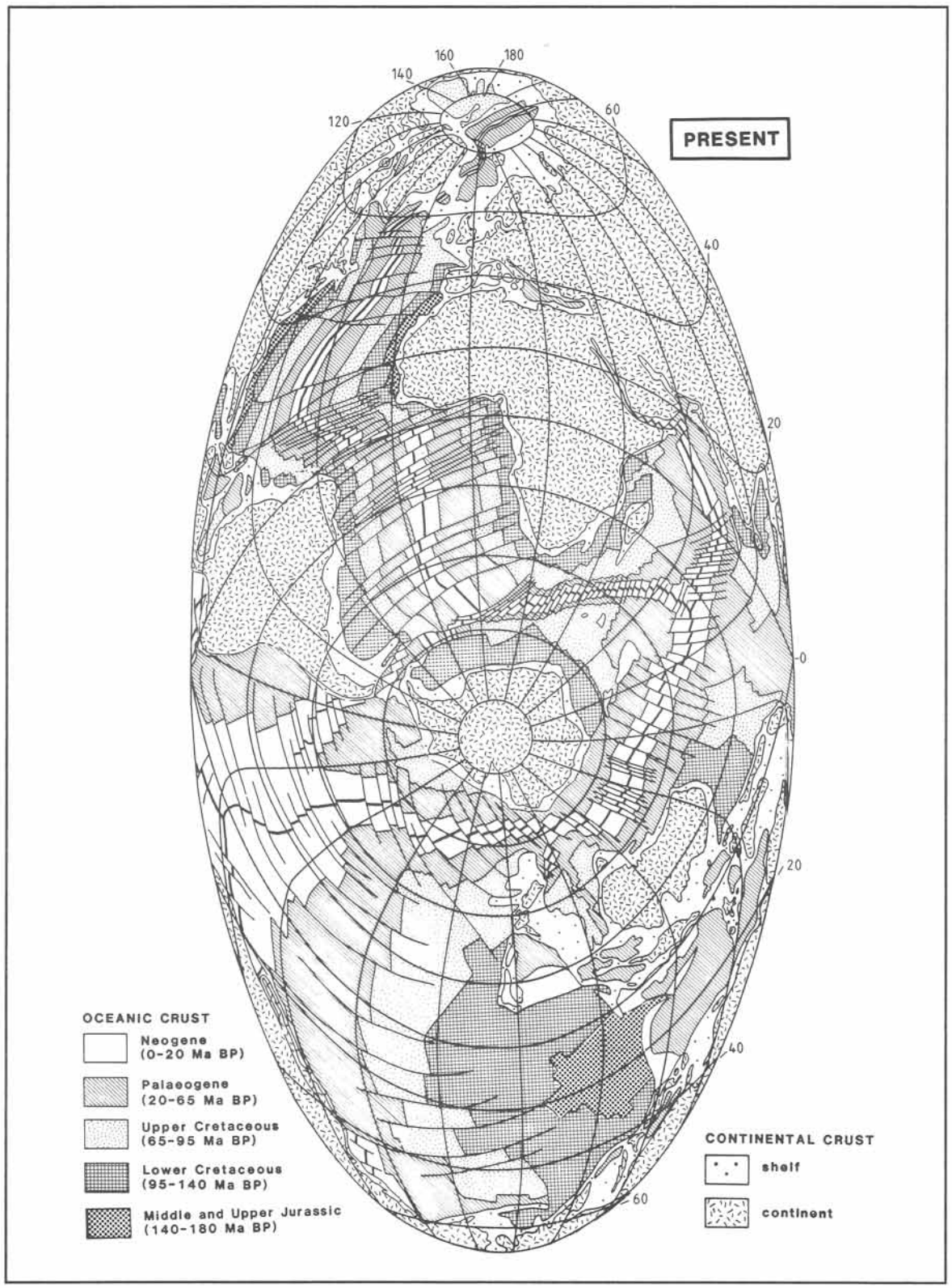

Figure 14-5: *Age distribution of the basaltic ocean floor in transverse Hammer-Aitoff projection.*

14-3 Flood basalts

Zones of incipient rifting are characterized by the intrusion of basic dikes. Progressive extension may lead to complete failure of the continental crust, accompanied by extrusion of basaltic lavas and the formation of oceanic crust. Continental rifting first produces basalts of the alkali magma series (alkali olivine basalts). It is only after the continental separation that the ocean floor crust of tholeiitic basalt forms. However, not all fractures in the continental crust succeed to form a separate plate boundary; these are the *failed rift-arms* or *aulacogens*. They are marked by dikes of alkali basalt, some of which manage to pour out large volumes of basaltic lavas onto the surface; these deposits are known as *flood basalts*. Figure 14-7 illustrates the breakup of Gondwana, some 140 million years ago, and outlines the regions where thick plateaus of stacked basalt flows have accumulated in Jurassic and Cretaceous rift zones. Continental alkali-basalts commonly contain more sodium and potassium than is typical for basalts of the ocean floor, which are not contaminated by partial melts of the sialic continental crust.

The progressive build-up of plateaus of flood basalts is continuing at present. Cenozoic basalts episodically erupt from fissures, splaying away from the opening Red Sea. The fissure system includes the aborted spreading zones of the African rift valley, Afar triangle, Danakil depression, and tears in the Arabian Peninsula (Fig. 14-8). Flood basalts typically are fissure eruptions, and the subrecent lava fields of the western province of Saudi Arabia have emanated from *en-echelon fractures*, splaying away from the Red Sea rift in what is referred to as the Makkah-Madinah-Nafud volcanic line (Fig. 14-9). Such fissure zones are commonly marked at the surface by a series of aligned *spatter cones* and *cinder cones* (Fig. 14-10a & b). Cinder cones are usually less than 300 meters high and are comprised of steep, 30° to 40° slopes, built from scoriaceous *pyroclastics*, i.e., ejected, airborne lava fragments (Fig. 14-10b). Such pyroclasts sometimes agglutinate into a hard deposit. Figures 14-11a and b are examples of regularly-spaced cinder cones, that mark the one-million-year-old fissure of Harrat Kishb, Saudi Arabia, and similar cones along the

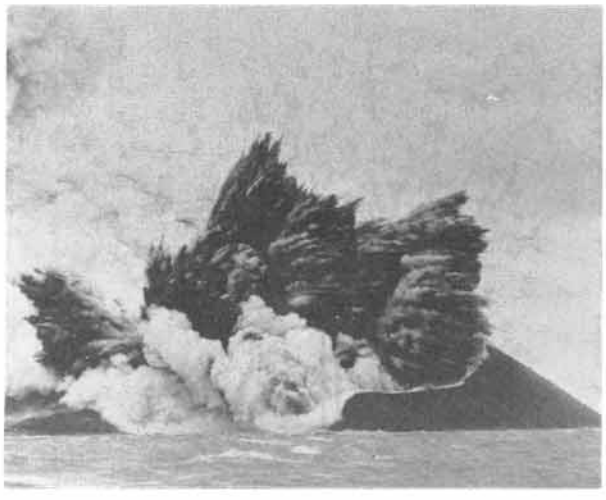

Figure 14-6: *Explosive eruption of Surtsey, Iceland.*

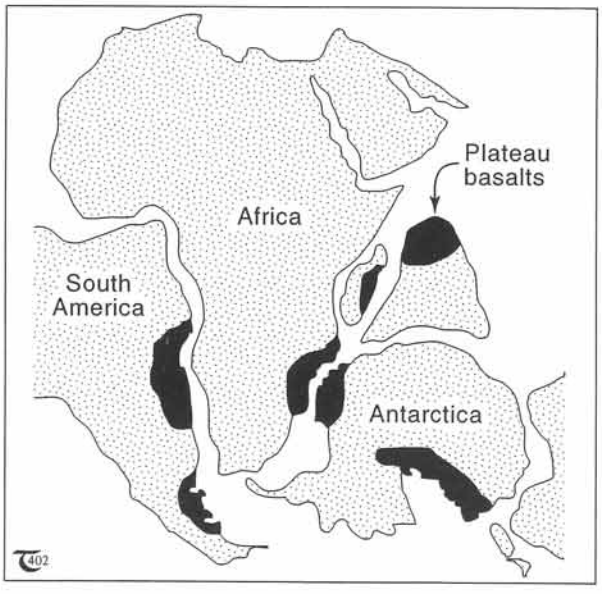

Figure 14-7: *Extent of plateau basalts along rift zones that broke up Gondwana about 140 million years ago. The age of the plateau basalts spans the entire epoch of modern plate movement.*

twenty-kilometer-long Laki fissure of 1783, Iceland. The Laki eruption represents the largest lava flood in recent history and was accompanied by a series of minor earthquakes. The map pattern of the Laki rift and associated cones is quite similar to that of the 2,100-year-old array of cones along the Great Rift Zone of the Craters of the Moon National Monument, Idaho (Fig. 14-12a & b).

A much larger plateau of Miocene flood basalts occupies the Columbia River Plateau, Washington, northwest of the volcanic province of the Craters of the Moon in the Snake River Plain (Fig. 14-13a). The Columbia basalts are locally up to 1,500 meters thick, cover an area of over 130,000 square kilometers, and may have formed in about ten million years. A still larger province of flood basalts occurs in the Deccan Plains, India, where 250,000 square kilometers of Cretaceous basalt lavas rest on the Precambrian basement (Fig. 14-13b). The Deccan *traps* ("steps") are up to two kilometers thick and include individual lava flows, ranging from one to sixty meter thick. The feeder fissures in the older provinces of flood basalts are no longer marked by spatter and scoria cones at the surface, which disappear by erosion in about four million years. But remnants of cinder cones commonly become entrapped within the sequence of flood basalts (Fig. 14-14).

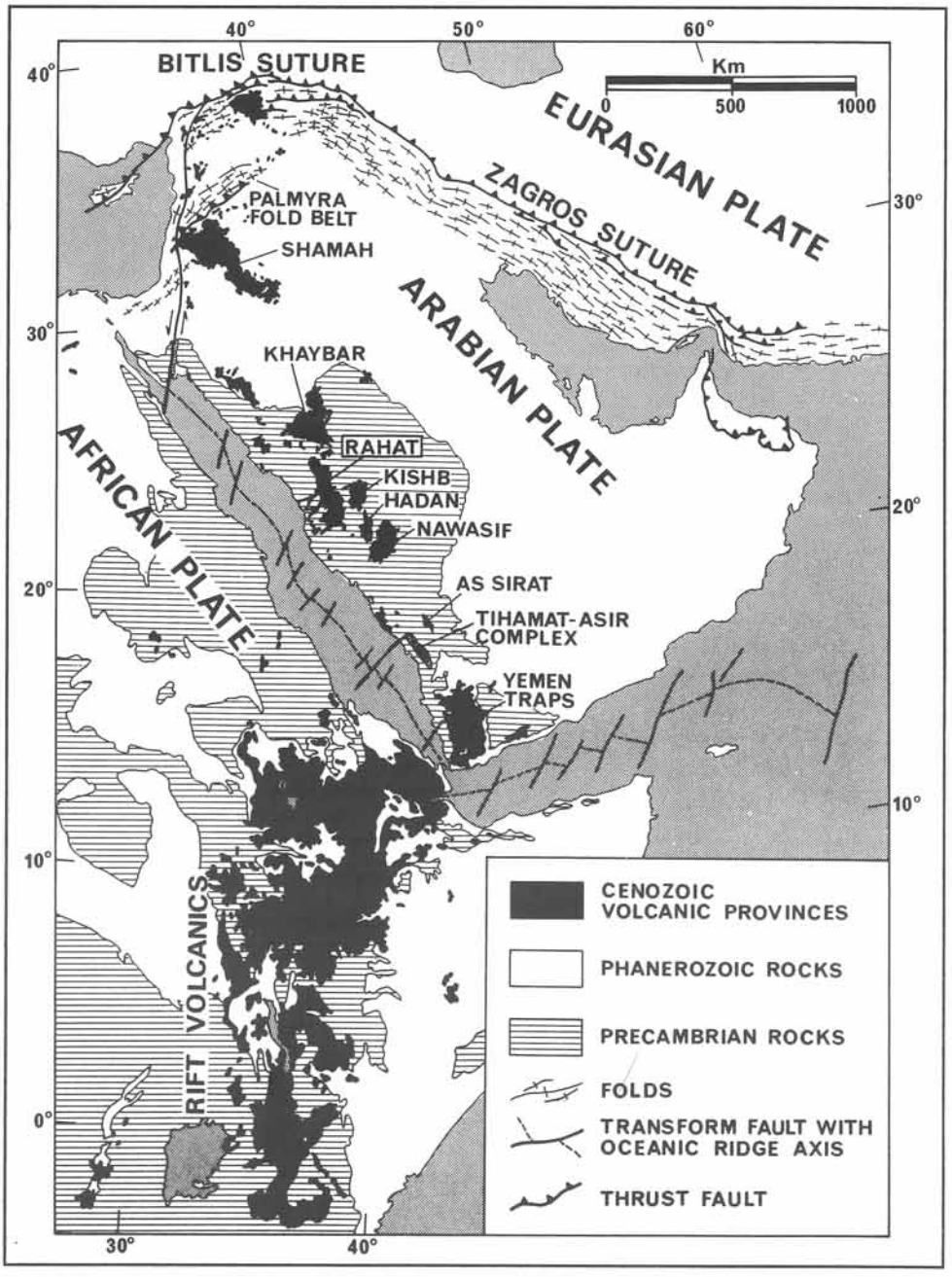

Figure 14-8: *Geological map of territory and recent basalts in the active rift zone of the Red Sea and the East African rift valley.*

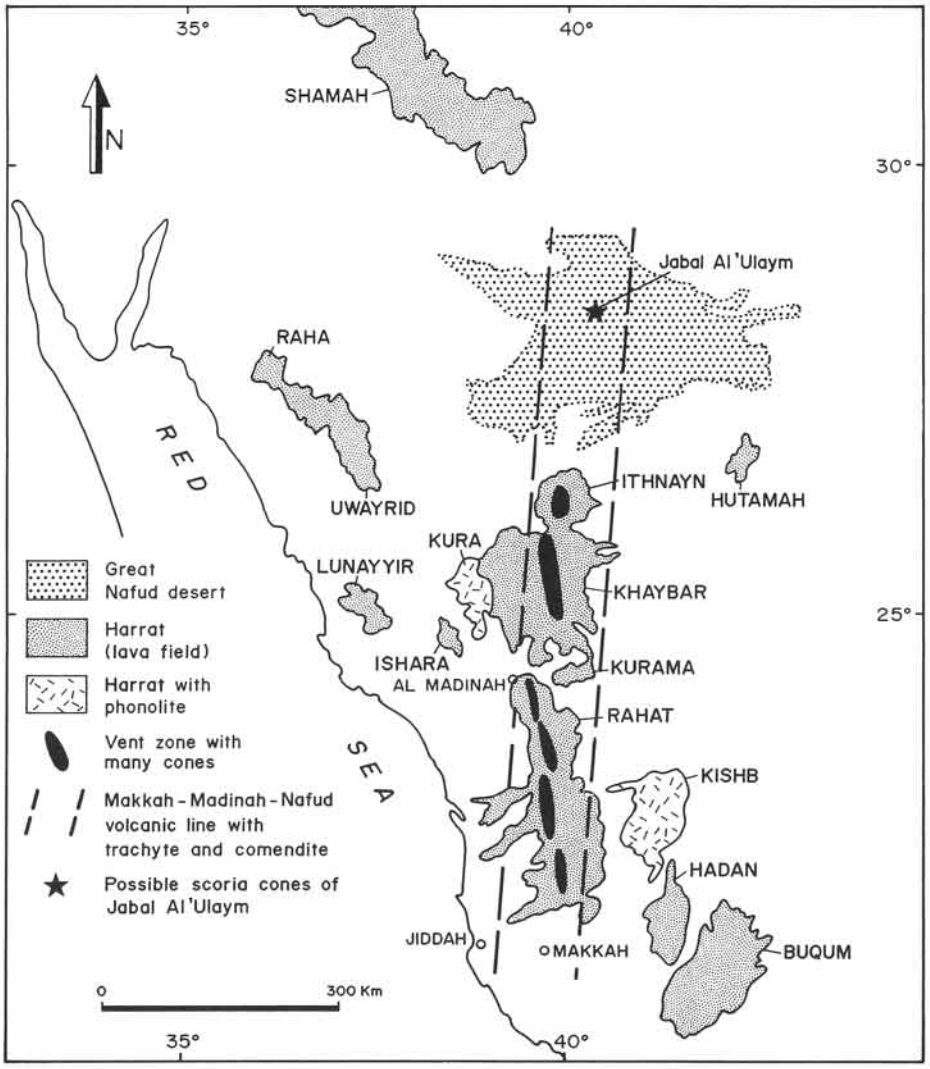

Figure 14-9: *Map of Neogene-Quaternary lava fields in western Arabia. The vent zones mark an en-echelon pattern of fractures, splaying away from the Red Sea rift zone.*

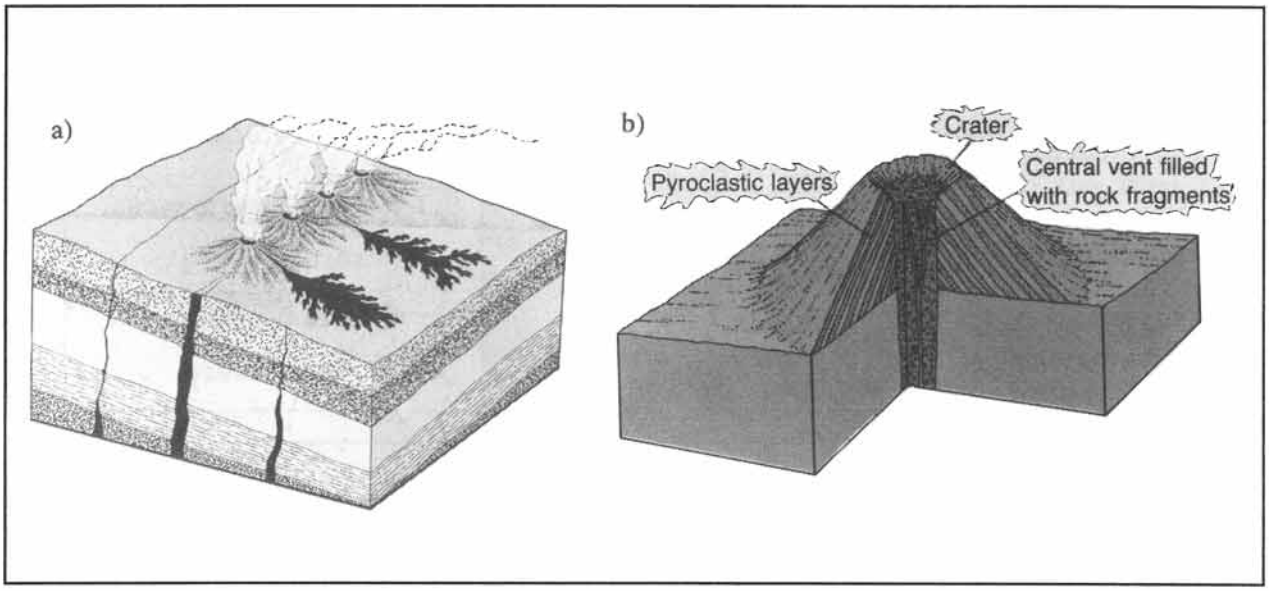

Figure 14-10: *The vent zones that feed flood basalts are commonly marked at the surface by a series of aligned cinder cones, that develop during a late stage in the eruption of each lava flood. a) Block diagram of aligned cinder cones. b) Detail of single cinder cone.*

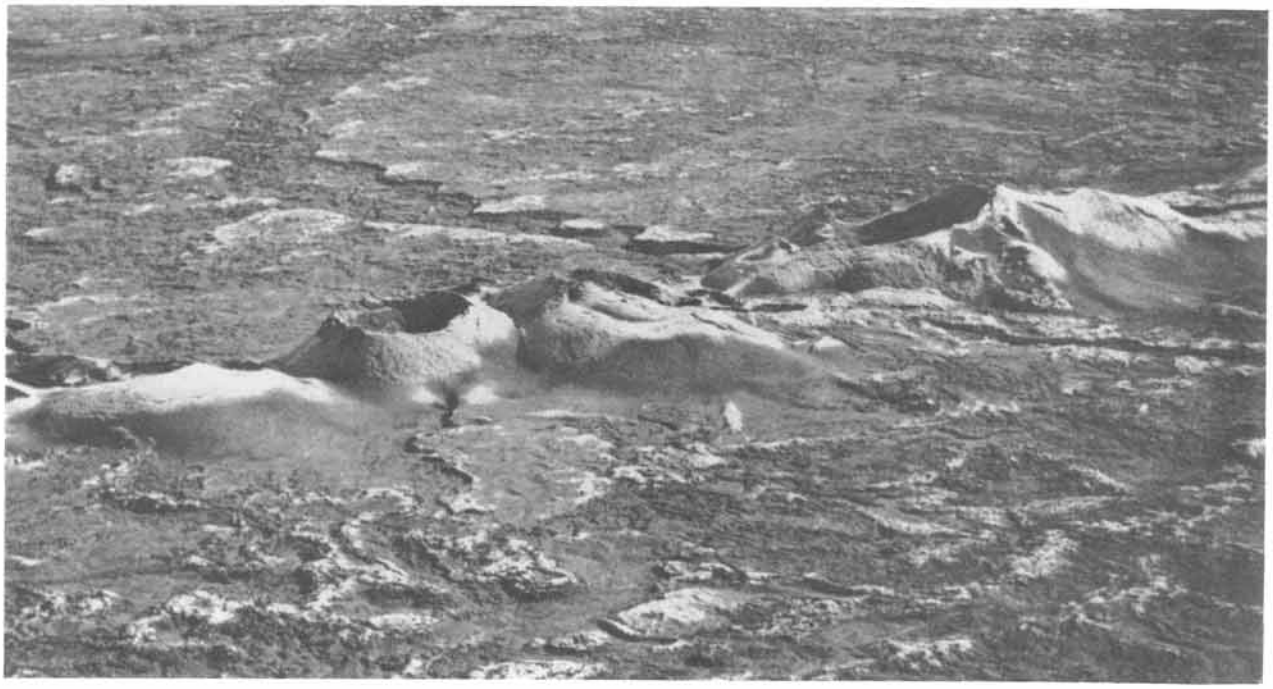

Figure 14-11a: *Cinder cones, formed in 1783, along part of the twenty-kilometer-long Laki fissure, Iceland.*

Figure 14-11b: *Aligned cinder cones of Harrat Kishb, Saudi Arabia.*

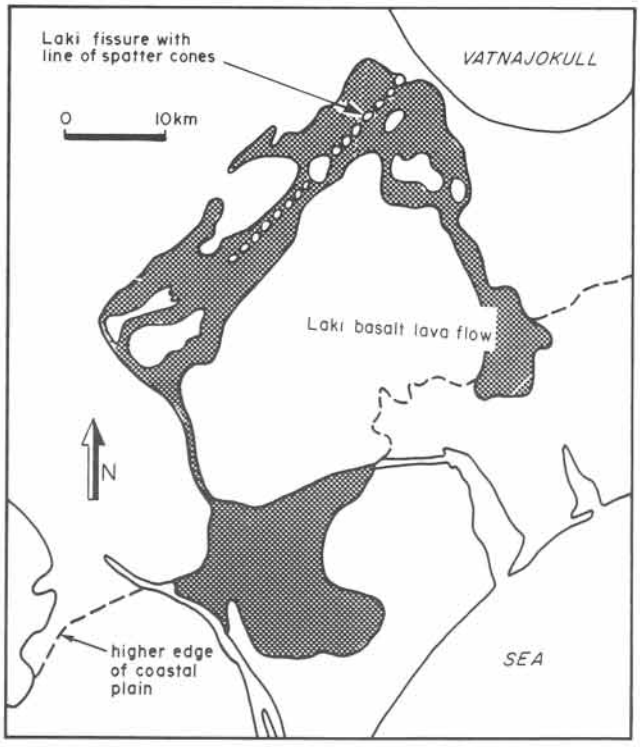

Figure 14-12a: *Map of the northeast-southwest trending Laki rift, showing the extent of the 1783 lava flood and the orientation of the cinder cones, Iceland.*

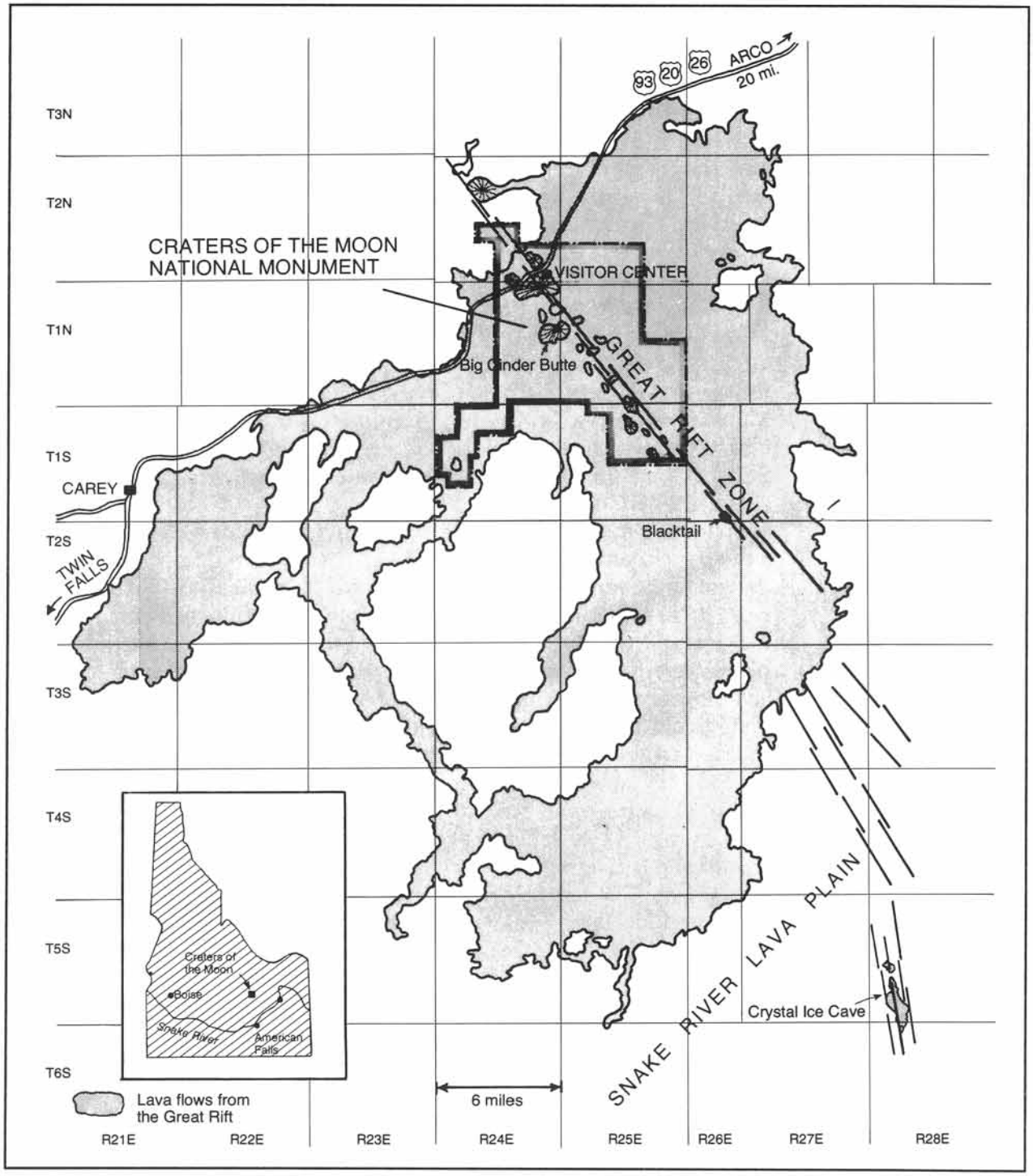

Figure 14-12b: *Map of the northwest-southeast trending Great Rift Zone, marked by cinder cones and the associated lava flows, Idaho. The cinder cones are part of the Craters of the Moon National Monument.*

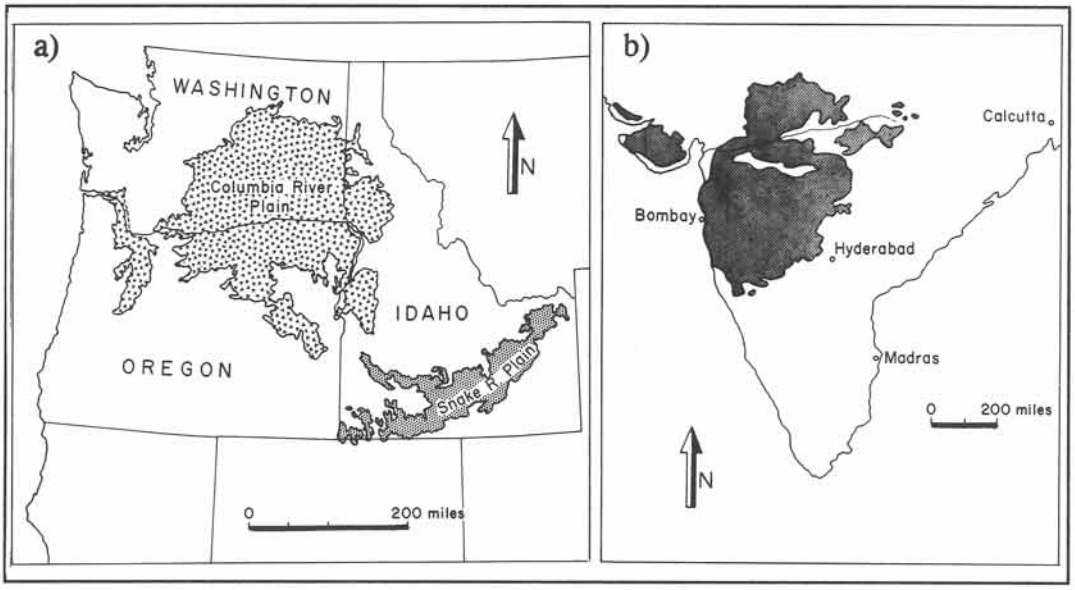

Figure 14-13: *a) Miocene flood basalts of the Columbia River Plateau, Washington. b) Cretaceous flood basalts of the Deccan traps, India.*

☐Exercise 14-1: Figure 14-14 is a schematic cross-section through a sequence of flood basalts. The succession includes shield volcanoes, feeder dikes, degraded cinder cones, erosion soils, and intercalations of continental sedimentary rocks. Discuss the geological history, implied by the section data.

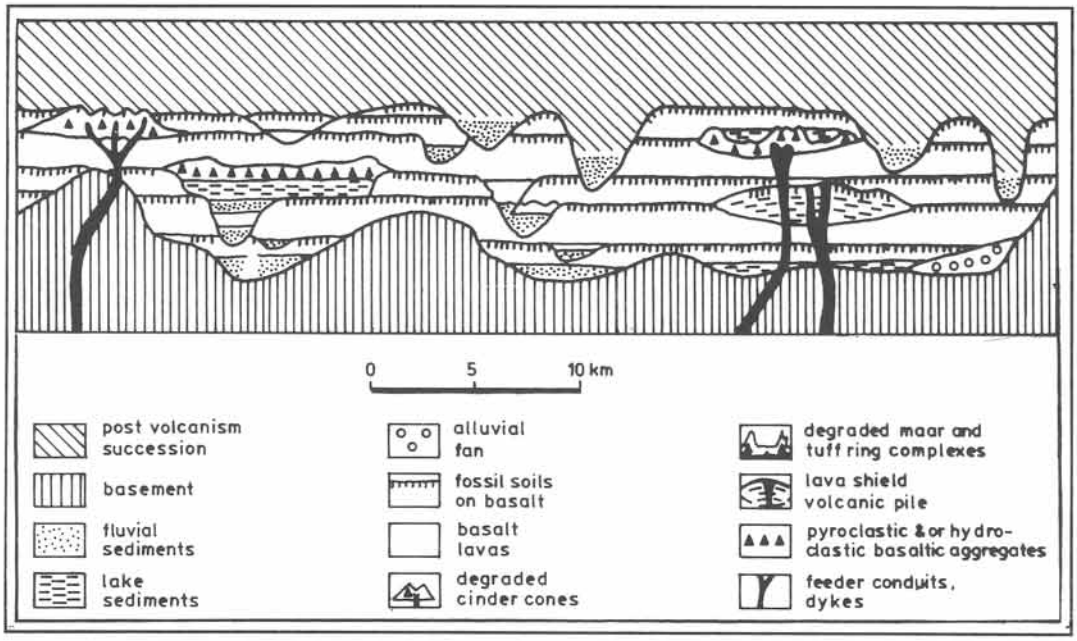

Figure 14-14: *Schematic cross-section of a flood basalt sequence. The vertical scale is of the order of one kilometer, and horizontal extent may be several hundred kilometers.*

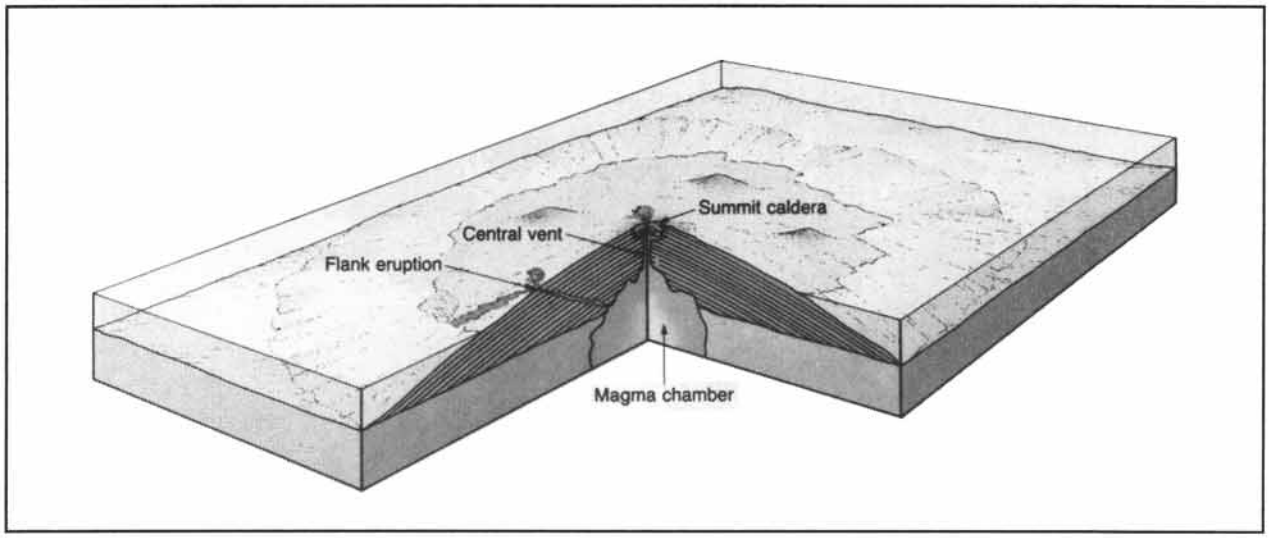

Figure 14-15: *Schematic perspective diagram of a shield volcano, built principally from stacked lava flows and only a small percentage of pyroclastics.*

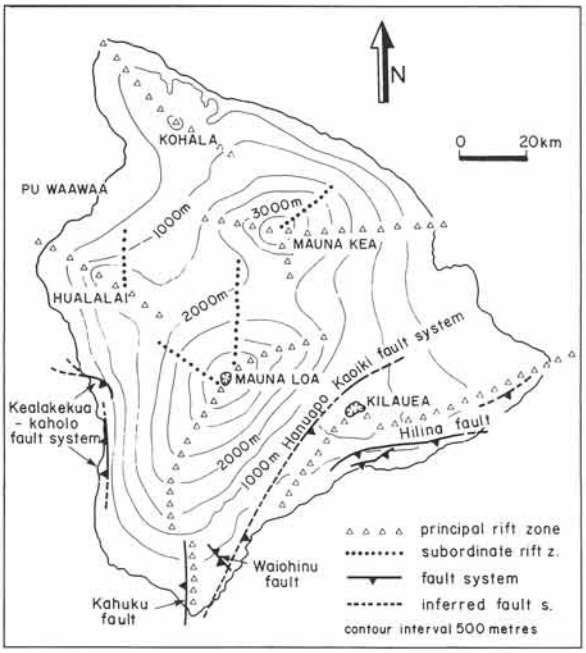

Figure 14-16: *The shield volcanoes of Hawaii; topographic contour map and location of the three principal shield centers, Mauna Kea, Mauna Loa, and Kilauea.*

14-4 Shield volcanoes

Rift zones and oceanic hot-spots may lead to the formation of basalt lavas, erupted from a single source. Basalt lavas have low viscosities and, therefore, spread out over large areas, forming shield volcanoes with width to height ratios of about ten (Fig. 14-15). *Shield volcanoes* contain few pyroclastic materials and are built up by successive lava flows accumulated by episodic eruptions over a time span of tens of thousands of years. The Kilauea volcano on the island of Hawaii has erupted over fifty times in recorded history. Mauna Loa, Hawaii's chief shield volcano, was built by eruption cycles, spanning about one million years (Fig. 14-16). The base of Mauna Loa rests on a five-kilometer-deep ocean floor, and its summit stands a full four kilometers above sea level. Most of the recent eruptions on Hawaii originate from linear fissures on the flanks of Mauna Loa (Fig. 14-17a to c). The Hawaiian Islands formed in a chain over a hot-spot. Movement of the Pacific plate has carried older shield volcanoes of this chain toward the northwest. Other examples of major shield volcanoes are Skalbreidur on Iceland and the Galapagos in the Pacific.

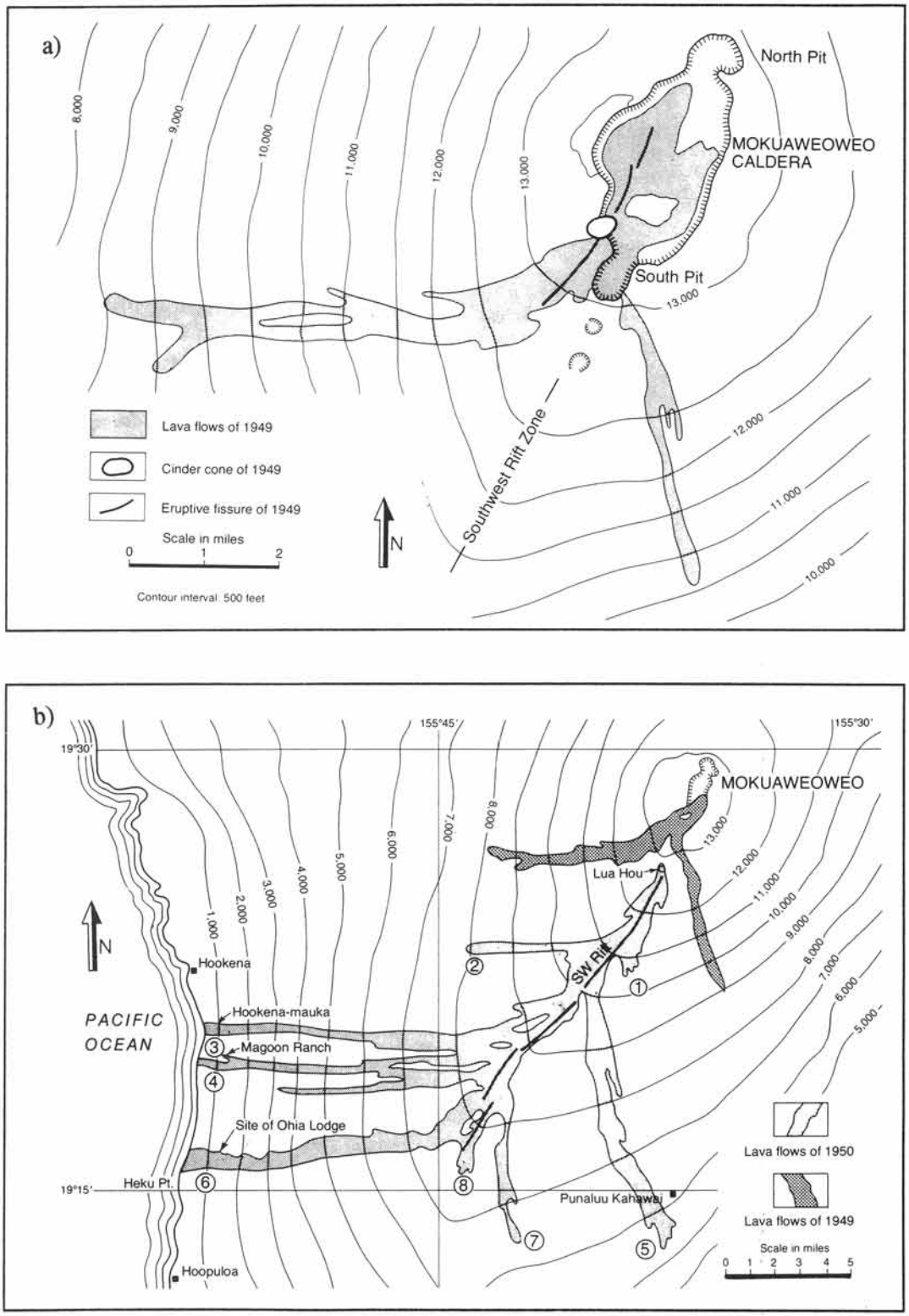

Figure 14-17: *Hawaiian fissure vents and associated lava flows on topographic base maps. a) Central rift in Mokuaweoweo collapse pit for 1949 flow. b) Southwest rift for 1950 flow.*

☐Exercise 14-2: Study the map of Figure 14-17c, and discuss the sequence of fissure eruptions that led to the eruption of the lava outbreaks, A to V, in chronological order.

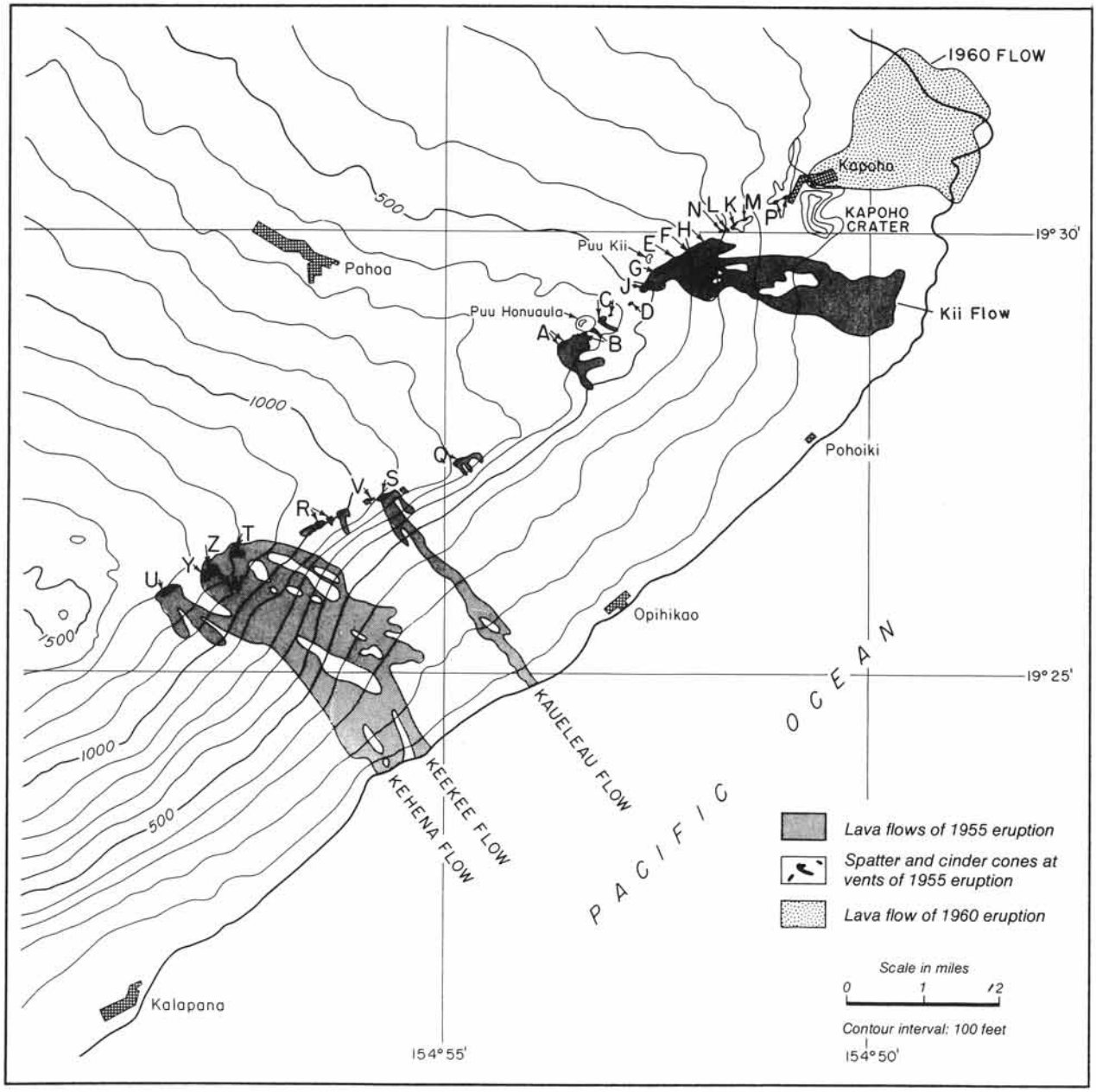

Figure 14-17c: *Rift zone east of Kilauea for lava flows of 1955 and 1960.*

14-5 Stratovolcanoes

The *stratovolcano* or *composite cone* is the archetype of the most abundant eruption cones (Fig. 14-18). Composite cones commonly form high mountains with concave slopes, contrasting with the convex shape of shield volcanoes. Fujiyama, on Japan's main island of Honshu, is a good example of a stratovolcano, rising up to nearly four kilometers high from a thirty-kilometer-wide basal diameter at sea level (Fig. 14-19a). Fujiyama lies on a line of active volcanoes on the Pacific plate, possibly representing a major fracture zone (Fig. 14-19b).

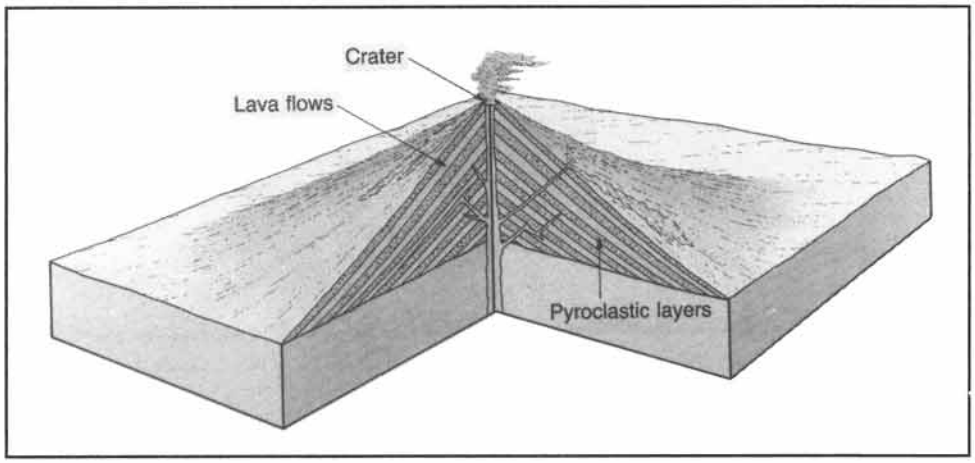

Figure 14-18: *Schematic perspective diagram of stratovolcano or composite cone, built of alternating layers of lava flows, epiclastics, and pyroclastics.*

Stratovolcanoes typically occur above slabs of oceanic lithosphere, descending into the mantle at active subduction zones. They frequently erupt, often explosively, and build stratovolcanoes from

Figure 14-19a: *Artistic representation of Mount Fuji (3776 m), Japan, with concave slopes characteristic of stratovolcanoes. Wood-block print by Hokusai - one of his thirty-six views of Mount Fuji.*

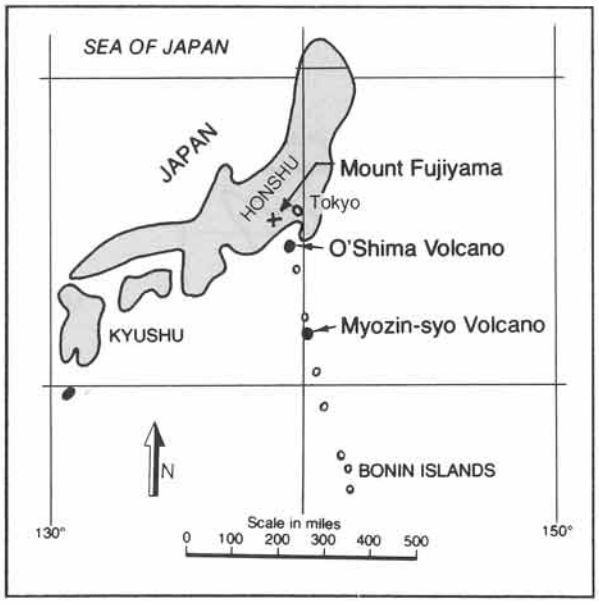

Figure 14-19b: *Location map of Mount Fuji and its alignment with volcanic islands off-shore.*

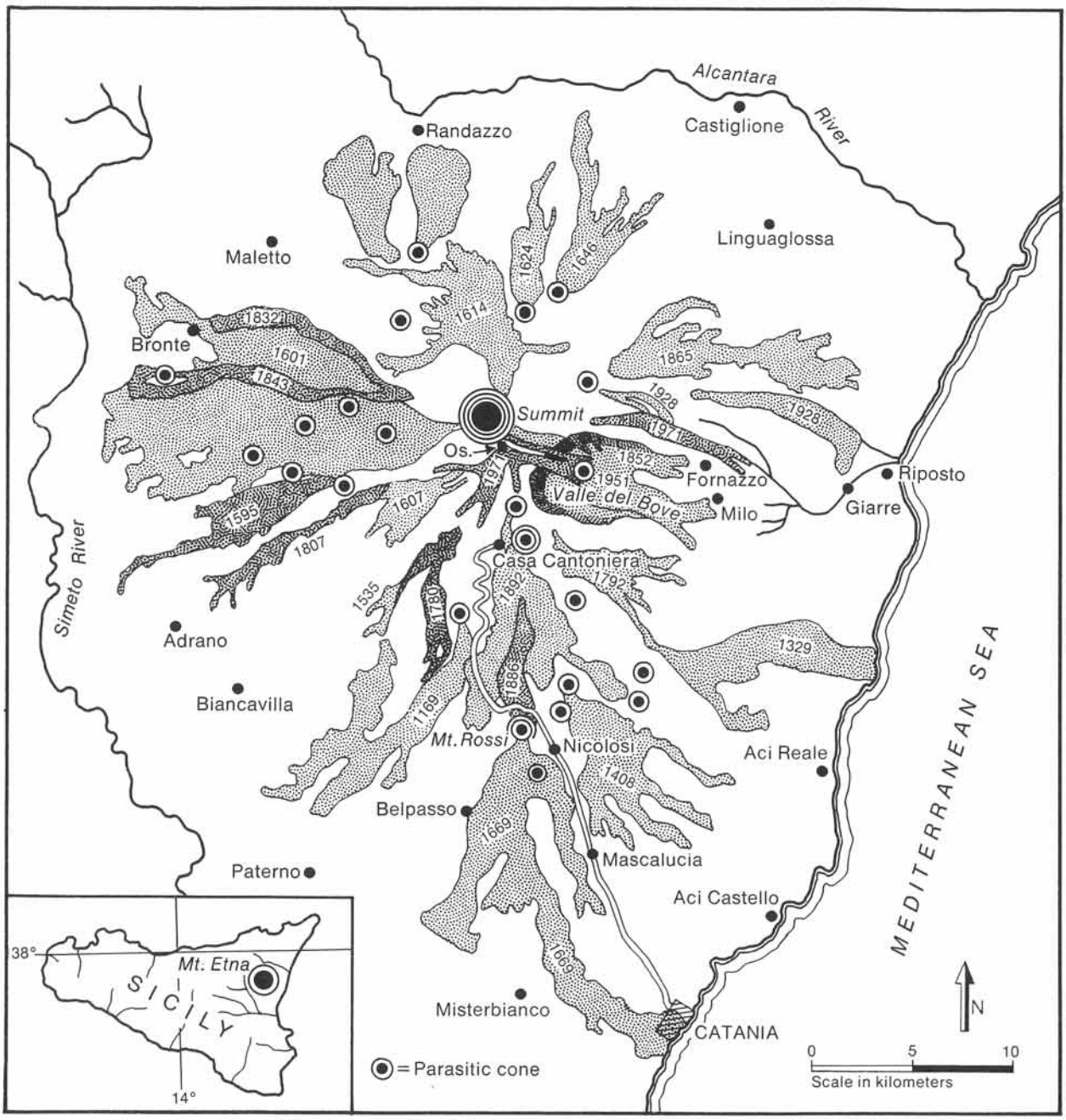

Figure 14-20: *Map of historic lava flows on Mount Etna, Sicily. The former volcanological observatory (marked: Os.) was destroyed during the 1991 eruption.*

interleafing layers of lava flows and pyroclastics. *Epiclastic deposits*, which consist of a mixture of rocks displaced by the eruption, are commonly encountered. The explosive character of stratovolcanoes originates from a higher water and gas content. The lavas erupting from them commonly contain a higher silica fraction than basic lavas. But no stratovolcano is wholly acid, because they, also, include basalt and andesite interstratified with acid lavas. Extreme compositions of stratovolcanoes occur in Mount Fuji (mainly basaltic) and Mt. Pelée (dominantly andesitic).

Figure 14-20 maps some of the principal lava flows observed at Mount Etna, Sicily, in recent history (1169-1971). Etna rises 3.5 kilometers above sea level and is extremely active. The most violent eruption in recent history occurred in 1669 and a fifteen-kilometer-long lava flow destroyed the city of Catania. It can be inferred that a volcano of Etna's size requires about one million years to build by episodic eruption of lavas and pyroclastics. The map pattern of the lava flows is chaotic and spreads away from the volcano summit. The detailed location of these lava flows is largely controlled by radial fissures, propagating from the summit downward.

Huge portions of the summit of mature stratovolcanoes may be blasted away after their slopes have become so steep that it is mechanically feasible to collapse them. The violent 1980 eruption of Mount St. Helens, Washington, was accompanied by massive sliding of its steep northern flank and a magnitude five earthquake (Fig. 14-21a to d). The slide lowered the volcano summit by about 400 meters, forming a two-kilometer-wide and 700-meter-deep breached crater. The sliding and summit collapse were triggered by increasing pore pressure, caused by expanding volcanic gases and magma, which lowered the frictional resistance of potential slide surfaces. Previous eruptions are known to have taken place from 1842 to 1857 and about 1,900 BC. The 1980 eruption caused 36 deaths, and 23 persons were reported permanently missing. Geologist David Johnston was killed by a pyroclastic flow, while monitoring the volcano more than nine kilometers away from the mountain peak. A significant number of casualties were caused by the debris-laden mudflows, rushing down the mountain slopes after the sudden melting of the snow and ice cover of Mt. St. Helens.

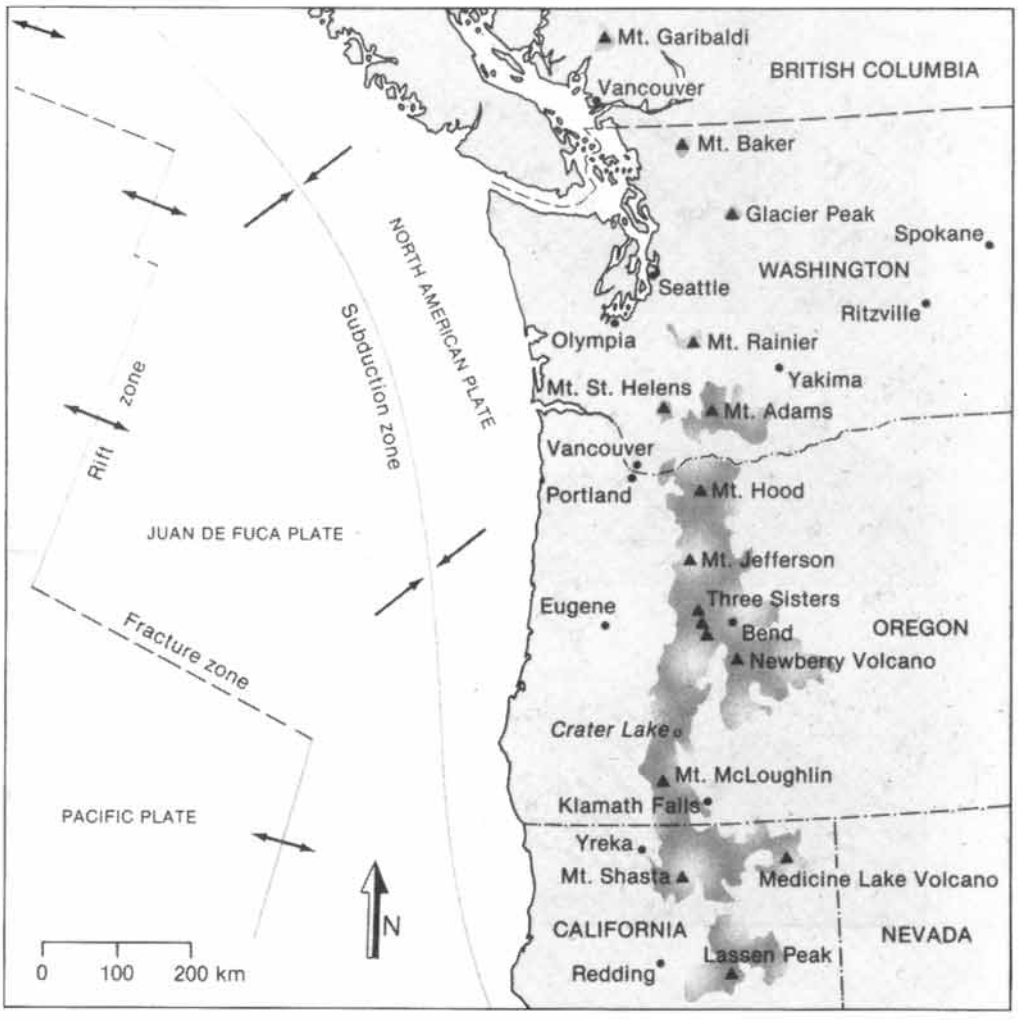

Figure 14-21a: *Location map of Mount St. Helens, Washington, and related volcanoes in the active belt of the Cascade Ranges. Dark-shaded areas are Quaternary extrusives.*

The violent eruptions of stratovolcanoes have claimed the majority of all human casualties and massive destruction related to volcanic activity. Some terrifying examples are: 30,000 deaths, caused by the glowing avalanche released during a 1902 eruption of Mount Pelée, Martinique; 16,000 deaths, caused by the 79 AD eruption of Mount Vesuvius, Italy; 36,000 deaths by ashfall and flood waves, set up by the 1883 eruption of Krakatao, Indonesia; 80,000 deaths by the famine, due to the 1815 eruption of Tambora, Indonesia, spoiling the crops; 25,000 deaths by mudflows from the 1985 eruption of the Nevado del Ruiz, Colombia.

☐Exercise 14-3: Estimate the length of transport involved in the displacement of the slide masses of the Mount St. Helens collapse.

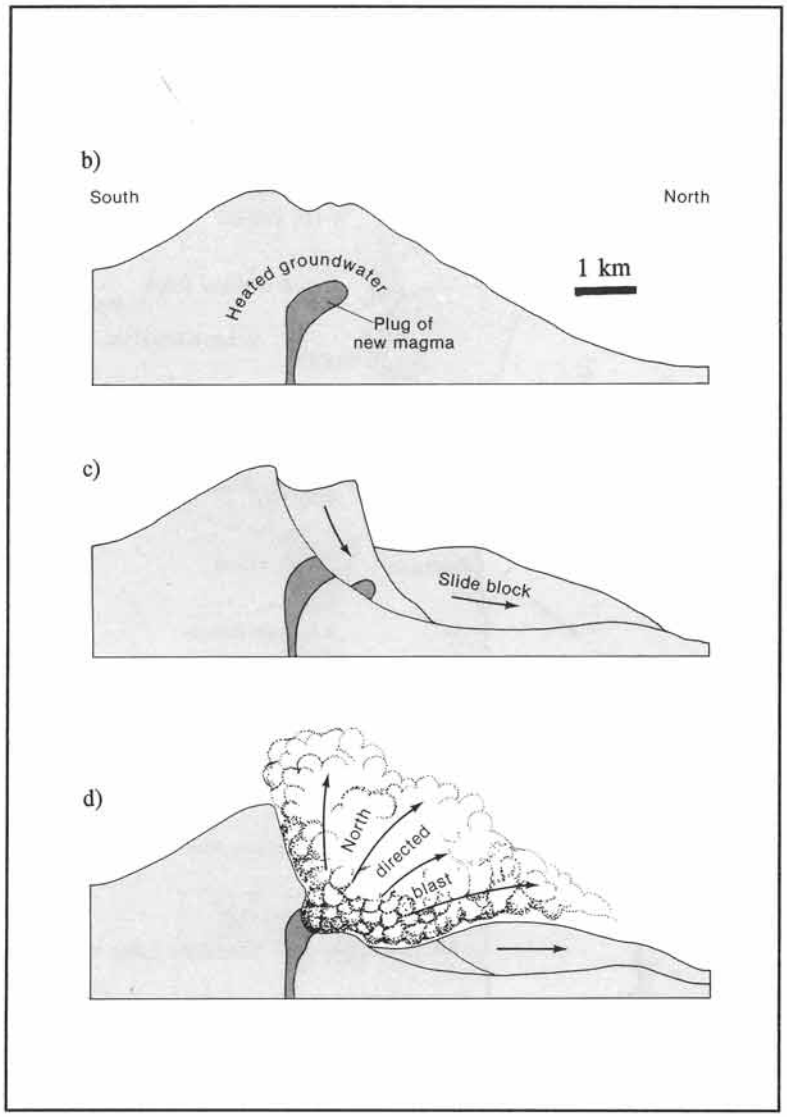

Figure 14-21: *b) to d) Collapse and sliding of Mount St. Helens during the violent 1980 eruption.*

14-6 Mudflows

The danger of *mudflows* or *lahars* (Indonesian) poses a serious hazard in volcanic terrains. They may be triggered by massive melting of ice caps following minor eruptions, by heavy rainfall that washes away unconsolidated deposits of recent ashfalls, or by overflowing of crater lakes by reactivation of dormant volcanoes. Mount Rainier, a dormant stratovolcano located about one hundred kilometers northeast of Mount St. Helens, is listed as a volcano likely to erupt before long. This more than four-kilometer-high volcano is largely covered by glaciers (Fig. 14-22a). Careful mapping has revealed the extent of two ancient mudflow deposits, i.e., the 500-year-old Electron mudflow and the 5,000-year-old Osceola mudflow (Fig. 14-22b). The Electron mudflow consists of 0.2 cubic kilometers; the Osceola flow has a volume of 2.5 cubic kilometers. The last eruption of Mount Rainier took place between 120 and 150 years ago. A map of potential hazards caused by a future eruption of Mount Rainier, published by the United States Geological Survey, outlines the risk areas for mudflows, lava flows, and ashfall (USGS map L-836 by D.R. Crandell, 1973).

Scarcity of volcanic hazard maps and poor public awareness still lead to tragedies, which might have been averted or limited if the potential dangers were better understood. In 1985, eruption of the Nevado del Ruiz volcano, Colombia, triggered mudflows. Several valleys were filled with mudflows, including the Lagunillas River, which buried the town of Armero, fifty kilometers away from the volcano summit. The mudflows reached speeds of forty to sixty kilometers per hour. Almost the entire population of 22,000 was either buried alive or drowned in muddy and debris-laden waters. The rampage was closely televised, with horrifying footage of failed attempts to rescue victims sinking away in the deep mud.

Geologists were aware of the potential danger posed by the dormant Nevado del Ruiz. Armero itself was built on the ruins of an earlier, 1845 mudflow, which had killed about 1,000 people. The delay between the 1985 eruption and the arrival of the mudflows in Armero was about two hours. However, there was no flood warning system - which is lacking in many regions of potential mudflow - and the population of Armero was taken by complete surprise.

☐Exercise 14-4: Order from your library or through interlibrary loan a copy of the USGS-Special Publication L-836. Study the hazard map, and discuss the merits of hazard control studies.

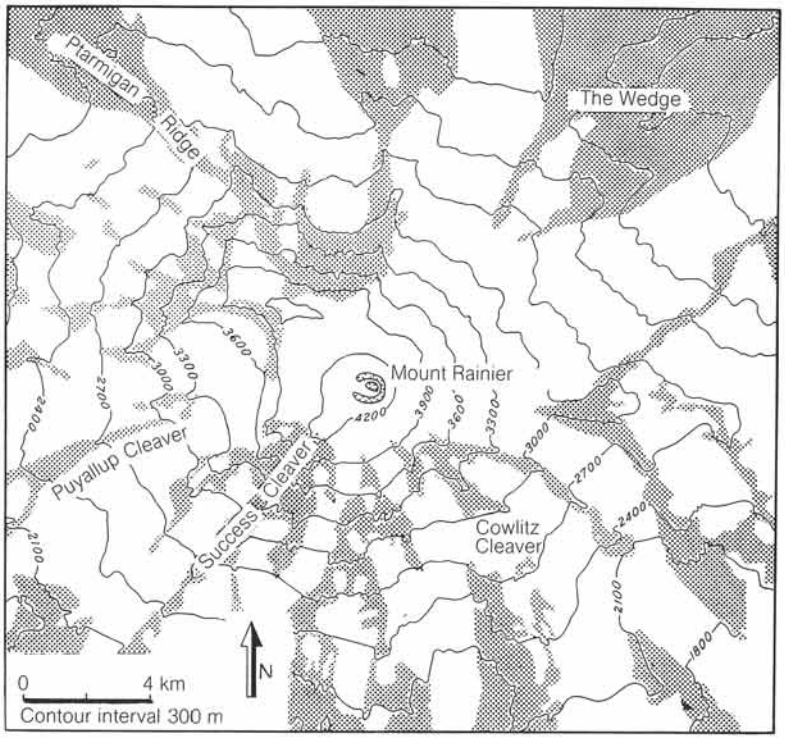

Figure 14-22a: *Topographic map of summit-area of Mount St. Rainier, Washington, marked with permanent glacier cover (white) and areas of bare rock (shaded).*

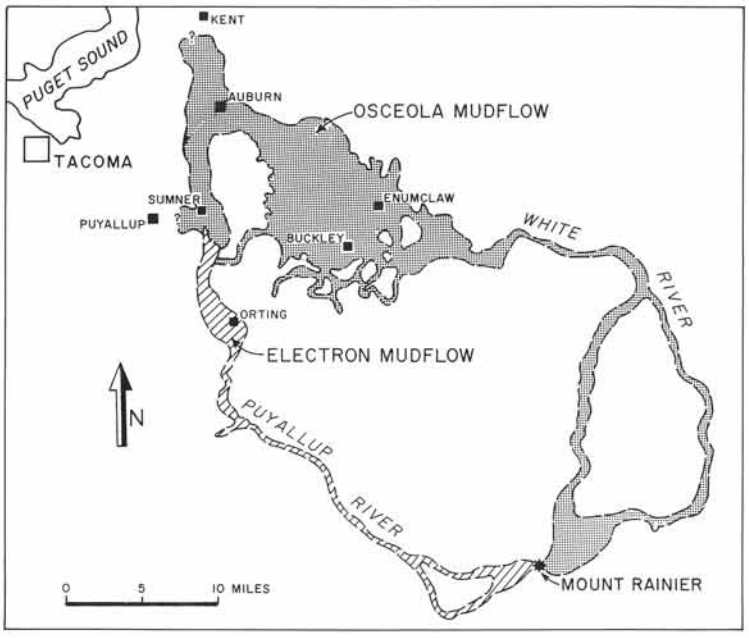

Figure 14-22b: *Regional map showing extent of the historic mudflows of Electron (500 years ago) and Osceola (5,000 years ago).*

14-7 Glowing avalanches

Apart from lava flows and mudflows, the eruption of stratovolcanoes is often accompanied by *glowing avalanches* or *nuée ardentes* (French). These are blasts of steam and hot gases, which engulf air and smoldering ejecta, consisting of rock fragments, lava bombs, and hot volcanic ashes. The resulting deposits, formed by the ejecta, range from ignimbrite, pumice, and tephra to felsic tuff, and block and ash deposits. For example, Mount Pelée erupted andesite domes and nuée ardente, which are filled with dense blocks of dome material.

The Roman city of Pompeii on the southern slope of the Vesuvius stratovolcano was struck by glowing avalanches in 79 AD, and subsequent ashfall buried the entire city in several-meter-deep pyroclastics (Fig. 14-23a & b). The city was forgotten and not rediscovered until about 1750. The excavation work now spans more than two centuries and is continuing at present. Numerous remains of persons and animals, trapped in the ashes, have been found in cavities formed by the ashes, which originally covered their bodies. Many of the cavities have been filled with gypsum, and the cured casts show the victims in agonizing positions (Fig 14-23c & d).

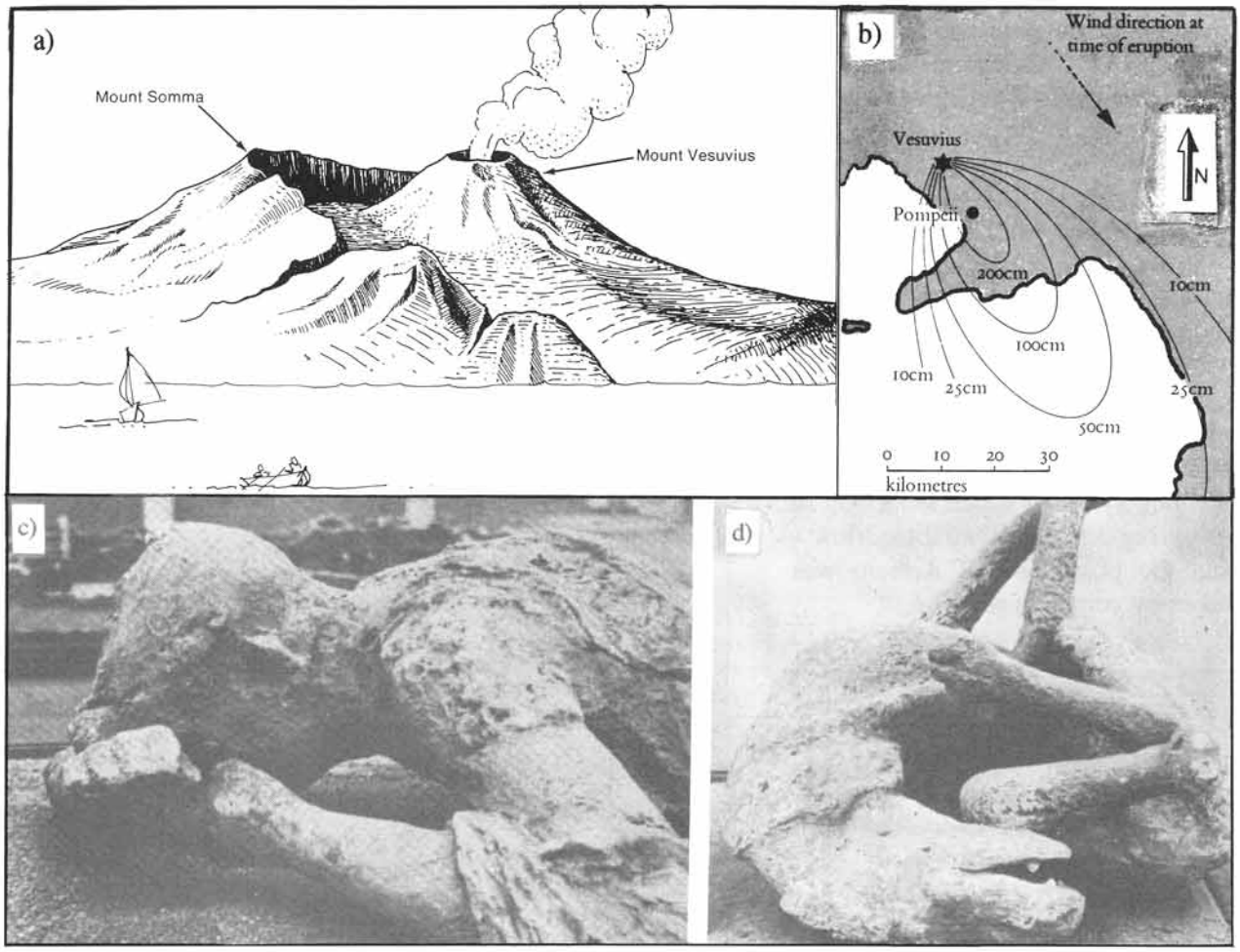

Figure 14-23: *Mount Vesuvius, Italy. a) Perspective view of Mount Vesuvius and its location within the caldera rim of Mount Somma. b) Isopach map of pyroclastics, deposited during the 79 AD eruption, which buried Pompeii. c) and d) Gypsum casts of victims of Pompeii (man and dog).*

The entire population of St. Pierre, Martinique, was killed by a nuée ardente, which flowed down from the erupting Mount Pelée in 1902 (Fig. 14-24a). Martinique is part of the volcanic island arc, located where the Caribbean plate overrides a subduction zone of Atlantic plate (Fig. 14-24b).

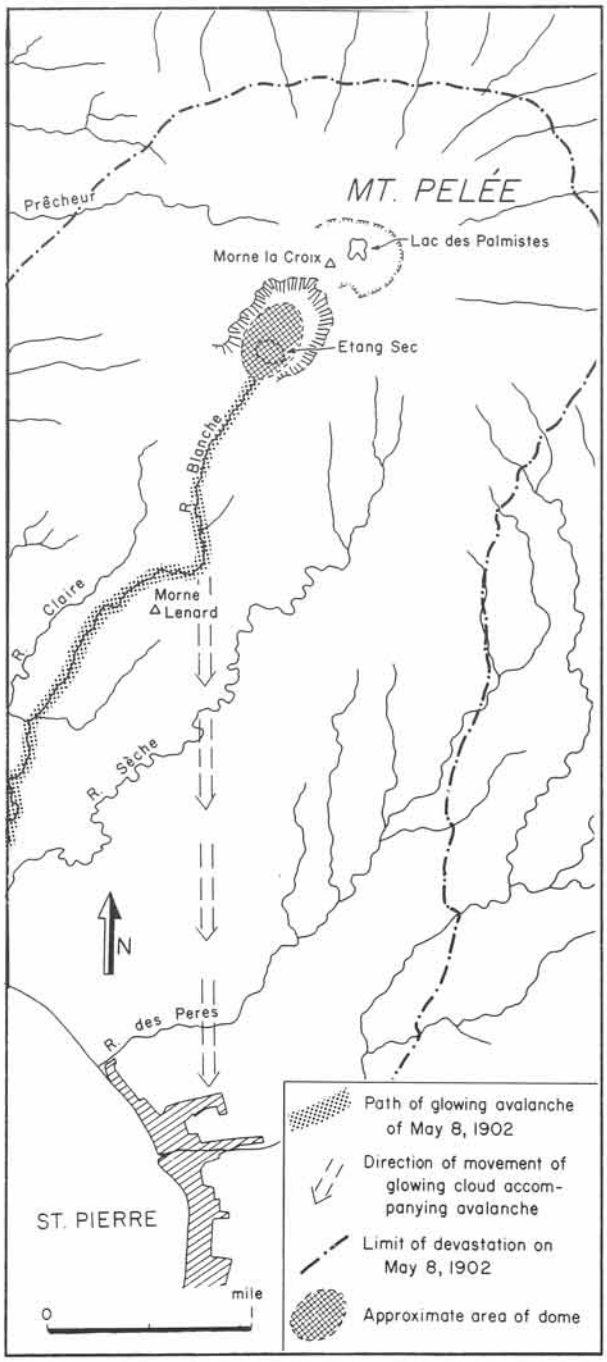

Figure 14-24a: Map of Mount Pelée, Martinique, and relative position of St. Pierre, hit by the nuée ardente of 1902.

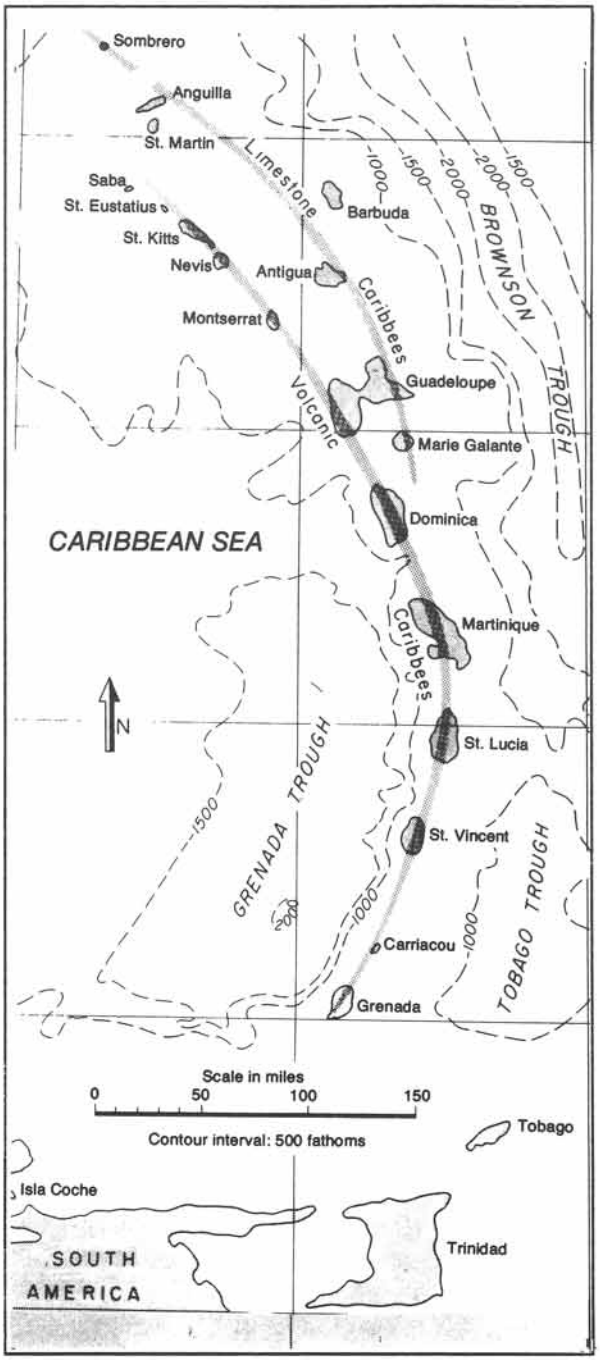

Figure 14-24b: Martinique is set within the volcanic island arc, which marks the leading edge of the Caribbean plate in the west overriding the subduction of the Atlantic plate in the east.

Figure 14-25: *Ruins of St. Pierre with Mount Pelée in the background, shortly after the glowing avalanche of May 8, 1902.*

The city of St. Pierre was actually destroyed by a surge of ash, which was part of a large pyroclastic flow over an area much wider than covered by the coarse, block-rich base of the flow. The nuée ardente collapsed thick masonry walls, uprooted large trees, and tore cannons from their mounts. The pressure wave capsized vessels moored in the harbor, and the hurricane of fire set ablaze the remaining ships. Only one out of eighteen vessels, the British steamship *Roddam*, managed to steam away with a dying crew, losing more than half of the men aboard due to burning and suffocation. The total destruction of St. Pierre was completed within a few minutes and left everything covered by a thin layer of smoldering volcanic ejecta (Fig. 14-25).

Figure 14-26 is a map of the Hibok-Hibok volcano, Camiguin Island, Philippines. An eruption in 1948 sent down mudflows, which destroyed part of Agoho village. A globule or dome of viscous lava started to grow in the summit of the crater early in 1949, episodically accompanied by explosions and minor glowing avalanches. However, massive nuée ardentes speeded down the slopes of Hibok-Hibok on 4 and 6 December, 1951 (Fig. 14-26). They killed about five hundred people in small villages southwest of Mambajao. The temperature of glowing avalanches reaches about seven hundred degrees centigrade, and they move fast, also. Glowing avalanches, emitted by Mount St. Helens, reached speeds of one hundred kilometers per hour.

The thickness of the ash deposits of the 79 AD Vesuvius eruption is dwarfed by the 1912 eruption of the Katmai volcano, Alaska (Fig. 14-27a). The isopach map of the ash deposits shows the maximum thickness reaches up to fifty feet close to the volcano proper (Fig. 14-27b). The explosive eruption took place at a vent at Novarupta, five kilometers west of the Mount Katmai summit. However, the massive release of ejecta from Novarupta was inferred to be coeval with caldera formation at Mount Katmai, lowering its summit by 400 meters and creating an oval depression of three to four kilometers wide and 600 meters deep. The area was not visited until several years after the eruption but was still fuming large quantities of white smoke, mostly escaping water vapor and gases (Fig. 14-28a). The director of the Katmai expeditions by the *National Geographic Society*, R.F. Griggs, termed it the Valley of Ten-Thousand Smokes. This ashfall deposit consists of pumiceous ash or *ignimbrite*, transported as a nuee ardente, which closely followed the topography of the terrain (Fig. 14-28b). The ignimbrite of the Valley of Ten-Thousand Smokes travelled a maximum distance of 22 kilometers from its source; ignimbrites have been mapped elsewhere at maximum distances of up to 225 kilometers from their eruption source.

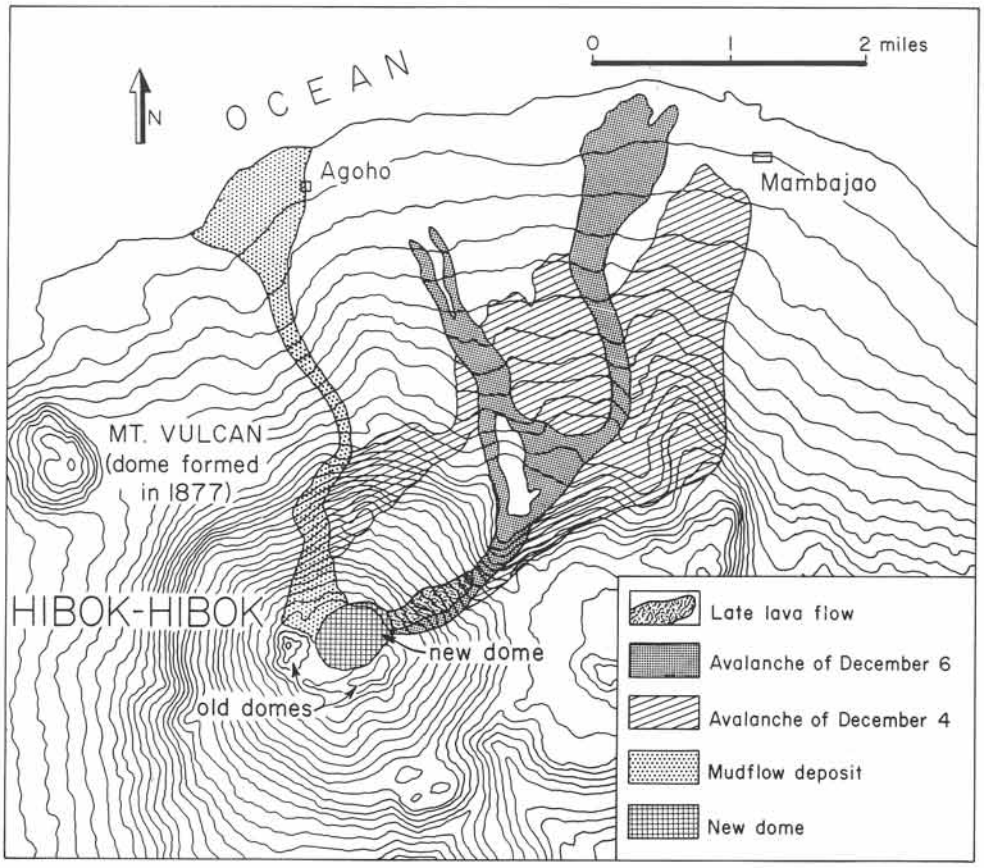

Figure 14-26: *Map of glowing avalanches and mudflows of Mount Hibok-Hibok, Camiguin Island, Philippines.*

Figure 14-27a: *Location map of Katmai volcano, Alaska.*

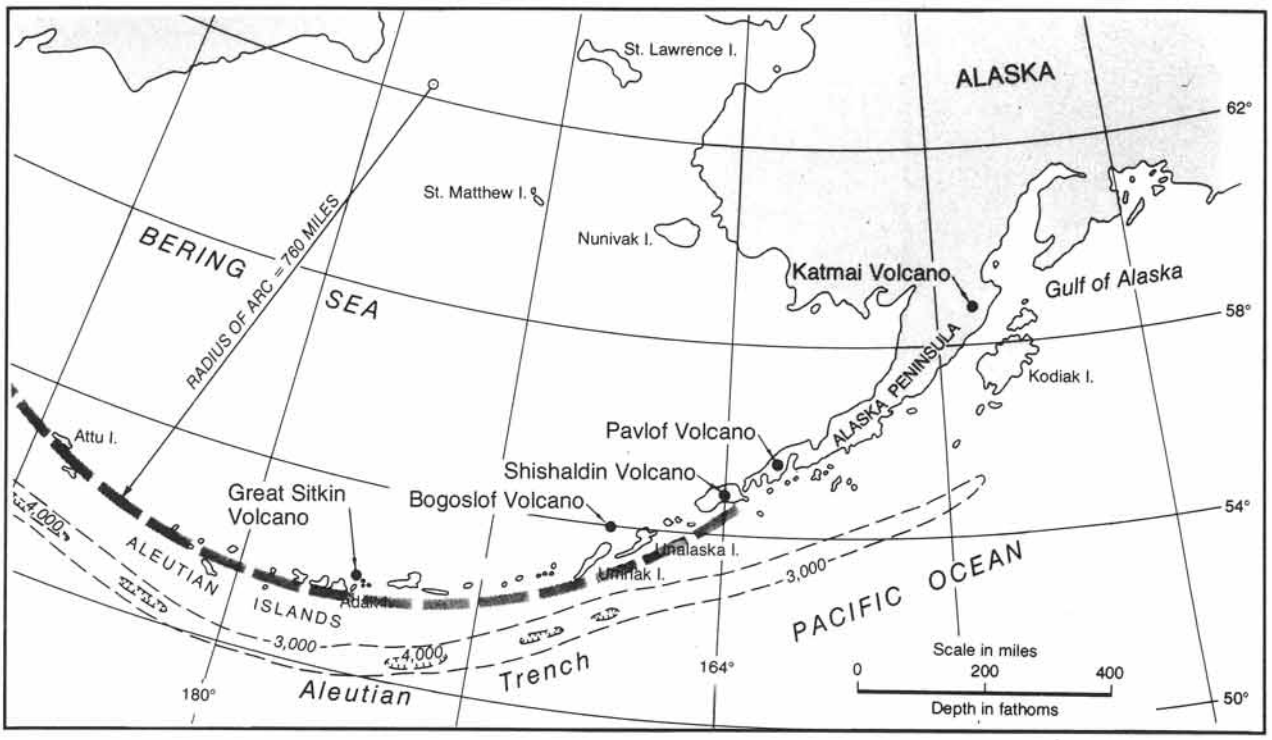

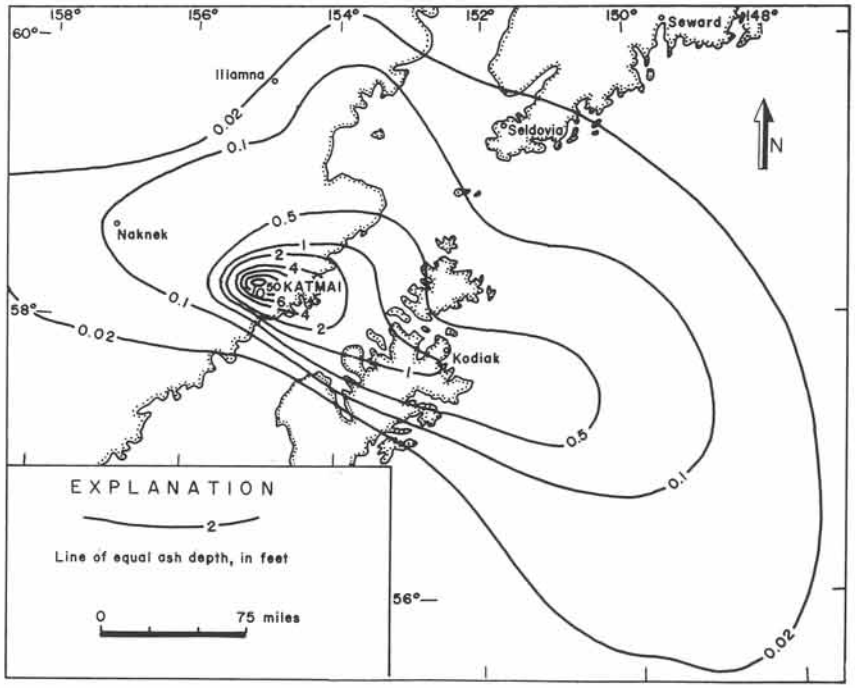

Figure 14-27b: *Isopach map for ash deposits of June 1912 eruption that created the Valley of Ten-Thousand Smokes.*

Figure 14-28: *Katmai volcano, Alaska. a) Valley of Ten-Thousand Smokes, as photographed by Griggs. b) Map showing the extent of the 1912 ignimbrite, associated with the glowing avalanche from the Novarupta vent.*

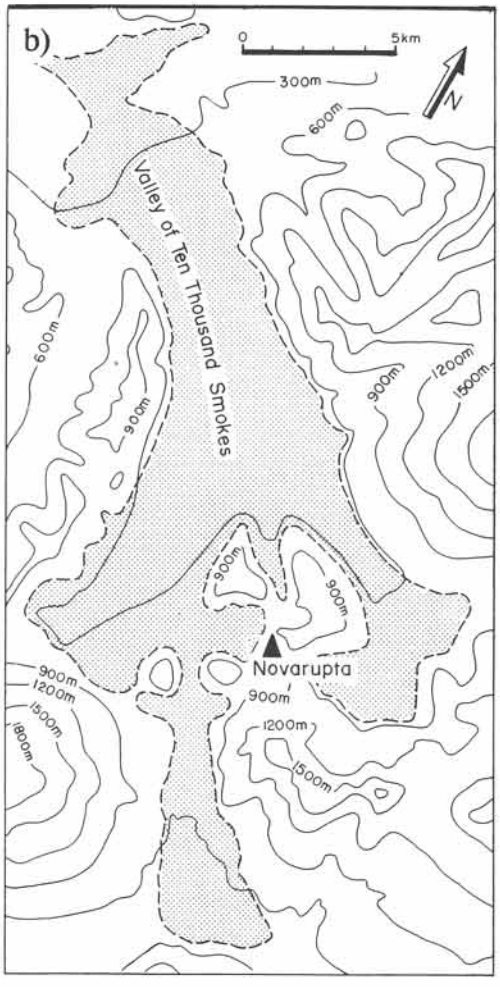

14-8 Craters and calderas

The collapse of Mount St. Helens, immediately prior to the May 18, 1980 eruption, was observed from a light aircraft about 400 meters above the summit. The gigantic, deep-seated landslide was an eye-opener and helps to understand better the historic disappearance of two major islands: Santorini and Krakatao.

A major island subsidence occurred about 1,500 BC in the volcanic archipelago of the Aegean Sea, Greece. The Minoan city of Akroteri, located on the flanks of the huge stratovolcano Santorini, suddenly subsided in a giant explosive eruption, accompanied by caldera collapse (Figs. 14-29a to c). The volume involved in the Santorini collapse is estimated at sixty cubic kilometers, more than three times larger than that of the Krakatao subsidence (see later). Santorini is considered one of the most likely locations for the legendary lost empire of Atlantis, which, according to Plato (427-347 BC), subsided into the ocean. The Santorini collapse must have been

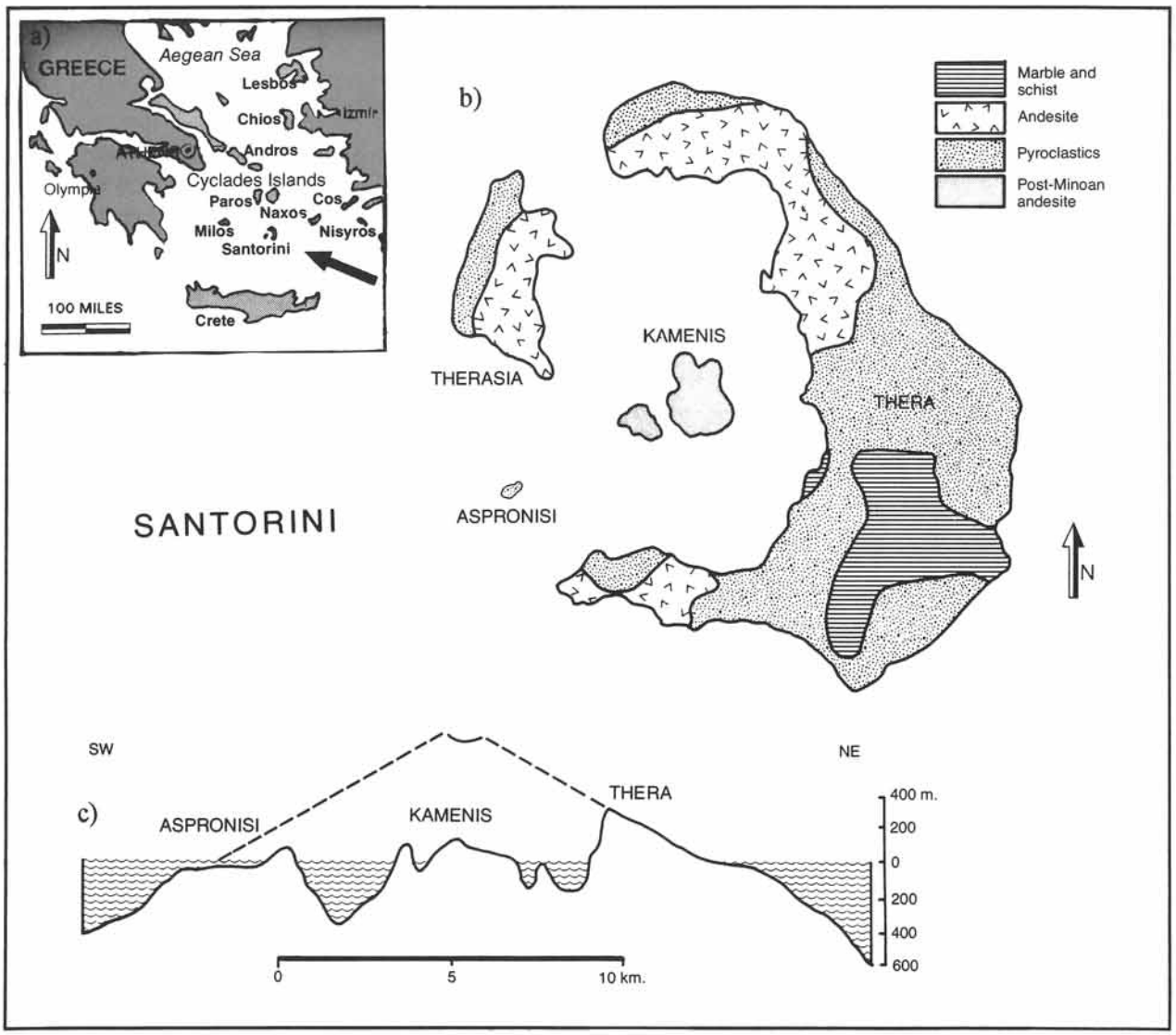

Figure 14-29: *Santorini volcanic complex, Aegean Sea, Greece. a) Location map. b) Geological map. c) Modern section and approximate outline of the volcano cone before its collapse, 1,500 BC.*

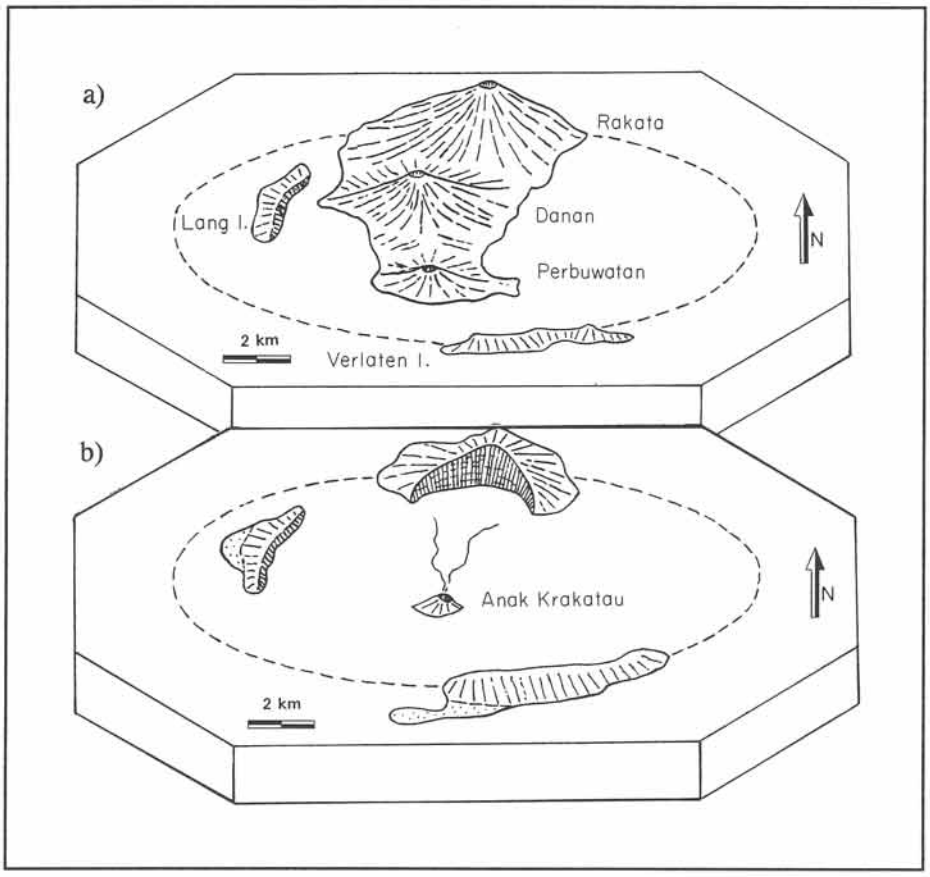

Figure 14-30: *a) & b) Perspective views of the Krakatao group before and after the eruption of 1883. Anak Krakatao, which emerged in 1930, is included.*

accompanied by a gigantic flood wave or *tsunami* (Japanese), and cities of the Minoan civilization on Crete, destroyed around 1,400 BC, are covered with pumice ashfall. Pumice layers of Thera, Santorini, have been excavated by French engineers to manufacture cement for construction of the Suez Canal. They uncovered man-made artifacts, which later were radiometrically dated at about 1410 BC (plus or minus 100 years). The Santorini volcano recovered by creating a new cone in the center of its collapsed caldera; the island of Kamenis rose in 197 BC with episodic additions until 1926. Incidentally, Wizard Island in Crater Lake, Oregon (section 13-3) is another example of a re-emergent volcano inside a caldera.

The main island of the Krakatao group, located in the Sunda Straits, Indonesia, almost completely vanished during an extremely violent eruption in 1883 (Figs. 14-30a & b). The rumbling explosion of the island was heard at thousands of kilometers distance. The 450-meter-high cone subsided in the blast and left the ground-floor 275 meters below sea level. The huge seismic tremors and submarine mass displacements caused a thirty-meter-high flood wave, which swept the coastlines of Sumatra and Java, killing 36,000 people (Fig. 14-31). It is not entirely clear whether the subsidence of Krakatao was due to lateral rock slides or vertical caldera subsidence or both. However, in 1930, volcanic eruptions pushed a new island above sea level (at the site of the formerly subsided volcano). It was appropriately named Anak Krakatao (Son of Krakatao). It now stands 200 meters high and measures nearly two kilometers in diameter.

The terms *caldera* and *crater* are somewhat mixed up in the literature, but for volcanologists they form by very different mechanisms. Craters result from outward explosion of debris and calderas by the inward subsidence of the volcanic superstructure into a partially erupted magma chamber. There is no hard rule about the field distinction, but, usually, calderas are defined as having diameters in excess of five kilometers, whereas craters are smaller than five kilometers in diameter. Volcanic subsidence features that

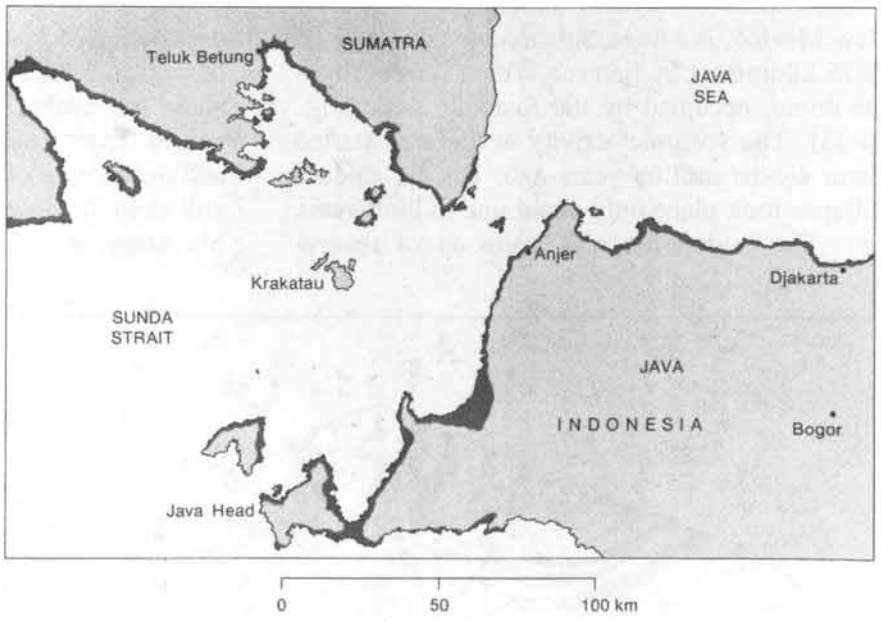

Figure 14-31: *Map of coastal area (shaded) inundated by tsunamis, originating from the 1883 collapse of Krakatao, killing an estimated 36,000 people.*

are less than five kilometers in diameter are termed *pits*. For example, the summit of Mauna Loa, Hawaii, hosts the Mokuaweoweo and several other, smaller *collapse pits* (Fig. 14-32).

☐Exercise 14-5: Calculate the volume (cubic kilometers) involved in the collapse of a volcano summit, which reduces its height by 300 meters. The slope of the original summit cone was 30°. Use the simple cone formula $V=\pi R^2h/3$, with base radius R and height h. Also, give an equation, expressing the volume in terms of height and slope, α, only.

Figure 14-32: *Oblique aerial view northward over the collapse pits of Mauna Loa, Hawaii. The summit of Mauna Kea appears in the background.*

The Valles Caldera in the Jemez Mountains, New Mexico, is a huge, subcircular caldera of 12 to 15 kilometers in diameter with a central rhyolite dome, occupied by the Redondo peak (Fig. 14-33). The volcanic activity in the area started about eleven million years ago, but the caldera collapse took place only about one million years ago. The caldera floor is made up of several jostled and tilted cauldron blocks, in between which new eruptions formed a dozen rhyolite domes. The caldera walls stand about 700 meters above the caldera floor. The volcanic activity has ceased, apart from the fuming of some solfatares and occurrence of hot springs. The welded tuffs and rhyolite flows on the slopes of the Jemez Mountains are developing inverted relief.

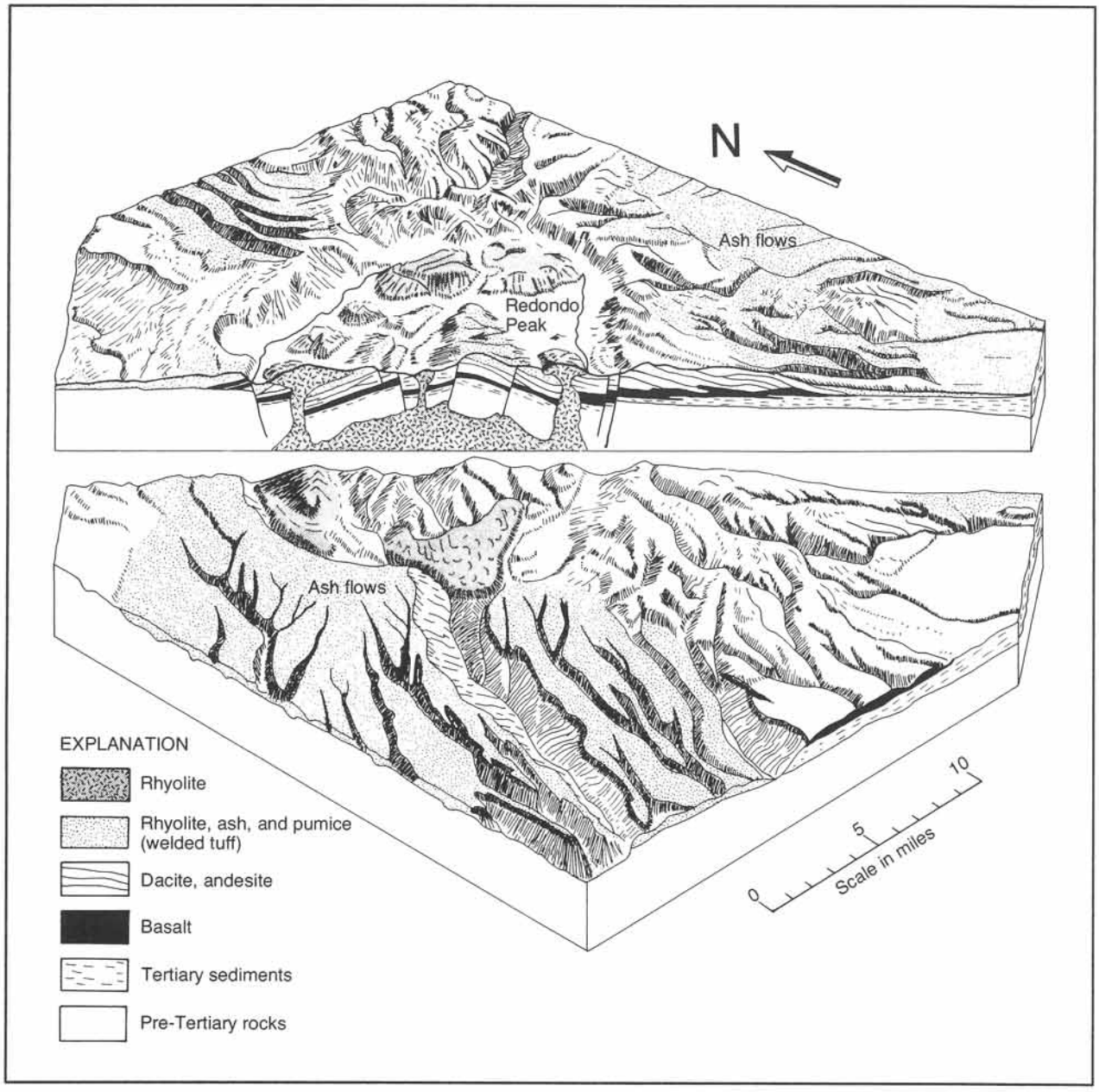

Figure 14-33: *Volcanic complex of Valles Caldera, Jemez Mountains, New Mexico.*

14-9 Eroded extrusives

Erosion slowly changes the relief and removes material from terrains with igneous extrusives. Figures 14-34a and b illustrate the change of a volcanic landscape after extensive erosion. The volcano cone is eroded away. All that remains in the landscape is a *volcanic neck*, the central feeder pipe of the former volcano. Shiprock Mountain, New Mexico, forms a magnificient example of such a volcanic neck. Shiprock towers some 400 meters above the surrounding desert plain with radial ridges, formed by dikes, emanating from the central stock (Fig. 14-34c). Lava sheets, if more

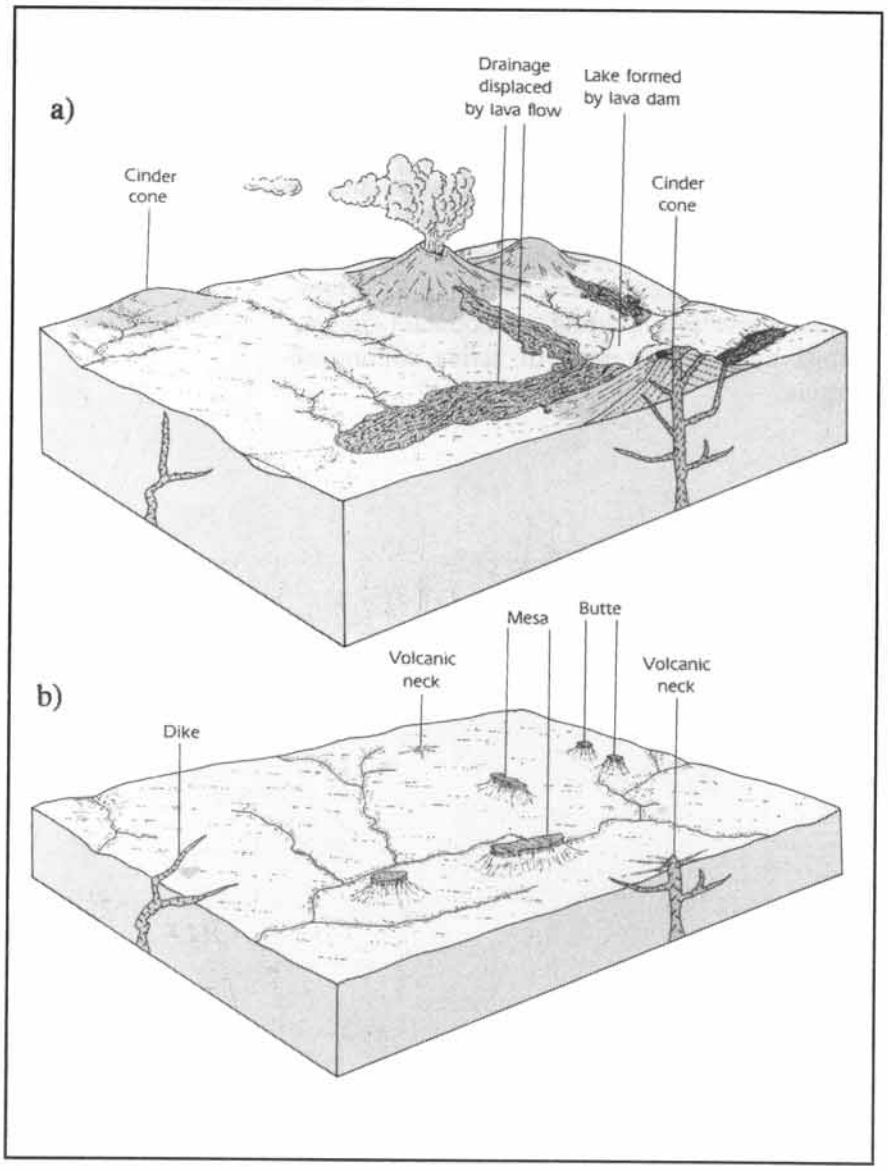

Figure 14-34: *Perspective diagram of volcanic landscape: (a) before, and (b) after, erosion. c) Shiprock Mountain, New Mexico, provides a spectacular example of a volcanic neck and radial dikes.*

resistant to erosion than the adjacent rock formations, may protect the underlying rocks from eroding away, thus forming an inverted relief. Former valleys, followed by the lava streams, are turned into *mesas* and *buttes*, elevated above the surrounding plains. Ultimately, the mesas, necks, and some dikes are all that remain of the volcanic structures. The erosion is particularly rapid in volcanic provinces above subduction zones, because these are uplifting as mountain ranges, formed by the thickening of active continental margins.

☐Exercise 14-6: Sketch two speculative map views, showing what the Valles Caldera region may look like (a) five million, and (b) fifty million years from now.